SLAC – PUB – 4749
October 1988
(M)

ANTIPROTON ANNIHILATION IN QUANTUM CHROMODYNAMICS*

STANLEY J. BRODSKY

Stanford Linear Accelerator Center,
Stanford University, Stanford, California 94309, USA

1. INTRODUCTION

Quantum chromodynamics[1] has been extensively tested in high-momentum transfer inclusive reactions, where factorization theorems, asymptotic freedom and jet algorithms provide semiquantitative perturbative predictions. Tests of the confining nonperturbative aspects of the theory are either quite qualitative or at best indirect. In fact QCD is a theory of relatively low mass scales ($\bar{\Lambda}_{MS} \sim 200 \pm 100$ MeV, $(k_\perp^2)^{1/2} \sim 300$ MeV, etc.) and its most critical tests of the theory as a viable theory of strong and nuclear interactions must involve relatively low energies and momentum transfer.

Anti-proton annihilation has a number of important advantages as a probe of QCD in the low energy domain. Exclusive reaction in which *complete* annihilation of the valance quarks occur ($\bar{p}p \to \ell\bar{\ell}$, $\gamma\gamma$, $\phi\phi$, etc.) necessarily involve impact distances $b_\perp$ smaller than $1/M_p = 5$ fm^{-1} since baryon number is exchanged in the t-channel. There are a number of exclusive and inclusive $\bar{p}$ reactions in the intermediate momentum transfer domain which provide useful constraints on hadron wavefunctions or test novel features of QCD involving both perturbative and nonperturbative dynamics. In several cases ($\bar{p}p \to \bar{\ell}\ell$, $\bar{p}p \to J/\psi$, $\bar{p}p \to \gamma\gamma$), complete leading twist (leading power law) predictions are available. These reactions not only probe the subprocesses $\bar{q}\bar{q}\bar{q}\ qqq \to \gamma\gamma$, etc., but they also are sensitive to the normalization and shape of the proton distribution amplitude $\phi_p(x_i, x_2, x_3; Q)$, the basic measure of the proton's three-quark valance wavefunction. Additionally, one can explore such processes in terms of quasielastic reactions inside of nuclear targets, e.g., $\bar{p}A \to (J/\psi)\ (A-1)$, and study an extraordinary feature of QCD: "color transparency." There is another class of exclusive reactions in QCD involving light nuclei, such as $\bar{p}d \to \gamma n$ and $\bar{p}d \to \pi^- p$ which can probe quark and gluon degrees of freedom of the nucleus at surprisingly low energy. These will be discussed in sec. 11.

Inclusive reactions involving antiprotons have the advantage that the parton distributions are well understood. In these lectures, I will particularly focus on lepton pair production $\bar{p}A \to \ell\bar{\ell}X$ as a means to understand specific nuclear features in QCD, including collision broadening, breakdown of the QCD "target length condition." Thus studies of low to moderate energy antiproton reactions with laboratory energies under 10 GeV could give further insights into the full structure of QCD.

* Work supported by the Department of Energy contract DE–AC03–76SF00515.
Invited Lectures presented at the International School of Physics with Low Energy Antiprotons: 3rd Course: Antiproton-Nucleon and Antiproton-Nucleus Interactions, Erice, Italy, June 10–18, 1988

2. QCD TESTS AND HADRON LIGHT-CONE WAVEFUNCTIONS

QCD has two essential properties which make calculations of processes at short distance or high-momentum transfer tractable and systematic. The critical feature is asymptotic freedom: the effective coupling constant $\alpha_s(Q^2)$ which controls the interactions of quarks and gluons at momentum transfer Q^2 vanishes logarithmically at large Q^2. Complementary to asymptotic freedom is the existence of factorization theorems for both exclusive and inclusive processes at large momentum transfer. In the case of exclusive processes (in which the kinematics of all the final state hadrons are fixed at large invariant mass), the hadronic amplitude can be represented as the product of a hard-scattering amplitude for the constituent quarks convoluted with a distribution amplitude for each incoming or outgoing hadron.[2-6] The distribution amplitude contains all of the bound-state dynamics and specifies the momentum distribution of the quarks in the hadron.[2] The hard-scattering amplitude can be calculated perturbatively as a function of $\alpha_s(Q^2)$. The analysis can be applied to form factors, exclusive photon-photon reactions, photoproduction, fixed-angle scattering, etc. In the case of the simplest processes, $\gamma\gamma \to M\overline{M}$ and the meson form factors, rigorous all-order proofs can be given. As we shall see, many of these predictions are directly applicable to antiproton-initiated reactions.

The predictions of perturbative QCD have been strikingly confirmed in inclusive e^+e^- and $\gamma\gamma$ collisions, deep inelastic lepton reactions, massive lepton pair production, and the whole array of large p_T jet and photon reactions. Measurements of exclusive processes at high-momentum transfer, especially form factors and two-body photon-photon reactions have led to detailed checks on the scaling behavior of the theory. Recent results[7] for $\gamma\gamma \to M\overline{M}$ are shown in fig. 1. In general, the experimental results on the scaling behavior of exclusive and inclusive reactions appear consistent with short-distance subprocesses based on the elementary scattering of spin 1/2 quarks and spin 1 gluons, the fundamental degrees of freedom of QCD.

The key to understanding hadronization and hadron matrix elements is the hadron wavefunction itself. A convenient description of hadron wavefunctions is given by the set of n-body momentum space amplitudes, $\psi_n(x_i, k_{\perp_i}, \lambda_i)$, $i = 1, 2, ...n$, defined on the free quark and gluon Fock basis at equal "light-cone time" $\tau = t + z/c$ in the physical "light-cone" gauge $A^+ \equiv A^0 + A^3 = 0$. (Here $x_i = k_i^+/p^+$, $\sum x_i = 1$, is the light-cone momentum fraction of quark or gluon i in the n — particle Fock state; $k_{\perp_i}$, with $\sum k_{\perp_i} = 0$, is its transverse momentum relative to the total momentum p^μ; and λ_i is its helicity.) The quark and gluon structure functions $G_{q/H}(x, Q)$ and $G_{g/H}(x, Q)$ which control hard inclusive reactions and the hadron distribution amplitudes $\phi_H(x, Q)$ which control hard exclusive reactions are simply related to these wavefunctions:

$$G_{q/H}(x, Q) = \sum_n \int^{Q^2} \Pi d^2 k_{\perp_i} \int \Pi dx_i \; |\psi_n(x_i, k_{\perp_i})|^2 \delta(x_q - x) \quad ,$$

and

$$\phi_H(x_i, Q) = \int^{Q^2} \Pi d^2 k_{\perp_i} \; \psi_{valence}(x_i, k_{\perp_i}) \quad .$$

Thus an important tool is the use of light-cone quantization to construct a consistent relativistic Fock state basis for the hadrons and their observables in terms of quark and gluon quanta. The distribution amplitudes and the structure functions are defined directly in terms of these light-cone wavefunctions.[2] The form factor of a hadron can be computed exactly in terms of a convolution of initial and final light-cone Fock state wavefunctions.[8] In the case of inclusive reactions all of the

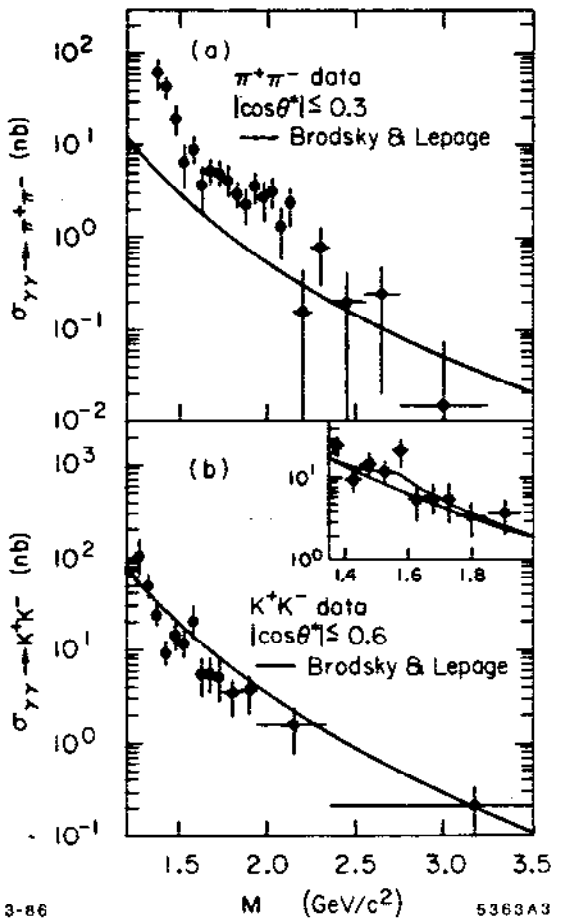

Fig. 1. Comparison of $\gamma\gamma \to \pi^+\pi^-$ and $\gamma\gamma \to K^+K^-$ meson pair production data with the parameter free perturbative QCD prediction of ref 2. The data are from ref 7.

hadron Fock states generally participate; the necessity for higher-particle Fock states in the proton is apparent from its large gluon momentum fraction and the recent results from the EMC collaboration[9] suggesting that, on the average, little of the proton's helicity is carried by the light quarks.[10] In the case of high-momentum transfer Q exclusive reactions perturbative QCD predicts that only the lowest particle number (valence) Fock state contributes to leading order in $1/Q$. The essential gauge-invariant input is the distribution amplitude[11] $\phi_H(x,Q)$. Its dependence in log Q is controlled by evolution equations derivable from perturbation theory[11] or the operator product expansion.[12] A more detailed discussion of the light-cone Fock state wavefunctions and their relation to observables is given in ref. 13.

The phenomenology of hadron wavefunctions in QCD is now just beginning. Constraints on the baryon and meson distribution amplitudes have been recently obtained using QCD sum rules and lattice gauge theory. The results are expressed in terms of gauge-invariant moments $< x_j^m >= \int \Pi dx_i \; x_j^m \; \phi(x_i,\mu)$ of the hadron's distribution amplitude.

A particularly important challenge relevant to antiproton exclusive processes is the construction of baryon distribution amplitudes. A three-dimensional "snapshot" of the proton's uud wavefunction at equal light-cone time as deduced from QCD sum rules at $\mu \sim 1$ GeV by Chernyak et al.[14] is shown in fig. 2. The moments

of the proton distribution amplitude computed by Chernyak et al., have now been confirmed in an independent analysis by Sachrajda and King.[15]

The moments of distribution amplitudes can also be computed using lattice gauge theory.[16] In the case of the pion distribution amplitudes, there is good agreement of the lattice gauge theory computations of Martinelli and Sachrajda[17] with the QCD sum rule results. This check has strengthened confidence in the reliability of the QCD sum rule method, although the shape of the meson distribution amplitudes are unexpectedly structured: the pion distribution amplitude is broad and has a dip at $x = 1/2$. In the case of the proton, the QCD sum rule prediction suggests that the u quark with helicity parallel to the proton helicity carries nearly $2/3$ of the momentum in the three-quark valence Fock state. In fact, the QCD sum rule distributions, combined with the perturbative QCD factorization predictions, account well for the scaling, normalization of the pion form factor and also the branching ratio for $J/\psi \to p\bar{p}$. In addition, Maina has found that the data for large angle Compton scattering $\gamma p \to \gamma p$ are also well described.[18] However, a very recent lattice calculation of the lowest two moments by Martinelli and Sachrajda[18] does not show skewing of the average fraction of momentum of the valence quarks in the proton.

These initial results are interesting — suggesting a highly structured oscillating momentum-space valence wavefunctions. The results from both the lattice calculations and QCD sum rules demonstrate that the light quarks are highly relativistic, at least in mesons. This gives further indication that while nonrelativistic potential models are useful for enumerating the spectrum of hadrons (because they express the relevant degrees of freedom), they may not be reliable in predicting wave function structure.

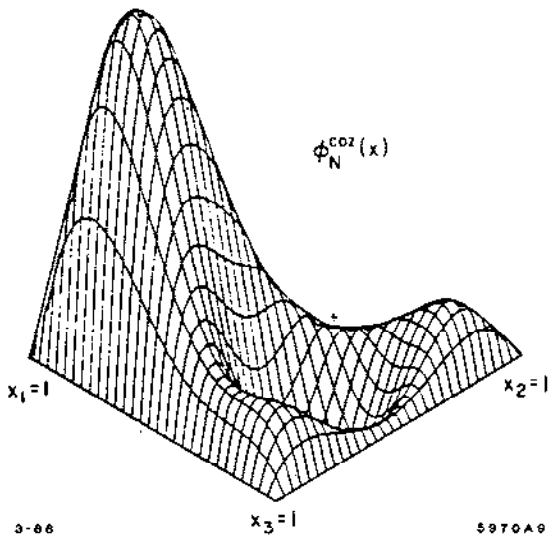

Fig. 2. The proton distribution amplitude $\phi_p(x_i, \mu)$ determined at the scale $\mu \sim 1$ GeV from QCD sum rules by Chernyak, Ogloblin and Zhitnitski.

The sum rule model form for the nucleon distribution amplitude together with the QCD factorization formulae, predicts the correct sign and magnitude as well as scaling behavior of the proton and neutron form factors.[19] (See fig. 3.)

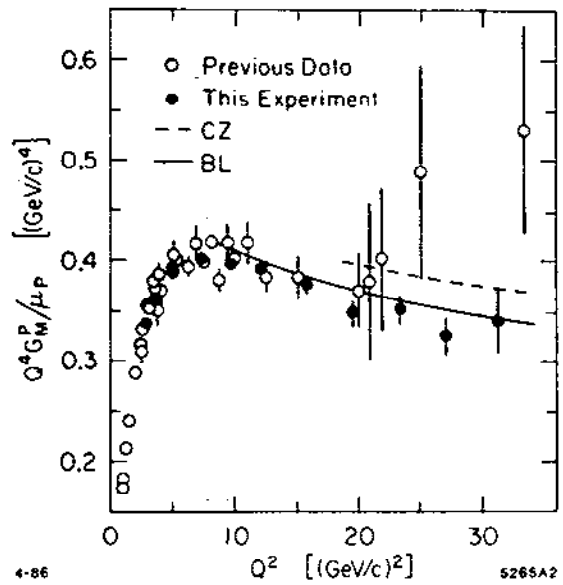

Fig. 3. Comparison of the scaling behavior of the proton magnetic form factor with the theoretical predictions of refs. 2 and 4. The CZ predictions[4] are normalized in sign and magnitude. The data are from ref. 19.

A new nonperturbative method "discretized light-cone quantization," (DLCQ)[20] has been developed which has the potential for providing detailed information on all the hadron's Fock light-cone components. The basic idea is to diagonalize the QCD Hamiltonian on the light-cone Fock states, using a computationally-convenient discrete momentum space basis. The eigenvalues M^2 of H_{LC} provide the spectrum of the theory; the eigenvectors yield the Fock state wavefunctions $\psi_n(x_i, k_{\perp i}, \lambda_i)$. So far the method has been successfully applied to gauge theories and Yukawa theory (scalar gluons) in one-space and one-time dimension. New results for the spectrum and wavefunctions for QCD[1+1] are presented in sec. 15.

3. THE TIME-LIKE PROTON FORM FACTOR

As an introduction to the application of QCD to exclusive antiproton reactions, I will first review the leading-twist perturbative QCD predictions for $\bar{p}p \to \bar{\ell}\ell$, i.e., the time-like proton form factors $F_1(s)$ and $F_2(s)$. According to the QCD factorization analysis for exclusive processes, the main dynamics is contained [to leading order in $1/s, s = (\bar{p} + p)^2$] in the $\bar{q}\bar{q}\bar{q}\ qqq \to \gamma^* \to \bar{\ell}\ell$ amplitude. To leading order in $\alpha_s(Q^2)$ the latter can be computed from minimally connected PQCD tree graphs containing two off-shell gluons and two off-shell quark lines. (See fig. 4.) To leading order in $1/s$, it is sufficient to compute the subprocess amplitude taking the incident antiquarks and quarks collinear with their respective incident hadron direction, $p_i^\mu = x_i p^\mu$. One easily finds $T_H \sim \alpha_s^2(Q^2)/(Q^2)^2 f(x_i, y_j)$, where f is a rational function of the momentum fractions. By definition, higher-loop corrections to T_H are computed such that in intermediate states all quark propagators are noncollinear, and thus off-shell by order Q. This generates corrections of higher order in $\alpha_s(Q^2)$, with no additional logarithms. The contributions where partons in the intermediate state are collinear yields the evolution of the proton and antiproton distribution amplitudes.

After computing the hard-scattering amplitude T_H to the desired order in $\alpha_s(Q^2)$, one then convolutes the amplitude with the distribution amplitudes of the $\bar{p}$ and p. The distribution amplitude $\phi_p(x_i, s)$, $(\sum_{i=1,2,3} x_i = 1)$ is a nonperturbative wavefunction, but its logarithm dependence on s is computable from first principles (e.g.,

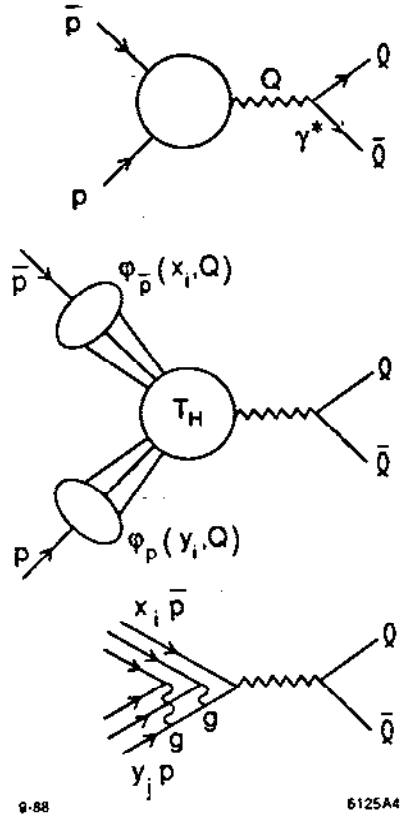

Fig. 4. Calculation of electromagnetic $\bar{p}p$ annihilation in PQCD.

renormalization group plus operator product expansion) since this is controlled by the large momentum tail of the wavefunction:

$$\frac{\partial}{\partial \ell n\ s}\phi(x_i,s) = \int_0^1 dy_i\ V(y_i,x_i,\alpha_s(s))\phi(y_i,s) \quad .$$

This equation is of the form of an evolution equation where $\ell n\ s$ plays the role of the "time." The solution has the form

$$\phi(x_i,s) = \sum_n C_n(x_i)\left(\ell n \frac{s}{\Lambda^2}^{\gamma_n}\right)^{\gamma_n} \quad ,$$

where the $C_n(x_i)$ are a known set of orthonormal polynomials. The γ_n are computable fractional powers, anomalous dimensions characteristic of the interpolating local operators for three quarks with the proton quantum numbers.

Thus the $\bar{p}p \to \bar{\ell}\ell$ time-like Fock Dirac factor (helicity conserving) has the form

$$F_1(Q^2) = \left[\frac{\alpha_s(Q^2)}{Q^2}\right]^2 \sum_{n,m} b_{nm}\left(\frac{\ell n\ s}{\Lambda^2}\right)^{-\gamma_n-\gamma_m} \quad .$$

The coefficients $b_{n,m}$ reflect the nonperturbative input and are determined by the initial data for $\phi(x_i,s_o)$ in the evolution equation. The power law scaling, $F_1(s) \sim 1/s^2$, and $d\sigma/dt\ (\bar{p}p \to \bar{\ell}\ell) \sim 1/s^6$ are consistent with the quark counting rules $F(Q^2) \sim (1/Q^2)^{n-1}$, $(d\sigma/dt)_{AB\to CD} \sim f(\theta_{cm})/s^{N_{tot}-2}$ where n is the number of fields in the bound state, and N_{tot} is the total number of incident and outgoing fields in $A + B \to C + D$; e.g., $(n = 3, \quad N_{tot} = 8 \quad \text{for} \quad \bar{p}p \to \ell\bar{\ell})$.

It is important to note that the leading power-law behavior originates in the minimum three-particle Fock state of the $\bar{p}$ and p, at least in physical gauge, such as $A^+ = 0$. Higher Fock states give contributions higher order in $1/s$. For $\bar{p}p \to \ell\bar{\ell}$

this means that initial-state interaction such as one gluon exchange are dynamically suppressed. (See fig. 5.) Soft-gluon exchange is suppressed since the incident p or $\bar{p}$ color neutral wavefunction in the three-parton state with impact operation $b_\perp \sim 0(1/\sqrt{s}$. Hard-gluon exchange is suppressed by powers of $[\alpha s(s)]$.

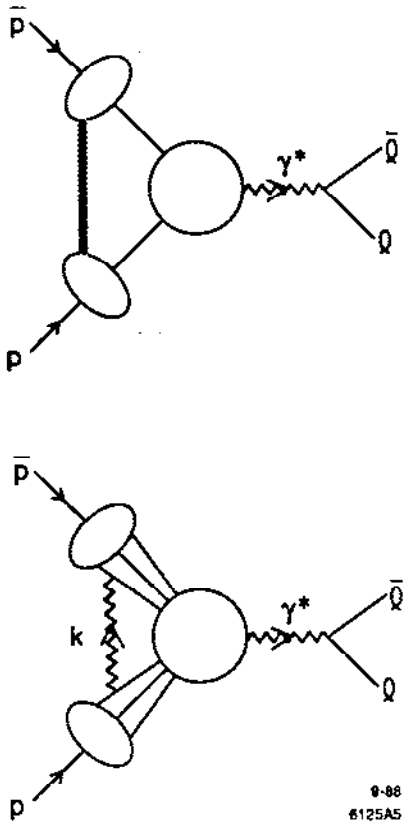

Fig. 5. Analysis of initial-state interactions in PQCD.

The absence of a soft initial-state interaction in $\bar{p}p \to \bar{\ell}\ell$ is a remarkable consequence of gauge theory and is quite contrary to normal treatments of initial interactions based on Glauber theory. This novel effect has experimental consequences: it can be studied in quasielastic $\bar{p}A \to \bar{\ell}\ell\ (A-1)$ reaction. Here we have in mind reactions in which there are no extra hadrons produced and the produced leptons are coplanar with the beam. (The nucleus $(A-1)$ can be left excited). Since PQCD predicts the absence of initial-state elastic and inelastic interactions, the number of such events could be strictly additive in the number Z of protons in the nucleus, every proton in the nucleus is equally available for short-distance annihilation. In traditional Glauber theory only the surface protons can participate because of the strong absorption of the $\bar{p}$ as it traverses the nucleus.

The above description is the ideal result for large s. QCD predicts that additivity is approached monotonically with increasing energy, corresponding to two effects: a) the effective transverse size of the $\bar{p}$ wavefunction is $b_\perp \sim 1/\sqrt{s}$, and b) the formation time for the $\bar{p}$ is sufficiently long, such that the Fock state stays small during transit of the nucleus.

The above example is an important example of the PQCD effect called "color transparency;" similar behavior is expected for all hard annihilation processing $\bar{p}p \to \gamma M$, $\bar{p}p \to J/\psi$, etc. In the case of exclusive high P_T processes in which hadrons are produced in the final state, each the final state hadron is produced with a small

color singlet wavefunction; thus one predicts negligible attenuation of these hadrons in the quasielastic nucleus reaction.

A test of color transparency in quasielastic $pp \to pp$ scattering has recently been performed at BNL. This is discussed in more detail in secs. 4 and 9. In the next section I will discuss the general problem of hadronization in the nuclear environment for both exclusive and inclusive reactions. More detailed discussions of exclusive reactions in QCD are then given in secs. 5–13.

4. QCD HADRONIZATION IN NUCLEI

The least-understood process in QCD is *hadronization* — the mechanism which converts quark and gluon quanta to color-singlet integrally-charged hadrons. One way to study hadronization is to perturb the environment by introducing a nuclear medium surrounding the hard-scattering short distance reaction. This is obviously impractical in the theoretically simplest processes — e^+e^- or $\gamma\gamma$ annihilation. However, for large momentum transfer reactions occurring in a nuclear target, such as deep inelastic lepton scattering or massive lepton pair production, the nuclear medium provides a nontrivial perturbation to jet evolution through the influence of initial- and/or final-state interactions. In the case of large momentum transfer quasiexclusive reactions, one can use a nuclear target to filter and influence the evolution and structure of the hadron wavefunctions themselves. The physics of such nuclear reactions is surprisingly interesting and subtle — involving concepts and novel effects quite orthogonal to usual expectations.

In the case of inclusive reactions, the essential test of QCD involving $\bar{p}$ reactions is the Drell-Yan process $\bar{p}A \to \ell^+\ell^- X$ and $\bar{p}A \to \gamma\gamma X$. One of the remarkable consequences of QCD factorization for inclusive reactions at large p_T is the absence of inelastic initial- or final-state interactions of the high-energy particles in a nuclear target. Since structure functions measured in deep inelastic lepton scattering are essentially additive (up to the EMC deviations), factorization implies that the $q\bar{q} \to \mu^+\mu^-$ subprocesses in Drell–Yan reactions occurs with equal probability on each nucleon throughout the nucleus. At first sight this seems surprising since one expects energy loss from inelastic initial-state interactions.

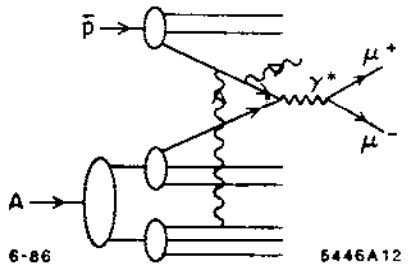

Fig. 6. Induced radiation from the propagation of an antiquark through a nuclear target in massive lepton production. Such inelastic interactions are coherently suppressed at parton energies large compared to a scale proportional to the length of the target.

In fact, inelastic reactions such as hard gluon bremsstrahlung induced in the nucleus which could potentially decrease the incident parton energy (illustrated in fig. 6) are suppressed by coherence if the quark energy (in the laboratory frame) is large compared to the target length: $E_q > \mu^2\ L_A$. Here μ^2 is the difference of mass squared between the incident quark and the quark-gluon pair produced in the initial or final state collision. This phenomenon has its origin in studies of QED

processes by Landau and Pomeranchuk. The QCD analysis is given by Bodwin, Lepage and myself.[26] The result can be derived by showing that the hard inelastic radiation emitted from differing scattering centers destructively interferes provided the target length condition is maintained. The destructive interference occurs when the momentum transfer μ^2/E_q due to the induced radiation is smaller than the inverse of the separation between two scattering centers in the nucleus. Soft radiation and elastic collisions, however, are still allowed, so one predicts collision broadening of the initial parton transverse momentum. Recent measurements of the Drell–Yan process $\pi A \to \mu^+\mu^- X$ by the NA–10 group[25] at the CERN–SPS confirm that the cross section for muon pairs at large transverse momentum is increased in a tungsten target relative to a deuteron target. (See fig. 7). Since the total cross section for lepton-pair production scales linearly with A (aside from relatively small EMC–effect corrections), there must be a corresponding decrease of the ratio of the differential cross section at low values of the di-lepton transverse momentum. This is also apparent in the data. Further measurements of low-energy $\bar{p}$ Drell–Yan reactions are needed to understand the limits of validity of QCD factorization and to explore the re-emergence of traditional Glauber inelastic scattering at low-antiquark energies. We discuss this further in sec. 14.

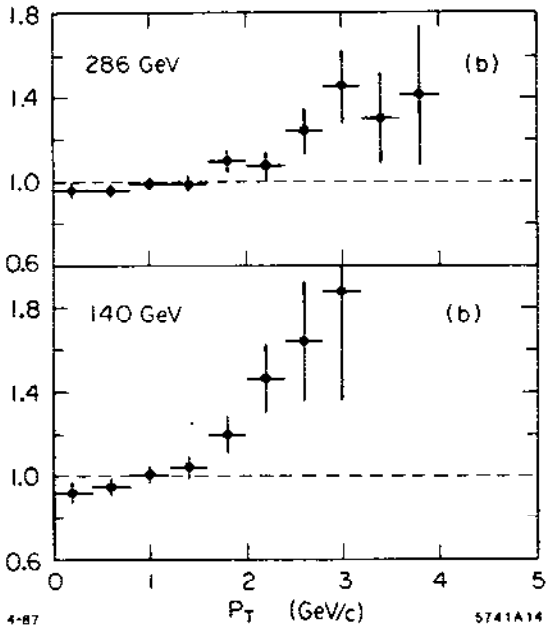

Fig. 7. The ratio $\sigma(\pi^- W \to \mu^+\mu^- X)/\sigma(\pi^- D \to \mu^+\mu^- X)$ as a function of the pair transverse momentum (from ref. 25).

The nucleus thus plays two complimentary roles in quantum chromodynamics:

1. A nuclear target can be used as a control medium or background field to modify or probe quark and gluon subprocesses. Some novel examples are *color transparency*, the predicted transparency of the nucleus to hadrons participating in high-momentum transfer exclusive reactions, and *formation zone phenomena*, the absence of hard, collinear, target-induced radiation by a quark or gluon interacting in a high-momentum transfer inclusive reaction if its energy is large compared to a scale proportional to the length of the target. (Soft radiation and elastic initial-state interactions in the nucleus still occur.) *Coalescence* with co-moving spectators is discussed as a mechanism which can lead to increased open charm hadroproduction, but which also suppresses forward charmonium production (relative to lepton pairs) in heavy ion collisions. There are also novel

features of nuclear diffractive amplitudes — high energy hadronic or electromagnetic reactions which leave the entire nucleus intact and give nonadditive contributions to the nuclear structure function at low x_{Bj}.

2. Conversely, the nucleus can be studied as a QCD structure. At short distances nuclear wavefunctions and nuclear interactions necessarily involve *hidden color*, degrees of freedom orthogonal to the channels described by the usual nucleon or isobar degrees of freedom. At asymptotic momentum transfer, the deuteron form factor and distribution amplitude are rigorously calculable. One can also derive new types of testable scaling laws for exclusive nuclear amplitudes in terms of the reduced amplitude formalism. We discuss this topic in detail in sec. 11.

5. PERTURBATIVE QCD ANALYSIS OF EXCLUSIVE REACTIONS

Perturbative QCD predictions for exclusive processes such as $p\bar{p}$ annihilation into two photons at high-momentum transfer and high invariant pair mass can provide severe tests of the theory.[27] The simplest, but still very important example,[28] of the QCD analysis of an exclusive reaction is the calculation of the Q^2-dependence of the process $\gamma^*\gamma \to M$ where M is a pseudoscalar meson such as the η. The invariant amplitude contains only one form factor: $M_{\mu\nu} = \epsilon_{\mu\nu\sigma\tau} p_\eta^\sigma q^\tau F_{\gamma\eta}(Q^2)$.

It is easy to see from power counting at large Q^2 that the dominant amplitude (in light-cone gauge) gives $F_{\gamma\eta}(Q^2) \sim 1/Q^2$ and arises from diagrams (see fig. 8) which have the minimum path carrying Q^2; i.e., diagrams in which there is only a single quark propagator between the two photons. The coefficient of $1/Q^2$ involves only the two-particle $q\bar{q}$ Fock component of the meson wavefunction. More precisely the wavefunction is the distribution amplitude $\phi(x, Q)$, defined below, which evolves logarithmically on Q. Higher particle number Fock states give higher power-law falloff contributions to the exclusive amplitude.

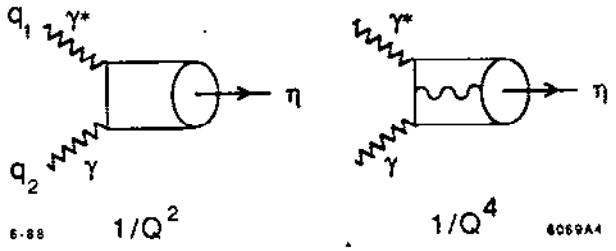

Fig. 8. Calculation of the $\gamma - \eta$ transition form factor in QCD from the valence $q\bar{q}$ and $q\bar{q}g$ Fock states.

The TPC/$\gamma\gamma$ data[29] shown in fig. 9 are in striking agreement with the predicted QCD power: a fit to the data gives $F_{\gamma\eta}(Q^2) \sim (1/Q^2)^n$ with $n = 1.05 \pm 0.15$. Data for the η' from Pluto and the TPC/$\gamma\gamma$ experiments give similar results, consistent with scale-free behavior of the QCD quark propagator and the point coupling to the quark current for both the real and virtual photons. In the case of deep inelastic lepton scattering, the observation of Bjorken scaling tests these properties when both photons are virtual.

The QCD power law prediction, $F_{\gamma\eta}(Q^2) \sim 1/Q^2$, is consistent with dimensional counting[30] and also emerges from current algebra arguments (when both photons are very virtual).[31] On the other hand, the $1/Q^2$ falloff is also expected in vector meson dominance models. The QCD and VDM predictions can be readily discriminated by

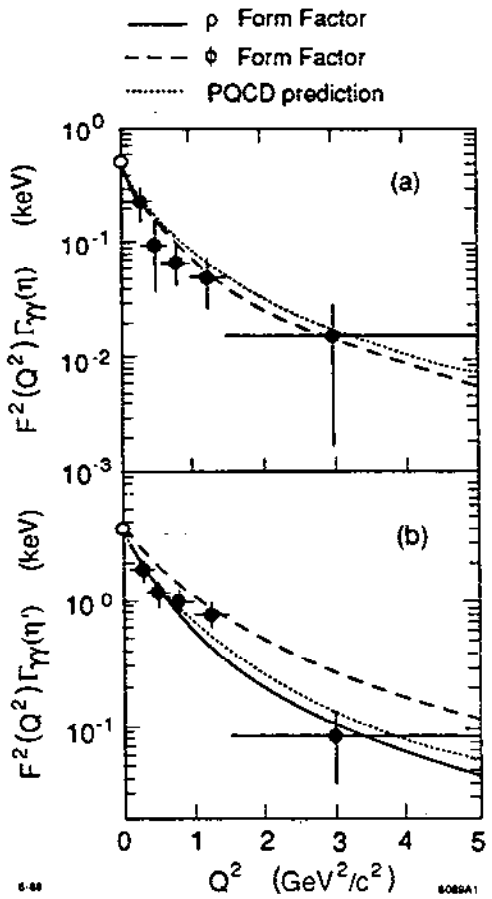

Fig. 9. Comparison of TPC/$\gamma\gamma$ data[29] for the $\gamma - \eta$ and $\gamma - \eta'$ transition form factors with the QCD leading twist prediction of ref. 27. The vector meson dominance predictions are also shown.

studying $\gamma^*\gamma^* \to \eta$. In VDM one expects a product of form factors; in QCD the falloff of the amplitude is still $1/Q^2$ where Q^2 is a linear combination of Q_1^2 and Q_2^2. It is clearly very important to test this important feature of QCD.

The analysis of $\gamma^*\gamma \to \eta$ given here is the prototype of the general QCD analysis of exclusive amplitudes at high-momentum transfer:[32] at large p_T the power behavior of the amplitude is controlled by the minimum tree diagram connecting the valence quarks in the initial and final state — this is the hard scattering amplitude T_H which shrinks to a local operator at asymptotic momentum transfer — effectively the quarks interact when they are all at relative impact separation $b_T \sim 1/p_T$. One then convolutes T_H with the distribution amplitudes $\phi(x_i, Q)$ of the hadrons — analogs of the "wavefunction at the origin" in nonrelativistic quantum mechanics — to construct the hadronic amplitude. (See also sec. 3) This convolution is the basis of the factorization theorem for QCD exclusive reactions: to leading order in $1/p_T$, the nonperturbative dynamics associated with the hadronic bound states is isolated in universal, process-independent distribution amplitudes.[32] In cases such as $\gamma\gamma$ annihilation into meson pairs and meson form factors, the analysis is completely rigorous in the sense that it can be carried out systematically to all orders in perturbation theory.

A striking feature of the QCD description of exclusive processes is "color transparency:"[33] The only part of the hadronic wavefunction that scatters at large momentum transfer is its valence Fock state where the quarks are at small relative impact separation. Such a fluctuation has a small color-dipole moment and thus has negli-

gible interactions with other hadrons. Since such a state stays small over a distance proportional to its energy, this implies that quasielastic hadron-nucleon scattering at large momentum transfer as illustrated in fig. 10 can occur additively on all of the nucleons in a nucleus with minimal attenuation due to elastic or inelastic final state interactions in the nucleus, i.e., the nucleus becomes "transparent." By contrast, in conventional Glauber scattering, one predicts strong, nearly energy-independent initial- and final-state attenuation.

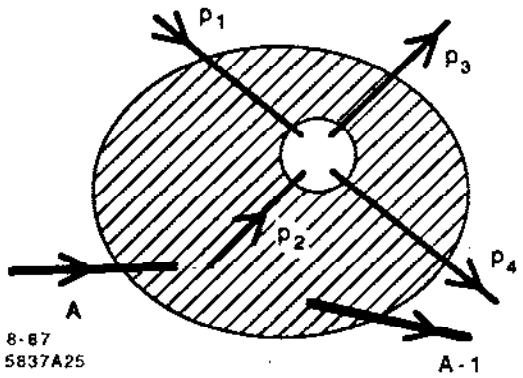

Fig. 10. Quasielastic pp scattering inside a nuclear target. Normally one expects such processes to be attenuated by elastic and inelastic interactions of the incident proton and the final-state interaction of the scattered proton. Perturbative QCD predicts minimal attenuation; i.e., "color transparency," at large momentum transfer.

A recent experiment[34] at BNL measuring quasielastic $pp \to pp$ scattering at $\theta_{\rm cm} = 90°$ in various nuclei appears to confirm the color transparency prediction — at least for p_{lab} up to 10 GeV/c. (See fig. 11.) Descriptions of elastic scattering which involve soft hadronic wavefunctions cannot account for the data. However, at higher energies, $p_{lab} \sim 12$ GeV/c, normal attenuation is observed in the BNL experiment. This is the same kinematical region $E_{\rm cm} \sim 5$ GeV where the large spin correlation in A_{NN} are observed.[35] Both features may be signaling new s-channel physics associated with the onset of charmed hadron production[36] or interference with Landshoff pinch singularity diagrams.[37] Much more testing of the color transparency phenomena is required, particularly in quasielastic lepton-proton scattering, Compton scattering, antiproton-proton scattering, etc.

As I have discussed in the introduction, the essential nonperturbative input for exclusive reactions at high-momentum transfer is the hadron "distribution amplitude" $\phi(x,Q)$ which describe the longitudinal momentum distribution of the quarks in the valence, lowest particle-number Fock state.[28] Hadron wavefunctions can be conveniently defined as coefficients on a Fock basis at fixed $\tau = t + z/c$ in the light-cone gauge. Then

$$\phi(x,Q) = \int d^2k_\perp \theta(Q^2 - k_\perp^2)\psi_V(x,k_\perp) \; ;$$

i.e., $\phi(x,Q)$ is the probability amplitude to find the quark and antiquark in the meson (or three quarks in a baryon) collinear up to the transverse momentum scale Q. Here $x = (k^0 + k^z)/(p^0 + p^z)$. More generally, the distribution amplitude can be defined as a gauge-invariant matrix-element product of quark fields evaluated between the QCD vacuum and the hadron state. At large Q^2 one can use an operator product expansion or an evolution equation to determine $\phi(x,Q)$ from an initial value $\phi(x,Q_0)$ determined by nonperturbative input. The distribution amplitude contains all of the bound-state dynamics and specifies the momentum distribution of the quarks in the

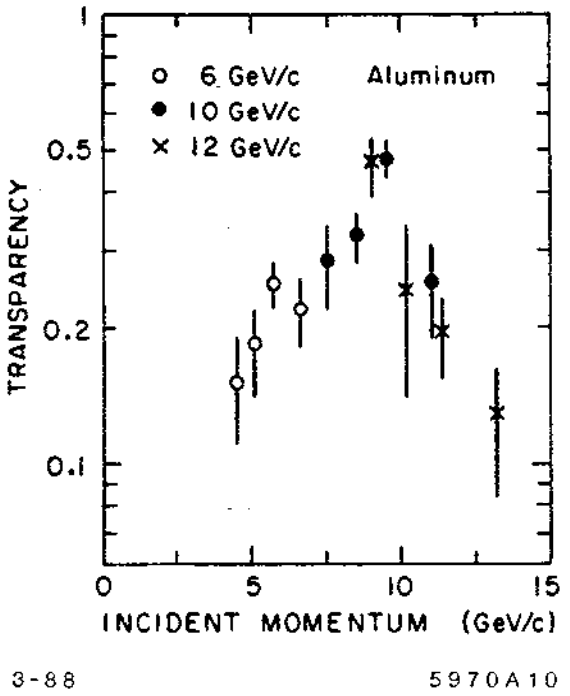

Fig. 11. Measurements of the transparency ratio $T = \frac{Z_{eff}}{Z} = \frac{d\sigma}{dt}[pA \to p(A-1)]/\frac{d\sigma}{dt}[pA \to pp]$ *near 90° on Aluminum (from ref. 34). Conventional theory predicts that T should be small and roughly constant in energy. Perturbative QCD*[33] *predicts a monotonic rise to* $T = 1$.

hadron. The hard-scattering amplitude can be calculated perturbatively as a function of $\alpha_s(Q^2)$. The analysis can be applied to form factors, exclusive photon-photon reactions, photoproduction, fixed-angle scattering, etc.

Exclusive two-body processes $\gamma\gamma \to H\overline{H}$ at large $s = W_{\gamma\gamma}^2 = (q_1 + q_2)^2$ and fixed $\theta_{\rm cm}^{\gamma\gamma}$ provide a particularly important laboratory for testing QCD, since the large momentum-transfer behavior, helicity structure, and often even the absolute normalization can be rigorously predicted.[27,38] The angular dependence of some of the $\gamma\gamma \to H\overline{H}$ cross sections reflects the shape of the hadron distribution amplitudes $\phi_H(x_i, Q)$. The $\gamma_\lambda\gamma_{\lambda'} \to H\overline{H}$ amplitude can be written as a factorized form

$$M_{\lambda\lambda'}(W_{\gamma\gamma}, \theta_{\rm cm}) = \int_0^1 [dy_i]\, \phi_H^*(x_i, Q)\, \phi_{\overline{H}}^*(y_i, Q)\, T_{\lambda\lambda'}(x, y; W_{\gamma\gamma}, \theta_{\rm cm}) \quad ,$$

where $T_{\lambda\lambda'}$ is the hard scattering helicity amplitude. To leading order $T \propto \alpha(\alpha_S/W_{\gamma\gamma}^2)^{1,2}$ and $d\sigma/dt \sim W_{\gamma\gamma}^{-4,-6} f(\theta_{\rm cm})$ for meson and baryon pairs, respectively.

Lowest order predictions for pseudoscalar and vector-meson pairs for each helicity amplitude are given in ref. 27. In each case the helicities of the hadron pairs are equal and opposite to leading order in $1/W^2$. The normalization and angular dependence of the leading order predictions for $\gamma\gamma$ annihilation into charged meson pairs are almost model independent; i.e., they are insensitive to the precise form of the meson distribution amplitude. If the meson distribution amplitudes is symmetric in x and $(1-x)$, then the same quantity $\int_0^1 dx\, [\phi_\pi(x,Q)/(1-x)]$ controls the x-integration for both $F_\pi(Q^2)$ and to high accuracy $M(\gamma\gamma \to \pi^+\pi^-)$. Thus for charged pion pairs Lepage and I found the relation:

$$\frac{\frac{d\sigma}{dt}(\gamma\gamma \to \pi^+\pi^-)}{\frac{d\sigma}{dt}(\gamma\gamma \to \mu^+\mu^-)} \cong \frac{4|F_\pi(s)|^2}{1-\cos^4\theta_{\rm cm}}$$

Note that in the case of charged kaon pairs, the asymmetry of the distribution amplitude may give a small correction to this relation.

The scaling behavior, angular behavior and normalization of the $\gamma\gamma$ exclusive pair production reactions are nontrivial predictions of QCD. Recent Mark II meson pair data and PEP4/PEP9 data for separated $\pi^+\pi^-$ and K^+K^- production in the range $1.6 < W_{\gamma\gamma} < 3.2$ GeV near 90° are in satisfactory agreement with the normalization and energy dependence predicted by QCD. (See fig. 1.) In the case of $\pi^0\pi^0$ production, the $\cos\theta_{\rm cm}$ dependence of the cross section can be inverted to determine the x-dependence of the pion distribution amplitude. The one-loop corrections to the hard-scattering amplitude for meson pairs have been calculated by Nizic.[38] The QCD predictions for mesons containing admixtures of the $|gg\rangle$ Fock state is given by Atkinson, Sucher and Tsokos.[38]

The perturbative QCD analysis has been extended to baryon-pair production in comprehensive analyses by Farrar et al.[39] and by Gunion et al.[38] Predictions are given for the "sideways" Compton process $\gamma\gamma \to p\bar{p}$, $\Delta\overline{\Delta}$ pair production, and the entire decuplet set of baryon pair states. The arduous calculation of 280 $\gamma\gamma \to qqq\overline{qqq}$ diagrams in T_H required for calculating $\gamma\gamma \to B\overline{B}$ is greatly simplified by using two-component spinor techniques. The doubly charged Δ pair is predicted to have a fairly small normalization. Experimentally, such resonance pairs may be difficult to identify under the continuum background.

The normalization and angular distribution of the QCD predictions for proton-antiproton production shown in fig. 12 depend in detail on the form of the nucleon distribution amplitude, and thus provide severe tests of the model form derived by Chernyak, Ogloblin and Zhitnitsky from QCD sum rules.[40]

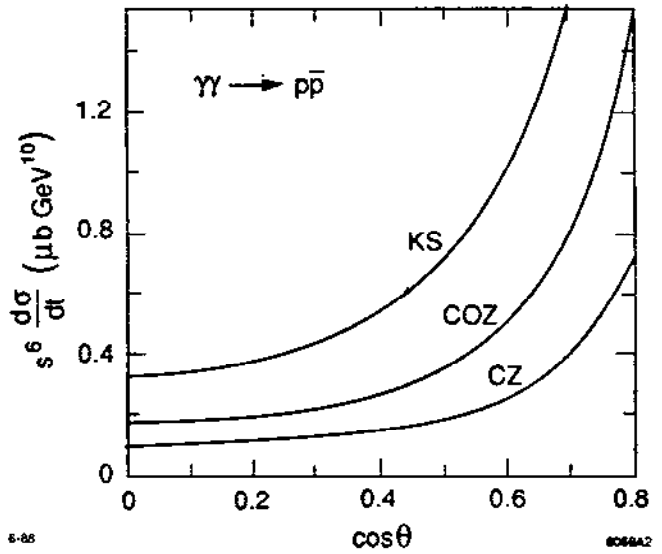

Fig. 12. Perturbative QCD predictions by Farrar and Zhang for the $\cos(\theta_{cm})$ dependence of the $\gamma\gamma \to p\bar{p}$ cross section assuming the King–Sachrajda (KS), Chernyak, Ogloblin and Zhitnitsky (COZ), and original Chernyak and Zhitnitsky (CZ) forms for the proton distribution amplitude, $\phi_p(x_i, Q)$.

An important check of the QCD predictions can be obtained by combining data from $\gamma\gamma \to p\bar{p}$ and the annihilation reaction, $p\bar{p} \to \gamma\gamma$, with large angle Compton scattering $\gamma p \to \gamma p$.[41]

This comparison checks in detail the angular dependence and crossing behavior expected from the theory. Furthermore, in $p\bar{p}$ collisions one can study time-like photon production into e^+e^- and examine the virtual photon mass dependence of the Compton amplitude. Predictions for the q^2 dependence of the $p\bar{p} \to \gamma\gamma^*$ amplitude can be obtained by crossing the results of Gunion and Millers.[38]

The region of applicability of the leading power-law predictions for $\gamma\gamma \to p\bar{p}$ requires that one be beyond resonance or threshold effects. It presumably is set by the scale where $Q^4 G_M(Q^2)$ is roughly constant, i.e., $Q^2 > 3$ GeV^2. Present measurements may thus be too close to threshold for meaningful tests.[42] It should be noted that unlike the case for charged meson-pair production, the QCD predictions for baryons are sensitive to the form of the running coupling constant and the endpoint behavior of the wavefunctions.

The QCD predictions for $\gamma\gamma \to H\overline{H}$ can be extended to the case of one or two virtual photons, for measurements in which one or both electrons are tagged. Because of the direct coupling of the photons to the quarks, the Q_1^2 and Q_2^2 dependence of the $\gamma\gamma \to H\overline{H}$ amplitude for transversely polarized photons is minimal at W^2 large and fixed $\theta_{\rm cm}$, since the off-shell quark and gluon propagators in T_H already transfer hard momenta; i.e., the 2γ coupling is effectively local for Q_1^2, $Q_2^2 \ll p_T^2$. The $\gamma^*\gamma^* \to \bar{B}B$ and $M\overline{M}$ amplitudes for off-shell photons have been calculated by Millers and Gunion.[38] New results on charged $\pi\rho$ pair production were also presented to this meeting by Kessler and Tamazouzt. In each case, the predictions show strong sensitivity to the form of the respective baryon and meson distribution amplitudes.

We also note that photon-photon collisions provide a way to measure the running coupling constant in an exclusive channel, independent of the form of hadronic distribution amplitudes. The photon-meson transition form factors $F_{\gamma\to M}(Q^2)$, $M = \pi^0, \eta^0, f$, etc., are measurable in tagged $e\gamma \to e'M$ reactions. QCD predicts

$$\alpha_s(Q^2) = \frac{1}{4\pi} \frac{F_\pi(Q^2)}{Q^2 |F_{\pi\gamma}(Q^2)|^2} \quad ,$$

where to leading order the pion distribution amplitude enters both numerator and denominator in the same manner.

6. APPLICABILITY OF PERTURBATIVE QCD TO EXCLUSIVE PROCESSES

Isgur and Llewellyn Smith[43] have recently raised a number of questions concerning the application of perturbative QCD to exclusive reactions in the momentum transfer range presently accessible to experiment. The issues involved are very important for understanding the basis of virtually all perturbative QCD predictions. In the following I will review and discuss the main points at issue:

(1) Isgur and Llewellyn Smith, and also Radyshkin,[44] argue that the normalization of the PQCD amplitude is of order $(\alpha_s/\pi)^n(\lambda^2/Q^2)^n$ where λ is a typical hadronic scale. If this were the correct estimate, the perturbative contributions would be too small to compete with the rapidly-falling "soft" nonperturbative contributions until very large momentum transfers Q.

In fact, the PQCD prediction for the pion form factor at large Q^2 is nominally of order $16\pi\alpha_s f_\pi^2$, a factor of order $16\pi^2$ times larger than the above estimate. The actual coefficient of the leading twist, leading power law term depends on the integral $\int_0^1 dx\ \frac{\phi_\pi(x,Q)}{(1-x)}$, and is thus only moderately sensitive to the shape of the meson distribution amplitude in the endpoint region.

The normalization and sign of the leading power law terms predicted by PQCD are in agreement with the measurements of the meson and baryon form factors as well as large invariant mass exclusive photon-photon meson pair production cross sections if one uses the hadron distribution amplitudes predicted by Chernyak et al.[40] and Sachrajda and King[15] from QCD sum rules. As discussed in sec. 2, the recent lattice gauge theory analysis of the moments of the meson distribution amplitude by Martinelli and Sachrajda[17] give results consistent with those of Chernyak and Zhitnitsky.

It might also be noted that in QED, the "soft" contributions to the positronium form factor from Coulomb photon exchange are the *same* order in α as the "hard" contributions from transverse photon exchange. There are no extra powers of α in the hard amplitude! Once the electrons are relativistic, i.e., for $Q^2 \sim M^2$, the hard, perturbative contribution dominates.[45]

(2) Isgur and Llewellyn Smith argue that the momentum transfer flowing through the gluon propagator in the hard scattering amplitude for an exclusive reaction is typically too small to trust the perturbative expansion. This seems to be of particular concern for the skewed, highly relativistic distribution amplitudes obtained from the QCD sum rule analysis of Chernyak et al. since the integration region where x is large tends to be emphasized. In the case of the hard-scattering T_H amplitude for the pion form factor (illustrated in fig. 13), the struck quark is off-shell at order $(1-x)Q^2$ whereas the momentum transfer of the exchanged gluon is of order $(1-x)(1-y)Q^2$, which can be considerably smaller.

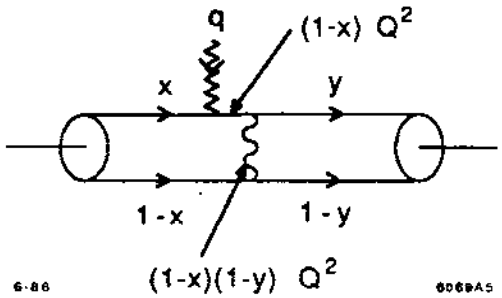

Fig. 13. Leading twist contribution to the meson form factor in QCD.

In fact, as shown by Lepage and myself,[28] the momentum transfer scale where one can analyze amplitudes perturbatively in QCD is controlled by the virtuality of the quark propagator not that of the exchanged gluon. [The range of the gluon virtuality is of course important in setting the scale of the effective coupling constant $\alpha_s(\bar{Q}^2)$.] If the struck quark is sufficiently off-shell, $|k_q^2| > \Lambda^2_{\rm QCD}$, one can easily show that multiple soft gluon exchange contributions are suppressed by powers of Q^2 relative to one-gluon exchange. The same considerations apply to the analysis of the evolution of deep inelastic structure functions: the critical scale is the off-shell virtuality of the quark propagators — not the minimum virtuality of the gluons. Even though the radiated gluons have low virtuality, one can compute the form of QCD evolution with elementary vector gluon couplings provided that the struck quark is sufficiently off-shell. Similarly, in computations of quark jet evolution, the perturbative gluon coupling dominates even though the gluon can be radiated near its mass shell. Requiring the gluon to have a minimum virtual mass corresponds to multiple jet production.

How can one reconcile the PQCD analysis with the concept that at low momentum transfer the interaction between quarks is nonperturbative? The concept of a nonperturbative potential (and estimates of scales involving the gluonium mass) can only be applicable to situations in which quarks are close to their mass shells and scatter at low relative velocity so that there is sufficient time to interact strongly. However, in the high momentum transfer form factor and deep inelastic scattering reactions, the struck quark is relatively far off its mass shell and interacts at high momentum relative to the spectator quarks. Thus its interactions may be computed perturbatively.

The above observations form the basis of the application of renormalization group equations and the operator product expansion to these reactions, and allows one to calculate the leading power behavior and the QCD logarithmic evolution of exclusive amplitudes for the pion form factor and $\gamma\gamma$ annihilation into meson pairs to all orders in perturbation theory.

The predictions[32] for the leading twist term in exclusive QCD hadronic amplitudes are thus unambiguous. Higher twist corrections to the quark and gluon propagator due to mass terms and intrinsic transverse momenta of a few hundred MeV give nominal corrections of higher order in $1/Q^2$. These finite mass corrections combine with the leading twist results to give a smooth approach to small Q^2. The PQCD scaling laws thus become valid at relatively low momentum transfer, the few GeV scale, consistent with what is observed in experiment, as in the results shown in figs. 1 and 9.[46]

(3) Independent of the underlying theory, the form factor of a hadron can be computed from the overlap of light-cone wavefunctions, summed over Fock states, as shown by Drell and Yan.[47] This is the starting point for all relativistic calculations including the PQCD analysis. Isgur and Llewellyn Smith, and also Radyshkin, argue that one can obtain reasonable agreement with the form factor data by parameterizing the three-point vertex amplitude using various models for the bound state wavefunctions.

However, phenomenological agreement with a parameterization of the vertex amplitude is not in contradiction with the PQCD analysis unless one can show that the QCD wavefunction with gluon exchange can be excluded in favor of purely nonperturbative forms. The analyses[48] of Dziembowski and Mankiewicz (which is consistent with QCD sum rules), Carlson and Gross, and Jacob and Kisslinger show that strictly soft wavefunctions, consistent with rotational invariance in the rest frame, and normalized correctly, cannot account for the pion or proton form factors in the power-law scaling regime.

Perhaps the most compelling evidence for the validity of the PQCD approach to exclusive processes is the observation[34] of color transparency in pp quasielastic scattering in nuclei, as discussed in sec. 4. The BNL data exclude models in which the scattering is dominated by soft wavefunctions.

The perturbative QCD predictions for the leading twist power-law contributions are generally consistent with data for exclusive processes when the momentum transfer exceeds several GeV.[49] It is difficult to understand the claim that these data are explained by higher twist or soft nonperturbative contributions since such effects necessarily fall at least one power of Q^2 faster than the dimensional counting prediction.

7. SUMMARY OF QCD PREDICTIONS FOR $\bar{p}p$ EXCLUSIVE PROCESSES

Dimensional counting rules[50] give a direct connection between the degree of hadron compositeness and the power-law fall of exclusive scattering amplitudes at

fixed center of mass angle: $M \sim Q^{4-n} F(\theta_{\rm cm})$ where n is the minimum number of initial and final state quanta. This rule gives the QCD prediction for the nominal power law scaling, modulo corrections from the logarithmic behavior of α_s, the distribution amplitude and small power-law corrections from Sudakov–suppressed Landshoff multiple scattering contributions. For $\bar{p}p$ one predicts

$$\frac{d\sigma}{d\Omega}\,(\bar{p}p \to \gamma\gamma) \simeq \frac{\alpha^2}{(p_T^2)^5}\, f^{\gamma\gamma}(\cos\theta, \ell n p_T)$$

$$\frac{d\sigma}{d\Omega}\,(\bar{p}p \to \gamma M) \simeq \frac{\alpha^2}{(p_T^2)^6}\, f^{\gamma M}(\cos\theta, \ell n p_T)$$

$$\frac{d\sigma}{d\Omega}\,(p\bar{p} \to M\overline{M}) \simeq \frac{1}{(p_T^2)^7}\, f^{M\overline{M}}(\cos\theta, \ell n p_T)$$

$$\frac{d\sigma}{d\Omega}\,(p\bar{p} \to B\overline{B}) \simeq \frac{1}{(p_T^2)^9}\, f^{B\overline{B}}(\cos\theta, \ell n p_T) \quad .$$

The angular dependence reflects the structure of the hard-scattering perturbative T_H amplitude, which in turn follows from the flavor pattern of the contributing duality diagrams. For example, a minimally-connected diagram such as that illustrated in fig. 14 is approximately characterized[51] as

$$T_H \sim \frac{1}{t^2}\,\frac{1}{s}\,\frac{1}{u} \quad .$$

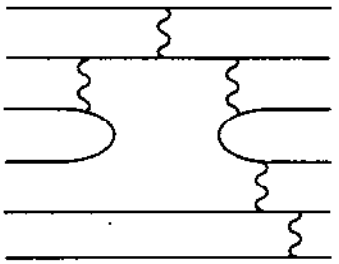

Fig. 14. A perturbative contribution to the hard-scattering amplitude in nucleon-nucleon collisions.

We emphasize that comparisons between channels related by crossing of the Mandelstam variables places a severe constraint on the angular dependence and analytic form of the underlying QCD exclusive amplitude. For example, it is possible to measure and compare

$$\bar{p}p \to \gamma\gamma \;:\; \gamma p \to \gamma p \;:\; \gamma\gamma \to \bar{p}p$$

$$\bar{p}p \to \gamma\pi^0 \;:\; \gamma p \to \pi^0 p \;:\; \pi^0 p \to \gamma p \;.$$

SLAC measurements[52] of the $\gamma p \to \pi^+ n$ cross section at $\theta_{CM} = \pi/2$ are consistent with the normalization and scaling (see fig. 15) $d\sigma/dt\,(\gamma p \to \pi^+ n) \simeq [1\,\text{nb}/(s/10\ \text{GeV})^7]$ $f(t/s)$. We thus expect similar normalization and scaling for $d\sigma/dt\,(\bar{p}p \to \gamma\pi^0)$; all angle measurements up to $s \lesssim 15$ GeV^2 appear possible given a high luminosity $\bar{p}$ beam.

Extensive measurements of the $pp \to pp$ cross section have been made at ANL, BNL and other laboratories.[51] The fixed-angle data on a log-log plot (see fig. 16) appears consistent with the nominal $s^{-10} f(\theta_{CM})$ dimensional counting production.

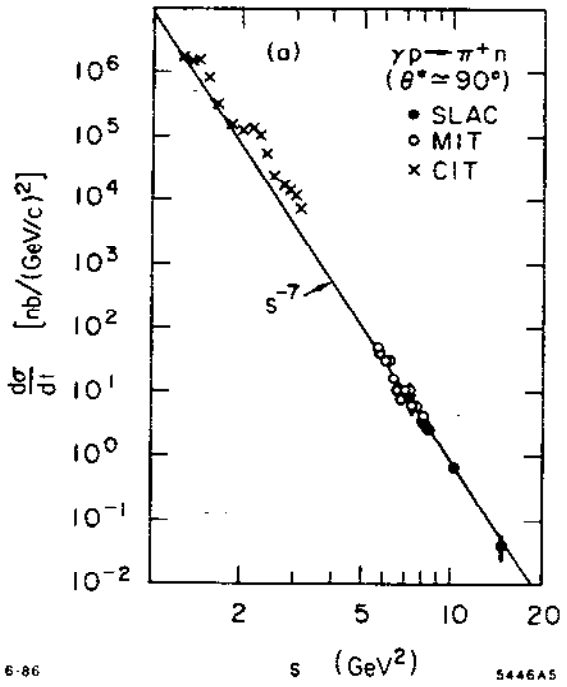

Fig. 15. Comparison of photoproduction data with the dimensional counting power-law prediction. The data are summarized in ref. 52.

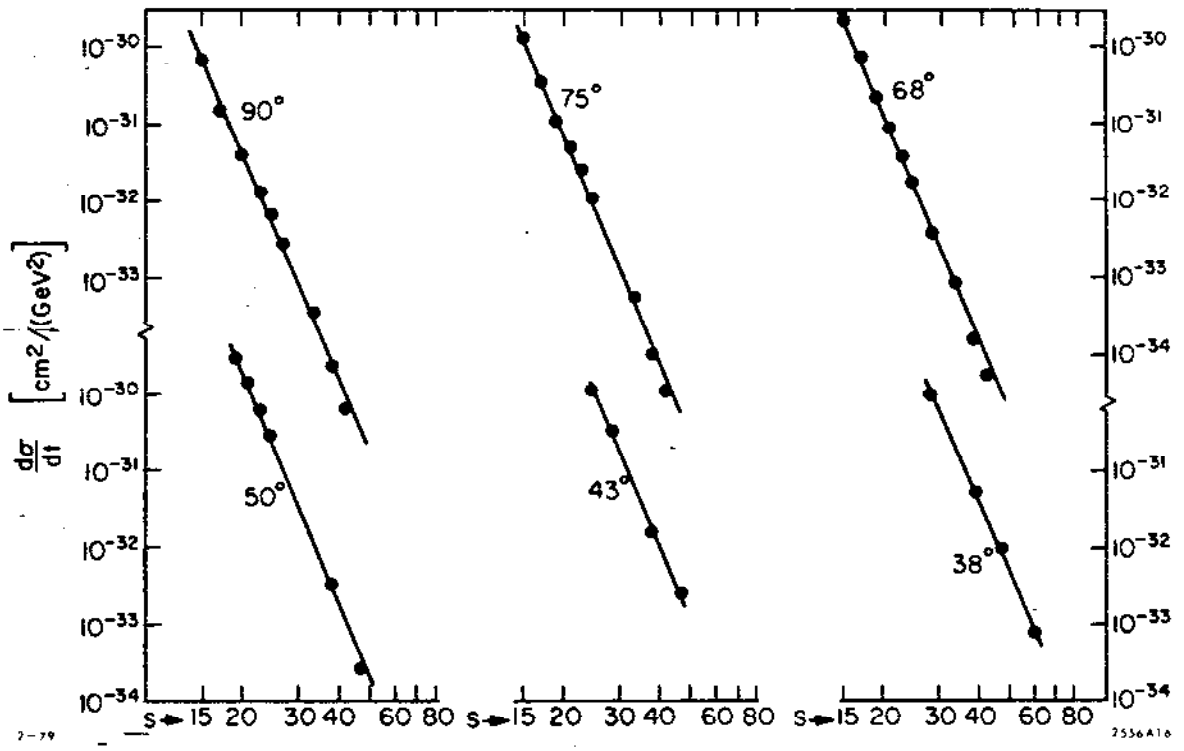

Fig. 16. Test of fixed θ_{CM} scaling for elastic pp scattering. The best fit gives the power $N = 9.7 \pm 0.5$ compared to the dimensional counting prediction N=10. Small deviations are not readily apparent on this log-log plot. The compilation is from Landshoff and Polkinghorne.

However, as emphasized by Hendry,[53] the $s^{10}d\sigma/dt$ cross section exhibits oscillatory behavior with p_T. Even more serious is the fact that polarization measurements[54]

show significant spin-spin correlations (A_{NN}), and the single spin asymmetry (A_N) is not consistent with predictions based on hadron helicity conservation (see sec. 6) which is expected to be valid for the leading power behavior.[55] Recent discussions of these effects have been given by Farrar[56] and Lipkin.[57] I discuss a new explanation of all of these effects in sec. 9. Clearly, $\bar{p}p \to \bar{p}p$ data in the large-angle, large-energy regime will also be helpful in clarifying these fundamental issues.

The simplest exclusive channels accessible to a $\bar{p}p$ facility are $\bar{p}p \to e^+e^-$, $\mu^+\mu^-$, $\tau^+\tau^-$ which to leading order in α provides a direct measurement of the Dirac and Pauli time-like proton form factor. The θ_{CM} angular dependence can be used to separate F_2 and F_1 and check the basic prediction,[2] $F_2(s)/F_1(s) \sim M^2/s$.

As discussed in sec. 3, perturbative QCD predicts asymptotic scaling of the form[2]

$s^2F_1(s) \sim f(\ell n\, s)$. A high-luminosity $\bar{p}$ facility could push time-like measurements of both form factors well beyond those available from e^+e^- storage rings. Since the normalization is similar to that of $p\bar{p} \to \gamma\gamma$, one should be able to measure the proton form factors out to center-of-mass energy squared as large as $s \sim 10$ GeV^2.

An important example of an exclusive process in QCD is the process $p\bar{p} \to \gamma\gamma$ as illustrated in fig. 17. To leading order in $1/p_T^2$,

$$M_{p\bar{p}\to\gamma\gamma}(p_T^2,\theta_{CM}) = \int_0^1 [dx] \int_0^1 [dy] \phi_{\bar{p}}(x,p_T) T_H(qqq + \bar{q}\bar{q}\bar{q} \to \gamma\gamma) \phi_p(y,p_T) \quad ,$$

where $\phi_p(x,p_T)$ is the antiproton distribution amplitude and $T_H \sim \alpha_s^2(p_T^2)/(p_T^2)$ gives the scaling behavior of the minimally connected tree-graph amplitude for the two-photon annihilation of three quarks and three antiquarks collinear with the initial hadron directions. (See fig. 18.) QCD thus predicts

$$\frac{d\sigma}{d\Omega_{CM}}\,(p\bar{p} \to \gamma\gamma) \simeq \frac{\alpha_s^4(p_T^2)}{(p_T^2)^5}\; f(p_T,\theta_{CM},\ell n p_T^2)\;.$$

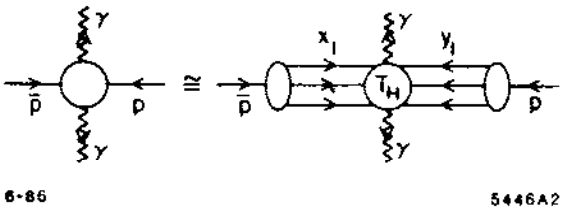

Fig. 17. Application of QCD factorization to $\bar{p}p$ annihilation into photons.

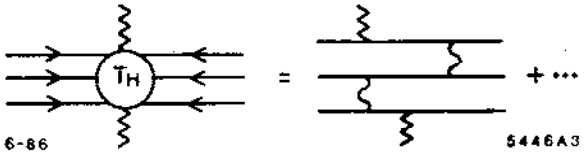

Fig. 18. Example of a lowest-order perturbative contribution to T_H for the process $\bar{p}p \to \gamma\gamma$.

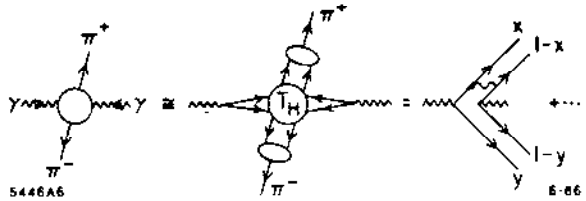

Fig. 19. Application of QCD to two-photon production of meson pairs.[58]

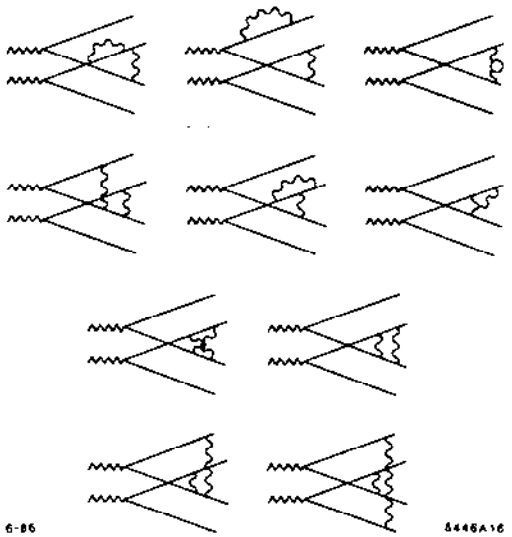

Fig. 20. Next-to-leading perturbative contribution to T_H for the process $\gamma\gamma \to M\bar{M}$. The calculation has been done by Nizic.[58]

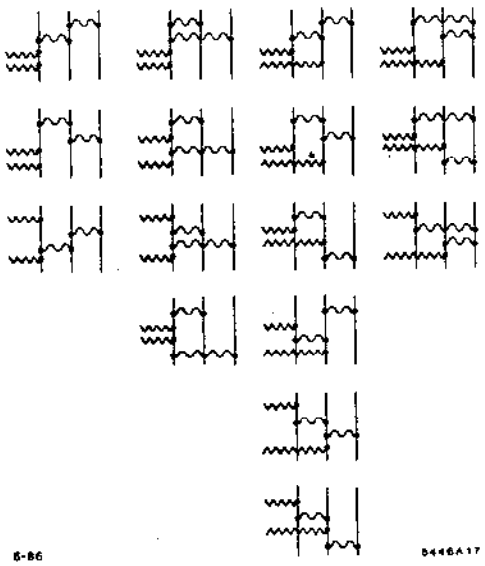

Fig. 21. Leading diagrams for $\gamma + \gamma \to \bar{p} + p$ calculated in refs. 59 and 60.

The complete calculations of the tree-graph structure (see figs. 19–21) of both $\gamma\gamma \to M\overline{M}$ and $\gamma\gamma \to B\overline{B}$ amplitudes has now been completed. One can use

crossing to compute T_H for $p\bar{p} \to \gamma\gamma$ to leading order in $\alpha_s(p_T^2)$ from the calculations reported by Farrar, Maina and Neri[59] and Gunion and Millers.[60] Examples of the predicted angular distributions are shown in figs. 22 and 23. The region of applicability of the leading power-law results is presumed to be set by the scale where $Q^4 G_M(Q^2)$ is roughly constant, i.e., $Q^2 > 3$ GeV^2. (See fig. 3.) Present two-photon collision measurements[61] are at energies too close to the $\bar{p}p$ threshold to meaningfully test the predictions.

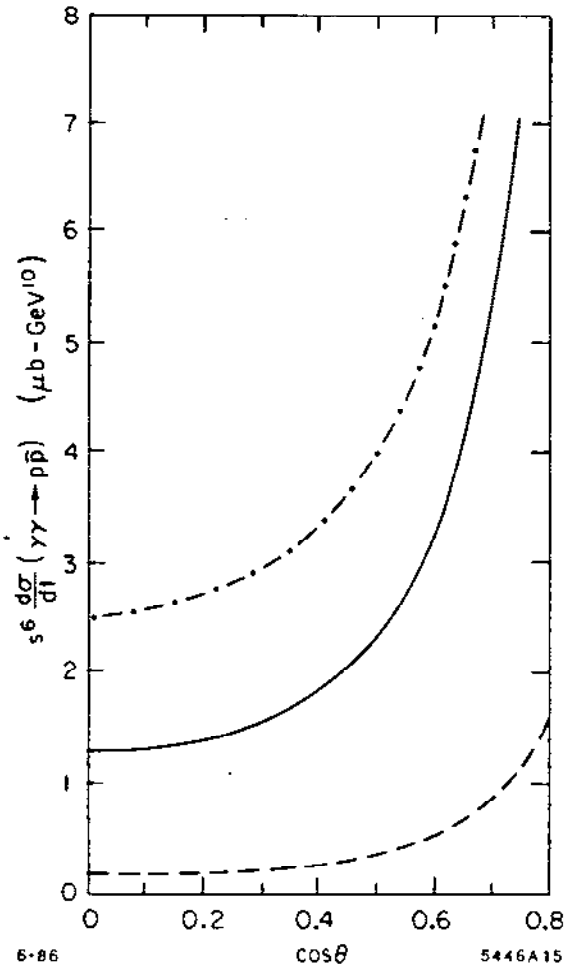

Fig. 22. QCD prediction for the scaling and angular distribution for $\gamma + \gamma \to \bar{p} + p$ calculated by Farrar et al.[59] The dashed-dot curve corresponds to $4\Lambda^2/s = 0.0016$ and a maximum running coupling constant $\alpha_s^{max} = 0.8$. The solid curve corresponds to $4\Lambda^2/s = 0.016$ and a maximum running coupling constant $\alpha_s^{max} = 0.5$. The dashed curve corresponds to a fixed $\alpha_s = 0.3$. The results are very sensitive to the endpoint behavior of the proton distribution amplitude. The CZ form is assumed.

As discussed in sec. 2, a model form for the proton distribution amplitude has been proposed by Chernyak and Zhitnitskii[4] based on QCD sum rules which leads to normalization and sign consistent with the measured proton form factor. (See fig. 2.) The CZ sum rule analysis has been recently corrected and modified by King and Sachrajda[62] but the final results are not known at this time. The CZ proton distribution amplitude yields predictions for $\gamma\gamma \to p\bar{p}$ in rough agreement with the experimental normalization, although the production energy is too low for a clear test. It should be noted that unlike meson pair production[58] the QCD predictions

scatterings can occur more or less independently, at widely separated points. The scattering process is no longer localized, and factorization does not occur. The s dependence of the contribution from this region can be readily estimated: a) the quark-quark scattering amplitudes each give $(1/s)^0$, by dimensional counting; b) phase space as restricted by in Eq. (116) gives a factor $(\lambda/\sqrt{s})^2$; c) the energy denominator gives a factor $1/D \sim 1/\lambda\sqrt{s}$. Thus the pinch region contributes

$$T_{PS} \sim \frac{1}{s^{3/2}} f(\theta_{CM}; x_a) \tag{117}$$

which apparently dominates the hard scattering contribution by a factor $\sqrt{s}$.

Two things work to suppress this pinch contribution. First the number of hard scattering amplitudes is much larger than the number of pinch singularity diagrams. More importantly, perhaps, radiative corrections to the individual quark-quark amplitudes build up Sudakov form factors that increase the effective power of $1/s$ to something like

$$\frac{3}{2} + \frac{4\,C_F}{\beta} \log\log\left(\frac{|t|}{\lambda^2}\right) \tag{118}$$

which grows infinitely large as $|t| \sim s \to \infty$. These corrections do not cancel here because the quarks and antiquarks scatter separately here, and not together as color singlets. So the pinch region is probably completely suppressed by Sudakov effects when s is sufficiently large. It turns out that a contribution still remains from a region intermediate between the pinch region and the hard-scattering region.[21] This results in a small correction to the power-law predicted by dimensional counting. For example, pp elastic scattering at wide angles should fall off roughly like $s^{-9.7}$, rather than s^{-10} as predicted by dimensional counting. Considerable progress has been made recently towards a complete analysis of such effects.[23]

Pinch singularities always show up as singularities in the hard scattering amplitude $T_H(x_a, x_b \ldots, Q)$ at points $x_a, x_b \ldots$ away from the endpoints 0 and 1. The integrals over $x_a, x_b \ldots$ are then singular. Not every midpoint singularity in T_H actually corresponds to a pinch. For example, singularities that are linear—*e.g.* $1/(x - c + i\epsilon)$—do not involve pinches. These cause no problems when integrating over x: the real part of the amplitude is obtained using a principal value prescription, while an imaginary part is generated by making the replacement $1/(x - c + i\epsilon) \to -2\pi i\delta(x - c)$. When the singularities are more severe they must be cut off by explicitly including Sudakov form factors in the pinch region. The dimensional-counting rule is modified only in these very singular situations.

4.6. How Large is Asymptotic Q?

The perturbative formalism we have described is only valid at large momentum transfers. A critical question[24] then is, How large is large? Here as in any application of perturbative QCD there are really two issues: 1) the convergence of perturbation theory; and 2) the relative importance of competing nonperturbative mechanisms. We examine each in term.

The perturbative expansion describing a short-distance process in QCD—*e.g.* $a_0+a_1\,\alpha_s(Q^2_{\rm eff})/\pi+\ldots$—converges quickly if the characteristic momentum $Q_{\rm eff}$ for the process is large compared with the QCD scale parameter $\Lambda_{QCD}\sim 200$ Mev. To determine $Q_{\rm eff}$ for large-$p_\perp$ exclusive processes we can examine the momentum flow in the hard-scattering amplitude. The pion's form factor, for example, is given by

$$F_\pi(Q^2)\approx\int_0^1 dx\int_0^1 dy\,\{\phi^*(y,(1-y)Q)\,e_q\,T_H(x,y,Q)\,\phi(x,(1-x)Q)+(q\leftrightarrow\bar q)\} \tag{119}$$

where the hard-scattering amplitude is

$$T_H(x,y,Q)=\frac{16\pi\,C_F\,\alpha_s}{(1-x)(1-y)Q^2}. \tag{120}$$

The running coupling in T_H is associated with gluon-exchange between the quark and the antiquark as they scatter from the initial to the final direction. Thus it is natural to set the scale of this coupling equal to the square of the gluon's four momentum: $\alpha_s\to\alpha_s((1-x)(1-y)Q^2)$ in T_H.[#13] The defining relation for $Q_{\rm eff}$ then is obviously

$$\int_0^1 dx\int_0^1 dy\,\phi^*\,\frac{\alpha_s((1-x)(1-y)Q^2)}{(1-x)(1-y)}\,\phi=\int_0^1 dx\int_0^1 dy\,\phi^*\,\frac{\alpha_s(Q^2_{\rm eff})}{(1-x)(1-y)}\,\phi. \tag{121}$$

A small complication is that the usual perturbative formula for $\alpha_s(Q^2)$ has an unphysical singularity at $Q=\Lambda_{QCD}$, and so the integral on the left-hand-side

#13 In earlier sections we set the scale equal to Q^2. The changes that result from the replacement $Q^2\to(1-x)(1-y)Q^2$ are higher order in α_s and so are irrelevant at very large Q^2. However we are now concerned with how small Q^2 can be made before perturbation theory fails, and for this purpose it is important to use the more physical scale in α_s.

of this equation is ill-defined. This is easily remedied by redefining the running coupling so that

$$\alpha_s(Q^2) = \frac{4\pi}{\beta_0 \log(c + Q^2/\Lambda^2_{QCD})} \tag{122}$$

where c is a constant ($\sim$ 1–3). This is a rather *ad hoc* remedy, but the ratio $Q_{\rm eff}/Q$ that results is fairly insensitive to both c and Q unless Q is very small.

The ratio $Q_{\rm eff}/Q$ is clearly quite sensitive to the x-dependence of the distribution amplitudes, with broader amplitudes giving more emphasis to the region $x, y \sim 1$ and thus lower $Q_{\rm eff}$'s. Assuming the asymptotic dependence $x(1-x)$, one finds that $Q_{\rm eff}/Q \approx 0.2$. In this case a form factor with momentum transfer of say 2 Gev actually probes QCD at scales of order only 400 MeV. The effective momentum transfer is smaller still with the broader distribution amplitudes suggested by QCD sum rules ($Q_{\rm eff}/Q \approx 0.1$). The running coupling constant is of order unity for such small $Q_{\rm eff}$'s and so perturbation theory is not likely to converge very well, if at all. Some perturbative properties, such as the dimensional-counting and helicity-conservation rules, are valid to all orders in perturbation theory; these might well be applicable even for such $Q_{\rm eff}$'s. However it should not be surprising if predictions for things like the magnitude of the form factor are off by factors of 2 or more. (Note, for example, that replacing $\alpha_s(Q^2)$ by $\alpha_s(Q^2_{\rm eff})$ more than doubles the perturbative prediction for the form factor at $Q = 2$ GeV.)

It has proven difficult to measure meson form factors for Q's much above a couple of GeV. However the proton form factor has been measured out beyond 5 Gev. Unfortunately the hard-scattering amplitudes for baryon form factors tend to be more singular in the low-momentum region than meson amplitudes resulting in smaller ratios of $Q_{\rm eff}/Q$: *e.g.* one finds that $Q_{\rm eff}/Q \approx 0.1$ for the asymptotic distribution amplitude $x_1x_2x_3$, and the ratio is smaller by another factor of a half to a third for the broader distribution amplitudes predicted by sum rules. So existing data for the proton form factor, although more accurate, still probes much the same region in effective momentum as does the data for the pion form factor.

The ratio $Q_{\rm eff}/Q$ is also relevant to the second important issue—the relative importance of nonperturbative contributions. We expect the quark-antiquark interaction in T_H to evolve smoothly from nonperturbative to perturbative behavior as $Q_{\rm eff}$ increases, with the crossover occurring around a few hundred MeV. Consequently the pion form factor, for example, could be predominantly perturbative by $Q = 2$ GeV since $Q_{\rm eff}$ is then of order a few hundred MeV. This is despite the fact that perturbative interactions bring in factors of α_s: the coupling $\alpha_s(Q^2_{\rm eff})$

is not particularly small when $Q_{\rm eff}$ is small, and thus it does not suppress such interactions much.[#14] With protons, perturbative behavior might set in at 3 GeV or higher, depending upon the distribution amplitude.

For larger Q's one must also worry about nonperturbative contributions coming from the endpoint region, particularly in the case of baryon form factors and scattering amplitudes. Perturbative arguments indicate that such contributions are suppressed by Sudakov form factors, but the extent of this suppression at accessible Q's is uncertain. The importance of this region also depends sensitively upon the behavior of the hadronic wavefunctions in the endpoint region: it is easy to make model wavefunctions in which there is little contribution from the endpoint region for Q's greater than a few GeV;[25,26,27] it is also easy to make models in which the region is important even at several GeV (ignoring Sudakov effects).[24] The situation is further complicated in the case of hadronic scattering amplitudes by our incomplete understanding of the Sudakov suppression of pinch singularities.

In the light of these uncertainties the best one can do is to assume the validity of the perturbative analysis, at least as a qualitative or semi-quantitative guide to large-$p_\perp$ exclusive processes. This model is quite plausibly correct, and in any case there is currently no other comprehensive theory of these processes. The validity of the perturbative model can then be judged by the extent to which it is capable of accounting for the broad range of available data.

#14 Of course perturbation theory will not converge well if α_s is large. When we speak of "perturbative behavior" here we are again thinking of behavior that is true to all orders—factorization, dimensional counting, helicity conservation.... It is important to realize that the validity of the factorized form for a large momentum transfer amplitude is not necessarily contingent on the applicability of perturbation theory. Indeed there is likely to be a region of momentum transfer where factorization, dimensional counting... are valid but where perturbation theory does not converge at all.

5. APPLICATIONS OF QCD TO THE PHENOMENOLOGY OF EXCLUSIVE REACTIONS

In the following sections we will discuss the phenomenology of exclusive reactions as tests of QCD and the structure of hadrons. The primary processes of interest are those in which all final particles are measured at large invariant masses compared to each other: *i.e.* large momentum transfer exclusive reactions. This includes form factors of hadrons and nuclei at large momentum transfer Q and large angle scattering reactions. Specific examples are reactions such as $e^-p \to e^-p$, $e^+e^- \to p\bar{p}$ which determine the proton form factor, two-body scattering reactions at large angles and energies such as $\pi^+p \to \pi^+p$ and $pp \to pp$, two-photon annihilation processes such as $\gamma\gamma \to K^+K^-$ or $\bar{p}p \to \gamma\gamma$, exclusive nuclear processes such as deuteron photo-disintegration $\gamma d \to np$, and exclusive decays such as $\pi^+ \to \mu^+\nu$ or $J/\psi \to \pi^+\pi^-\pi^0$. In this section we will summarize the main features of the QCD predictions developed in the previous sections.

QCD has two essential properties which make calculations of processes at short distance or high-momentum transfer tractable and systematic. The critical feature is asymptotic freedom: the effective coupling constant $\alpha_s(Q^2)$ which controls the interactions of quarks and gluons at momentum transfer Q^2 vanishes logarithmically at large Q^2 since it allows perturbative expansions in $\alpha_s(Q^2)$. Complementary to asymptotic freedom is the existence of *factorization theorems* for both exclusive and inclusive processes at large momentum transfer. In the case of "hard" exclusive processes (in which the kinematics of all the final state hadrons are fixed at large invariant mass), the hadronic amplitude can be represented as the product of a process-dependent hard-scattering amplitude $T_H(x_i, Q)$ for the scattering of the constituent quarks convoluted with a process-independent *distribution amplitude* $\phi(x, Q)$ for each incoming or outgoing hadron.[2] When Q^2 is large, T_H is computable in perturbation theory as is the Q-dependence of $\phi(x, Q)$. We have discussed the development of factorization for exclusive processes in detail in Section 4.

Quantum chromodynamics[1] has now been extensively tested in high momentum transfer inclusive reactions where the factorization theorems, perturbation theory, and jet evolution algorithms provide semi-quantitative predictions. Tests of the confining nonperturbative aspects of the theory are, however, either qualitative or at best indirect. In fact QCD is a theory of relatively low mass scales ($\Lambda_{\overline{MS}} \sim 200 \pm 100$ MeV, $< k_\perp^2 >^{1/2} \sim 300$ MeV), and eventually its most critical test as a viable theory of strong and nuclear interactions will involve relatively low energies and momentum transfer at the interface of the perturbative and nonperturbative domain.

The understanding of hadronization and the computation of hadron matrix elements clearly requires knowledge of the hadron wavefunctions. In Table I we give a summary of the main scaling laws and properties of large momentum transfer exclusive and inclusive cross sections which are derivable starting from the light-cone Fock space basis and the perturbative expansion for QCD.

As we have discussed in Section 3, a convenient relativistic description of hadron wavefunctions is given by the set of n-body momentum space amplitudes, $\psi_n(x_i, k_{\perp_i}, \lambda_i)$, $i = 1, 2, ...n$, defined on the free quark and gluon Fock basis at equal "light-cone time" $\tau = t + z/c$ in the physical "light-cone" gauge $A^+ \equiv A^0 + A^3 = 0$. (Here $x_i = k_i^+/p^+$, $\sum_i x_i = 1$, is the light-cone momentum fraction of quark or gluon i in the n — particle Fock state; $k_{\perp_i}$, with $\sum_i k_{\perp_i} = 0$, is its transverse momentum relative to the total momentum p^μ; and λ_i is its helicity.) The quark and gluon structure functions $G_{q/H}(x, Q)$ and $G_{g/H}(x, Q)$ which control hard inclusive reactions and the hadron distribution amplitudes $\phi_H(x, Q)$ which control hard exclusive reactions are simply related to these wavefunctions:

$$G_{q/H}(x, Q) \propto \sum_n \int^Q \Pi d^2 k_{\perp_i} \int \Pi dx_i \, |\psi_n(x_i, k_{\perp_i})|^2 \delta(x_q - x) \quad ,$$

and

$$\phi_H(x_i, Q) \propto \int^Q \Pi d^2 k_{\perp_i} \, \psi_{\text{valence}}(x_i, k_{\perp_i}) \quad .$$

In the case of inclusive reactions, such as deep inelastic lepton scattering, two basic aspects of QCD are relevant: (1) the scale invariance of the underlying lepton-quark subprocess cross section, and (2) the form and evolution of the structure functions. A structure function is a sum of squares of the light-cone wavefunctions. The logarithmic evolution of $G_q(x, Q^2)$ is controlled by the wavefunctions which fall off as $|\psi(x, \vec{k}_\perp)|^2 \sim \alpha_s(k_\perp^2)/k_\perp^2$ at large $k_\perp^2$. This form is a consequence of the pointlike $q \to qg$, $g \to gg$, and $g \to q\bar{q}$ splittings. By taking the logarithmic derivative of G with respect to Q one derives the evolution equations of the structure function. All of the hadron's Fock states generally participate; the necessity for taking into account the (non-valence) higher-particle Fock states in the proton is apparent from two facts: (1) the proton's large gluon momentum fraction and (2) the recent results from the EMC collaboration[28] suggesting that, on the average, little of the proton's helicity is carried by the light quarks.[29]

Table I

Table I Comparison of Exclusive and Inclusive Cross Sections

Exclusive Amplitudes	Inclusive Cross Sections
$\mathcal{M} \sim \Pi\, \phi(x_i, Q) \otimes T_H(x_i, Q)$	$d\sigma \sim \Pi\, G(x_a, Q) \otimes d\hat{\sigma}(x_a, Q)$
$\phi(x,Q) = \int^Q [d^2k_\perp]\, \psi^Q_{\rm val}(x, k_\perp)$	$G(x,Q) = \sum_n \int^Q [d^2k_\perp]\,[dx]'\, \lvert\psi^Q_n(x,k_\perp)\rvert^2$
Measure ϕ in $\gamma \to M\overline{M}$	Measure G in $\ell p \to \ell X$
$\sum_{i\in H} \lambda_i = \lambda_H$	$\sum_{i\in H} \lambda_i \neq \lambda_H$
Evolution	
$\dfrac{\partial \phi(x,Q)}{\partial \log Q^2} = \alpha_s \int [dy]\; V(x,y)\, \phi(y)$	$\dfrac{\partial G(x,Q)}{\partial \log Q^2} = \alpha_s \int dy\; P(x/y)\, G(y)\,.$
$\lim_{Q\to\infty} \phi(x,Q) = \prod_i x_i \cdot C_{\rm flavor}$	$\lim_{Q\to\infty} G(x,Q) = \delta(x)\, C$
Power Law Behavior	
$\dfrac{d\sigma}{dx}(A+B \to C+D) \cong \dfrac{1}{s^{n-2}}\, f(\theta_{c.m.})$	$\dfrac{d\sigma}{d^2p/E}(AB \to CX) \cong \sum \dfrac{(1-x_T)^{2n_s-1}}{(Q^2)^{n_{act}-2}}\, f(\theta_{c.m.})$
$n = n_A + n_B + n_C + n_D$	$n_{act} = n_a + n_b + n_c + n_d$
T_H : expansion in $\alpha_s(Q^2)$	$d\hat{\sigma}$: expansion in $\alpha_s(Q^2)$
Complications	
End point singularities	Multiple scales
Pinch singularities	Phase-space limits on evolution
High Fock states	Heavy quark thresholds
	Higher twist multiparticle processes
	Initial and final state interactions

In the case of exclusive electroproduction reactions such as the baryon form factor, again two basic aspects of QCD are relevant: (1) the scaling of the underlying hard scattering amplitude (such as $l + qqq \to l + qqq$), and (2) the form and evolution of the hadron distribution amplitudes. The distribution amplitude is defined as an integral over the lowest (valence) light-cone Fock state. The logarithmic variation of $\phi(x, Q^2)$ is derived from the integration at large $k_\perp$, *i.e.* wavefunctions which behave as $\psi(x, \vec{k}_\perp) \sim \alpha_s(k_\perp^2)/k_\perp^2$ at large $k_\perp^2$ This behavior follows from the simple one-gluon exchange contribution to the tail of the valence wavefunction. By taking the logarithmic derivative, one then obtains the evolution equation for the hadron distribution amplitude.

As we showed in Section 3, the form factor of a hadron at any momentum transfer can be computed exactly in terms of a convolution of initial and final light-cone Fock state wavefunctions.[10] In general, all of the Fock states contribute. In contrast, exclusive reactions with high momentum transfer Q, perturbative QCD predicts that only the lowest particle number (valence) Fock state is required to compute the contribution to the amplitude to leading order in $1/Q$.

For example, in the light-cone Fock expansion the proton is represented as a column vector of states ψ_{qqq}, ψ_{qqqg}, $\psi_{qqq\bar{q}q}$ .... In the light-cone gauge, $A^+ = A^0 + A^3 = 0$, only the minimal "valence" three-quark Fock state needs to be considered at large momentum transfer since any additional quark or gluon forced to absorb large momentum transfer yields a power-law suppressed contribution to the hadronic amplitude. Thus at large Q^2, the baryon form factor can be systematically computed by iterating the equation of motion for its valence Fock state wherever large relative momentum occurs. To leading order the kernel is effectively one-gluon exchange. The sum of the hard gluon exchange contributions can be arranged as the gauge invariant amplitude T_H, the final form factor having the form

$$F_B(Q^2) = \int_0^1 [dy] \int_0^1 [dx]\ \phi_B^\dagger(y_j, Q) T_H(x_i, y_j, Q) \phi_B(x_i, Q) \ .$$

The essential gauge-invariant input for hard exclusive processes is the distribution amplitude $\phi_H(x, Q)$. For example $\phi_\pi(x, Q)$ is the amplitude for finding a quark and antiquark in the pion carrying momentum fractions x and $1 - x$ at impact (transverse space) separations less than $b_\perp < 1/Q$. The distribution amplitude thus plays the role of the "wavefunction at the origin" in analogous non-relativistic calculations of form factors. In the relativistic theory, its dependence on log Q is controlled by evolution equations derivable from perturbation

theory or the operator product expansion. A detailed discussion of the light-cone Fock state wavefunctions and their relation to observables is given in Section 3 and in Ref. 30.

The distribution amplitude contains all of the bound-state dynamics and specifies the momentum distribution of the quarks in the hadron. The hard-scattering amplitude for a given exclusive process can be calculated perturbatively as a function of $\alpha_s(Q^2)$. Similar analyses can be applied to form factors, exclusive photon-photon reactions, and with increasing degrees of complication, to photoproduction, fixed-angle scattering, etc. In the case of the simplest processes, $\gamma\gamma \to M\overline{M}$ and the meson form factors, the leading order analysis can be readily extended to all-orders in perturbation theory.

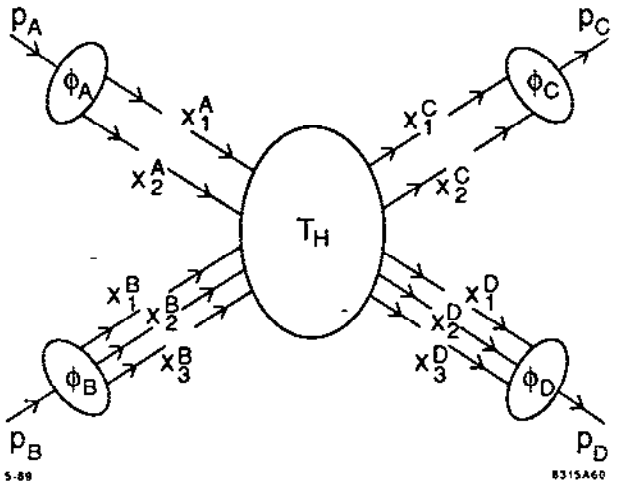

Figure 18. QCD factorization for two-body amplitudes at large momentum transfer.

In the case of exclusive processes such as photo-production, Compton scattering, meson-baryon scattering, etc., the leading hard scattering QCD contribution at large momentum transfer $Q^2 = tu/s$ has the form (helicity labels and suppressed) (see Fig. 18)

$$\mathcal{M}_{A+B\to C+D}(Q^2,\theta_{\rm c.m.}) = \int [dx]\phi_C(x_c,\tilde{Q})\ \phi_D(x_d,\tilde{Q})\ T_H(x_i;Q^2,\theta_{\rm c.m.}) \times \phi_A(x_a,\tilde{Q})\ \phi_B(x_b,\tilde{Q})$$

In general the distribution amplitude is evaluated at the characteristic scale $\tilde{Q}$ set by the effective virtuality of the quark propagators.

By definition, the hard scattering amplitude T_H for a given exclusive process is constructed by replacing each external hadron with its massless, collinear valence partons, each carrying a finite fraction x_i of the hadron's momentum. Thus T_H is the scattering amplitude for the constituents. The essential behavior of the amplitude is determined by T_H, computed where each hadron is replaced by its (collinear) quark constituents. We note that T_H is "collinear irreducible," *i.e.* the transverse momentum integrations of all reducible loop integration are restricted to $k_\perp^2 > \mathcal{O}(Q^2)$ since the small $k_\perp$ region is already contained in ϕ. If the internal propagators in T_H are all far-off-shell $\mathcal{O}(Q^2)$, then a perturbative expansion in $\alpha_s(Q^2)$ can be carried out.

Higher twist corrections to the quark and gluon propagator due to mass terms and intrinsic transverse momenta of a few hundred MeV give nominal corrections of higher order in $1/Q^2$. These finite mass corrections combine with the leading twist results to give a smooth approach to small Q^2. It is thus reasonable that PQCD scaling laws become valid at relatively low momentum transfer of order of a few GeV.

5.1. General Features of Exclusive Processes in QCD

The factorization theorem for large-momentum-transfer exclusive reactions separates the dynamics of hard-scattering quark and gluon amplitudes T_H from process-independent distribution amplitudes $\phi_H(x,Q)$ which isolates all of the bound state dynamics. However, as seen from Table I, even without complete information on the hadronic wave functions, it is still possible to make predictions at large momentum transfer directly from QCD.

Although detailed calculations of the hard-scattering amplitude have not been carried out in all of the hadron-hadron scattering cases, one can abstract some general features of QCD common to all exclusive processes at large momentum transfer:

1. Since the distribution amplitude ϕ_H is the $L_z = 0$ orbital-angular-momentum projection of the hadron wave function, the sum of the interacting constituents' spin along the hadron's momentum equals the hadron spin:[6]

$$\sum_{i \in H} s_i^z = s_H^z.$$

   In contrast, there are any number of non-interacting spectator constituents in inclusive reactions, and the spin of the active quarks or gluons is only statistically related to the hadron spin (except at the edge of phase space $x \to 1$).

2. Since all loop integrations in T_H are of order $\hat{Q}$, the quark and hadron masses can be neglected at large Q^2 up to corrections of order $\sim m/\hat{Q}$. The vector-gluon coupling conserves quark helicity when all masses are neglected–*i.e.* $\overline{u}_\uparrow \gamma^\mu u_\uparrow = 0$. Thus total quark helicity is conserved in T_H. In addition, because of (2), each hadron's helicity is the sum of the helicities of its valence quarks in T_H. We thus have the selection rule

$$\sum_{\text{initial}} \lambda_H - \sum_{\text{final}} \lambda_H = 0,$$

i.e. total hadronic helicity is conserved up to corrections of order m/Q or higher. Only (flavor-singlet) mesons in the 0^{-+} nonet can have a two-gluon valence component and thus even for these states the quark helicity equals the hadronic helicity. Consequently hadronic-helicity conservation applies for all amplitudes involving light meson and baryons.[31] Exclusive reactions which involve hadrons with quarks or gluons in higher orbital angular states are suppressed by powers.

3. The nominal power-law behavior of an exclusive amplitude at fixed $\theta_{c.m.}$ is $(1/Q)^{n-4}$, where n is the number of external elementary particles (quarks, gluons, leptons, photons, ...) in T_H. This dimensional-counting rule[5] is modified by the Q^2 dependence of the factors of $\alpha_s(Q^2)$ in T_H, by the Q^2 evolution of the distribution amplitudes, and possibly by a small power correction associated with the Sudakov suppression of pinch singularities in hadron-hadron scattering.

The dimensional-counting rules for the power-law falloff appear to be experimentally well established for a wide variety of processes.[32,33] The helicity-conservation rule is also one of the most characteristic features of QCD, being a direct consequence of the gluon's spin. A scalar-or tensor-gluon-quark coupling flips the quark's helicity. Thus, for such theories, helicity may or may not be conserved in any given diagram contribution to T_H depending upon the number of interactions involved. Only for a vector theory, such as QCD, can one have a helicity selection rule valid to all orders in perturbation theory.

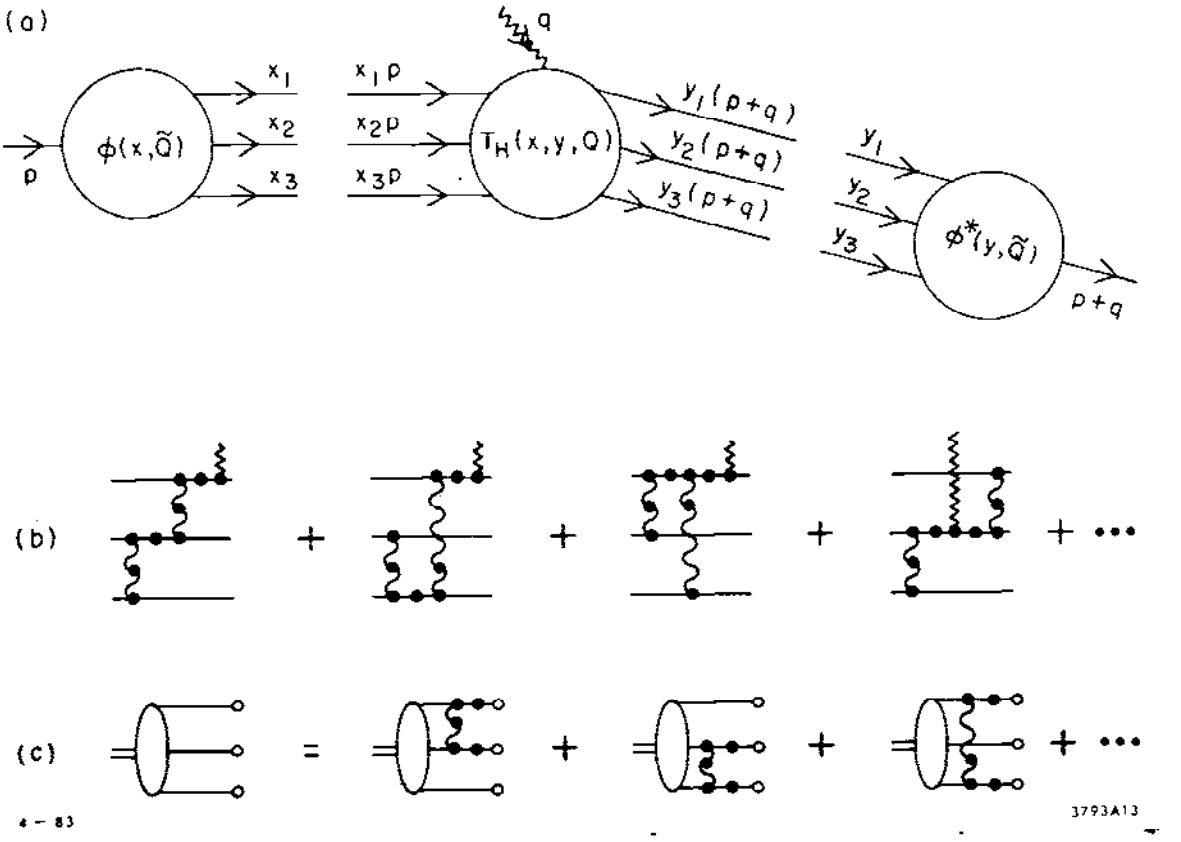

Figure 19. (a) Factorization of the nucleon form factor at large Q^2 in QCD. (b) The leading order diagrams for the hard scattering amplitude T_H. The dots indicate insertions which enter the renormalization of the coupling constant. (c) The leading order diagrams which determine the Q^2 dependence of the distribution amplitude $\phi(x,Q)$.

5.2. Electromagnetic Form Factors

Any helicity conserving baryon form factor at large Q^2 has the form: [see Fig. 19(a)]

$$F_B(Q^2) = \int_0^1 [dy] \int_0^1 [dx]\ \phi_B^\dagger(y_j,Q) T_H(x_i,y_j,Q) \phi_B(x_i,Q) \quad ,$$

where to leading order in $\alpha_s(Q^2)$, T_H is computed from $3q + \gamma^* \to 3q$ tree graph amplitudes: [Fig. 19(b).]

$$T_H = \left[\frac{\alpha_s(Q^2)}{Q^2}\right]^2 f(x_i,y_j)$$

and

$$\phi_B(x_i, Q) = \int [d^2k_\perp]\, \psi_V(x_i, \vec{k}_{\perp i})\theta(k_{\perp i}^2 < Q^2)$$

is the valence three-quark wavefunction [Fig. 19(c)] evaluated at quark impact separation $b_\perp \sim \mathcal{O}(Q^{-1})$. More detailed formulae for the baryon form factor are presented in Appendix I. Since ϕ_B only depends logarithmically on Q^2 in QCD, the main dynamical dependence of $F_B(Q^2)$ is the power behavior $(Q^2)^{-2}$ derived from scaling of the elementary propagators in T_H. More explicitly, the proton's magnetic form factor has the form:[4]

$$G_M(Q^2) = \left[\frac{\alpha_s(Q^2)}{Q^2}\right]^2 \sum_{n,m} a_{nm} \left(\log \frac{Q^2}{\Lambda^2}\right)^{-\gamma_n - \gamma_m}$$

$$\times \left[1 + \mathcal{O}(\alpha_s(Q)) + \mathcal{O}\left(\frac{1}{Q}\right)\right].$$

The first factor, in agreement with the quark counting rule, is due to the hard scattering of the three valence quarks from the initial to final nucleon direction. Higher Fock states lead to form factor contributions of successively higher order in $1/Q^2$. The logarithmic corrections derive from an evolution equation for the nucleon distribution amplitude. The γ_n are the computed anomalous dimensions, reflecting the short distance scaling of three-quark composite operators.[12] The results hold for any baryon to baryon vector or axial vector transition amplitude that conserves the baryon helicity. Helicity non-conserving form factors should fall as an additional power of $1/Q^2$.[6] Measurements[34] of the transition form factor to the $J = 3/2$ $N(1520)$ nucleon resonance are consistent with $J_z = \pm 1/2$ dominance, as predicted by the helicity conservation rule.[6] A review of the data on spin effects in electron nucleon scattering in the resonance region is given in Ref. 34. It is important to explicitly verify that $F_2(Q^2)/F_1(Q^2)$ decreases at large Q^2. The angular distribution decay of the $J/\psi \to p\overline{p}$ is consistent with the QCD prediction $\lambda_p + \lambda_{\overline{p}} = 0$.

Thus, modulo logarithmic factors, one obtains a dimensional counting rule for any hadronic or nuclear form factor at large Q^2 ($\lambda = \lambda' = 0$ or $1/2$)

$$F(Q^2) \sim \left(\frac{1}{Q^2}\right)^{n-1},$$

$$F_1^N \sim \frac{1}{Q^4}, \quad F_\pi \sim \frac{1}{Q^2}, \quad F_d \sim \frac{1}{Q^{10}},$$

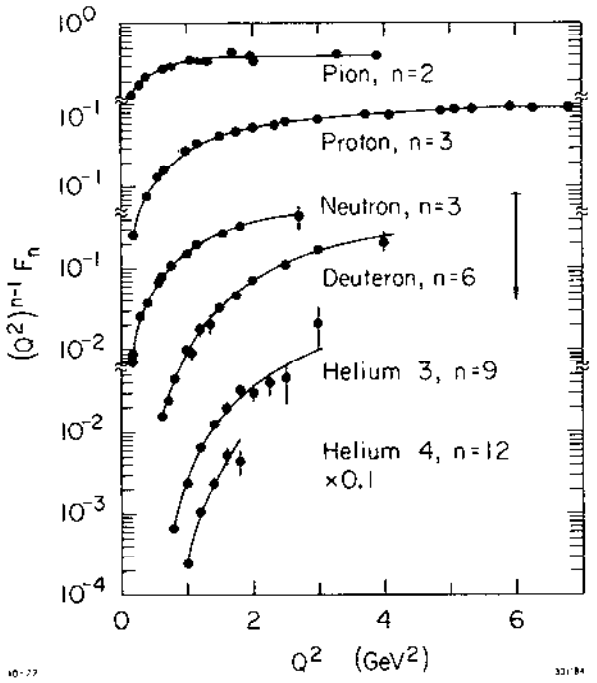

Figure 20. Comparison of experiment[35] with the QCD dimensional counting rule $(Q^2)^{n-1}F(Q^2) \sim const$ for form factors. The proton data extends beyond 30 GeV^2.

where n is the minimum number of fields in the hadron. Since quark helicity is conserved in T_H and $\phi(x_i, Q)$ is the $L_z = 0$ projection of the wavefunction, total hadronic helicity is conserved at large momentum transfer for any QCD exclusive reaction. The dominant nucleon form factor thus corresponds to $F_1(Q^2)$ or $G_M(Q^2)$; the Pauli form factor $F_2(Q^2)$ is suppressed by an extra power of Q^2. Similarly, in the case of the deuteron, the dominant form factor has helicity $\lambda = \lambda' = 0$, corresponding to $\sqrt{A(Q^2)}$.

The comparison of experimental form factors with the predicted nominal power-law behavior is shown in Fig. 20. We will discuss predictions for the normalization of the leading power terms in Section 5.6. As we have discussed in Section 4, the general form of the logarithmic corrections to the leading power contributions form factors can be derived from the operator product expansion at short distance[11,12] or by solving an evolution equation[4] for the distribution amplitude computed from gluon exchange [Fig. 19(c)], the only QCD contribution which falls sufficiently small at large transverse momentum to effect the large Q^2 dependence.

The comparison of the proton form factor data with the QCD prediction arbitrarily normalized is shown in Fig. 21. The fall-off of $(Q^2)^2 G_M(Q^2)$ with Q^2

is consistent with the logarithmic fall-off of the square of QCD running coupling constant. As we shall discuss below, the QCD sum rule[16] model form for the nucleon distribution amplitude together with the QCD factorization formulae, predicts the correct sign and magnitude as well as scaling behavior of the proton and neutron form factors.[36]

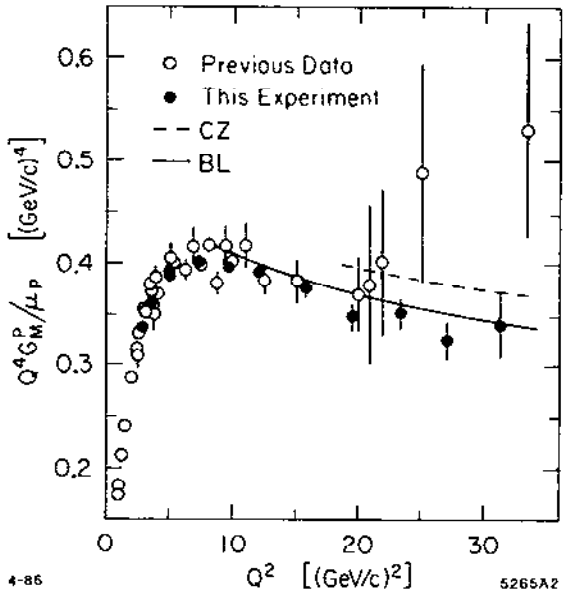

Figure 21. Comparison of the scaling behavior of the proton magnetic form factor with the theoretical predictions of Refs. 4 and 16. The CZ predictions[16] are normalized in sign and magnitude. The data are from Ref. 36.

5.3. Comparison of QCD Scaling with Experiment

Phenomenologically the dimensional counting power laws appear consistent with measurements of form factors, photon-induced amplitudes, and elastic hadron-hadron scattering at large angles and momentum transfer.[33] The successes of the quark counting rules can be taken as strong evidence for QCD since the derivation of the counting rules require scale invariant tree graphs, soft corrections from higher loop corrections to the hard scattering amplitude, and strong suppression of pinch singularities. QCD is the only field theory of spin $\frac{1}{2}$ fields that has all of these properties.

As shown in Fig. 22, the data for $\gamma p \to \pi^+ n$ cross section at $\theta_{CM} = \pi/2$ are consistent with the normalization and scaling $d\sigma/dt\ (\gamma p \to \pi^+ n) \simeq [1\,\mathrm{nb}/(s/10\ \mathrm{GeV})^7]\ f(t/s)$.

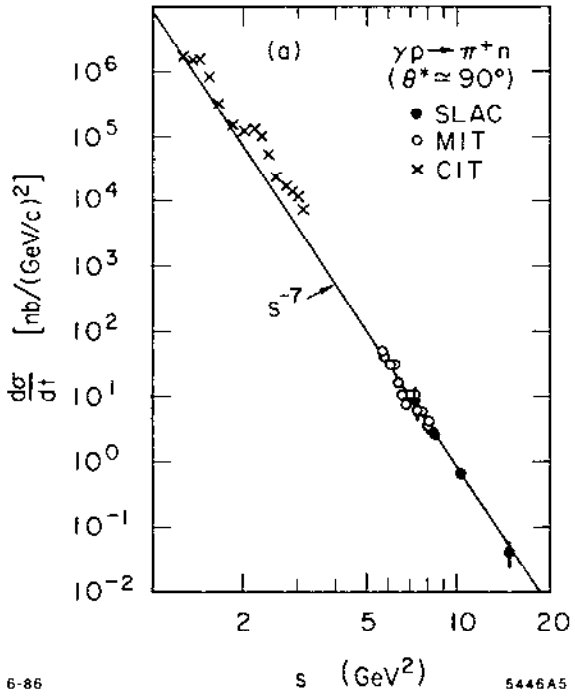

Figure 22. Comparison of photoproduction data with the dimensional counting power-law prediction. The data are summarized in Ref. 37.

The check of fixed angle scaling in proton-proton elastic scattering is shown in Figs. 23. Extensive measurements of the $pp \to pp$ cross section have been made at ANL, BNL and other laboratories. The scaling law $s^{10} d\sigma/dt(pp \to pp) \simeq const.$ predicted by QCD seems to work quite well over a large range of energy and angle. The best fit gives the power $N = 9.7 \pm 0.5$ compared to the dimensional counting prediction N=10. There are, however, measurable deviations from fixed power dependence which are not readily apparent on the log-log plot. As emphasized by Hendry[38] the $s^{10} d\sigma/dt$ cross section exhibits oscillatory behavior with p_T (see Section 9). Even more serious is the fact that polarization measurements[40] show significant spin-spin correlations (A_{NN}), and the single spin asymmetry (A_N) is not consistent with predictions based on hadron helicity conservation (see Section 6) which is expected to be valid for the leading power behavior.[6] Recent discussions of these effects have been given by Farrar[41] and Lipkin.[42] We discuss a new explanation of all of these effects in Section 9.

As emphasized by Landshoff, the ISR data for high energy elastic pp scattering at small $|t|/s$ can be parameterized in the form $d\sigma/dt \sim const/t^8$ for $2\ GeV^2 < |t| < 10\ GeV^2$. This suggests a role for triple gluon exchange pinch contributions at large energies where multiple vector exchange diagrams could

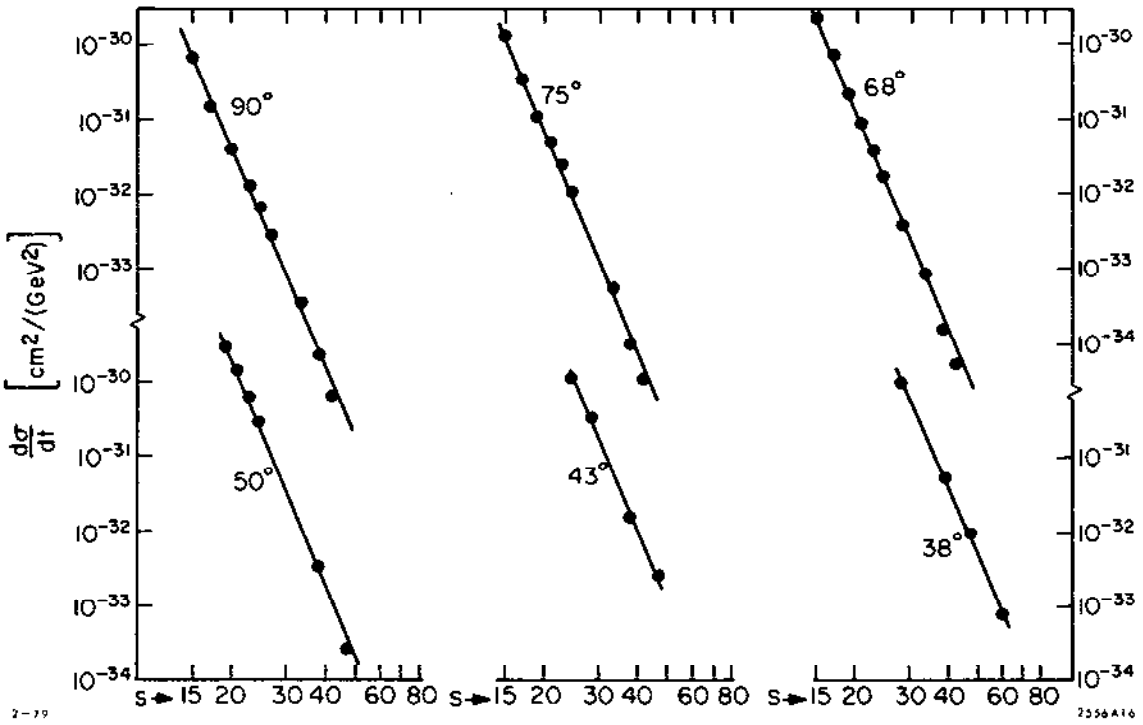

Figure 23. Test of fixed θ_{CM} scaling for elastic *pp* scattering. The data compilation is from Landshoff and Polkinghorne.

dominate. However, from Mueller's analysis[21] one expects stronger fall-off in t due to the Sudakov form factor suppression. This paradox implies that the role of the pinch singularity in large momentum transfer exclusive reactions is not well understood and deserve further attention.[43] As discussed in Section 4.5, pinch singularities are also expected to modify the dimensional counting scaling laws for wide-angle scattering, but the change in the exponent of s is small and hard to detect experimentally. However, Ralston and Pire[43] have suggested that the oscillatory behavior in the wide-angle *pp* scattering amplitude results from interference between the pinch contributions and the ordinary hard-scattering contributions to the *pp* amplitude. Thus *pp* scattering may provide a experimental handle on pinch contribution. However it is possible that the oscillations are specific to particular channels, in which case an alternative explanation is necessary. We discuss this further in Section 9. Pinch singularities do not arise in form factors, or such photon-induced processes as $\gamma\gamma \to M\overline{M}$,[16] $\gamma^* + \gamma \to M$,[4] $\gamma^* \to M_1 ... M_N$ at fixed angle,[44] $\gamma\gamma \to B\overline{B}$, $\gamma B \to \gamma B$, etc.[45,46]

5.4. Exclusive Anti-Proton Proton Annihilation Processes

Anti-proton annihilation has a number of important advantages as a probe of QCD in the low energy domain. Exclusive reaction in which *complete* annihilation of the valance quarks occur ($\bar{p}p \to \ell\bar{\ell}$, $\gamma\gamma$, $\phi\phi$, etc.) necessarily involve impact distances $b_\perp$ smaller than $1/M_p = 5$ fm^{-1} since baryon number is exchanged in the t-channel. There are a number of exclusive and inclusive $\bar{p}$ reactions which can provide useful constraints on hadron wavefunctions or test novel features of QCD involving both perturbative and nonperturbative dynamics. In several cases ($\bar{p}p \to \bar{\ell}\ell$, $\bar{p}p \to J/\psi$, $\bar{p}p \to \gamma\gamma$), complete leading twist (leading power law) predictions are available. These reactions not only probe the subprocesses $\overline{qqq}\ qqq \to \gamma\gamma$, etc., but they also are sensitive to the normalization and shape of the proton distribution amplitude $\phi_p(x_i, x_2, x_3; Q)$, the basic measure of the proton's three-quark valance wavefunction.

The fixed angle scaling laws for the $\bar{p}p$ channels are:

$$\frac{d\sigma}{d\Omega}\,(\bar{p}p \to e^+e^-) \simeq \frac{\alpha^2}{(p_T^2)^5}\ f^{e^+e^-}(\cos\theta, \ell n p_T)$$

$$\frac{d\sigma}{d\Omega}\,(\bar{p}p \to \gamma\gamma) \simeq \frac{\alpha^2}{(p_T^2)^5}\ f^{\gamma\gamma}(\cos\theta, \ell n p_T)$$

$$\frac{d\sigma}{d\Omega}\,(\bar{p}p \to \gamma M) \simeq \frac{\alpha^2}{(p_T^2)^6}\ f^{\gamma M}(\cos\theta, \ell n p_T)$$

$$\frac{d\sigma}{d\Omega}\,(p\bar{p} \to M\overline{M}) \simeq \frac{1}{(p_T^2)^7}\ f^{M\overline{M}}(\cos\theta, \ell n p_T)$$

$$\frac{d\sigma}{d\Omega}\,(p\bar{p} \to B\overline{B}) \simeq \frac{1}{(p_T^2)^9}\ f^{B\overline{B}}(\cos\theta, \ell n p_T) \quad .$$

The angular dependence reflects the structure of the hard-scattering perturbative T_H amplitude, which in turn follows from the flavor pattern of the contributing duality diagrams.

It is important to note that the leading power-law behavior originates in the minimum three-particle Fock state of the $\bar{p}$ and p, at least in physical gauge, such as $A^+ = 0$. Higher Fock states give contributions higher order in $1/s$. For $\bar{p}p \to \ell\bar{\ell}$ this means that initial-state interaction such as one gluon exchange are dynamically suppressed (see Fig. 24). Soft-gluon exchange is suppressed since the incident p or $\bar{p}$ color neutral wavefunction in the three-parton state with impact

operation $b_\perp \sim 0(1/\sqrt{s})$. Hard-gluon exchange is suppressed by powers of $\alpha_s(s)$. The absence of a soft initial-state interaction in these reactions is a remarkable consequence of gauge theory, and is quite contrary to normal treatments of initial interactions based on Glauber theory.

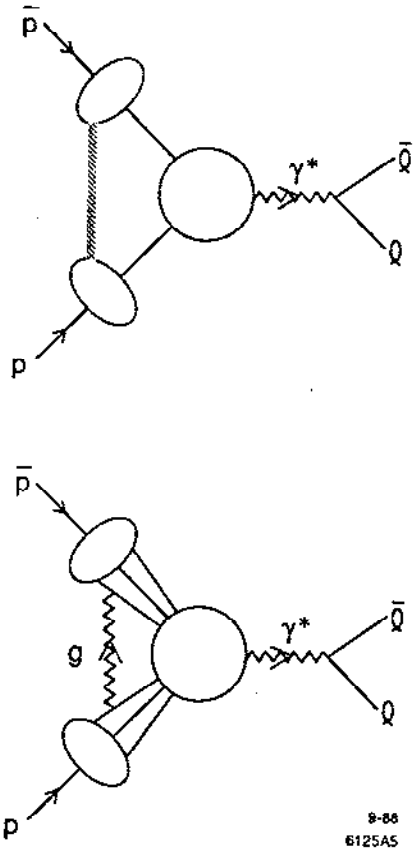

Figure 24. Analysis of initial-state interactions in PQCD.

We will discuss in Section 8.1 another class of exclusive reactions in QCD involving light nuclei, such as $\bar{p}d \to \gamma n$ and $\bar{p}d \to \pi^- p$ which can probe quark and gluon degrees of freedom of the nucleus at surprisingly low energy. We will also discuss the "color transparency" of nuclei in quasi-elastic processes like $\bar{p}A \to \ell\bar{\ell}(A-1)$.

5.5. Additional Tests of Gluon Spin in Exclusive Processes

The spin of the gluon can be tested in a wide variety of exclusive processes:

(a) $\gamma\gamma \to \rho\rho, K^*K^*, \ldots$. These cross sections can be measured using e^+e^- colliding beams. At large energies ($s \gtrsim 2 - 4GeV^2$) and wide angles, the final-state helicities must be equal and opposite. These processes can also be used as a sensitive probe of the structure of the quark distribution amplitudes.[16]

(b) Electroweak form factors of baryons. Relations, valid to all order in α_s, can be found among the various electromagnetic and weak-interaction for factors of the nucleons and other baryons.[47] These relations depend crucially upon quark-helicity conservation and as such test the vector nature of the gluon. Current data for the axial-vector and electromagnetic form factors of the nucleons is in excellent agreement with these QCD predictions, although a definitive test requires higher energies.

(c) $\pi p \to \pi p, pp \to pp, \ldots$. QCD predicts that total hadronic helicity is conserved from the initial state to the final state in all high-energy, wide-angle, elastic, and quasi-elastic hadronic amplitudes. One immediate consequence of this is the suppression of the backward peak relative to the forward peak in scalar-meson- baryon scattering. This follows because angular momentum cannot be conserved along the beam axis if only the baryons carry helicity, helicity is conserved, and the baryons scatter through 180°. Data[32] for πp and Kp scattering is consistent with this observation. However the hard-scattering amplitudes for these processes must be computed before a detailed interpretation of the data is possible.

In the case of $pp \to pp$ scattering, there are in general five independent parity-conserving and time-reversal-invariant amplitudes $\mathcal{M}(++ \to ++), \mathcal{M}(+- \to +-)$, $\mathcal{M}(-+ \to +-), \mathcal{M}(++ \to +-)$, and $\mathcal{M}(-- \to ++)$. Total-hadron-helicity conservation implies that $\mathcal{M}(++ \to +-)$ and $\mathcal{M}(-- \to ++)$ are power-law suppressed. The vanishing of the double-flip amplitude implies $A_{NN} = A_{SS}$, and

$$2A_{NN} - A_{LL} = 1 \quad (\theta_{c.m.} = 90^\circ).$$

Here A_{NN} is the spin asymmetry for incident nucleons polarized normal ($\hat{x}$) to the scattering plane. A_{LL} refers to initial spins polarized along the laboratory beam direction ($\hat{z}$) and A_{SS} refers to initial spin polarized (sideways) along y. Data at $p_{\rm lab} = 11.75\ GeV/c$ from Argonne[48] appears to be consistent with this prediction.

(d) Zeros of meson form factors. Asymptotically, the electromagnetic form factors of charged π's, K's, and $\rho(\lambda = 0)$'s have a positive sign in QCD. In a theory

of scalar gluons, these form factors become negative for Q^2 large, and thus must vanish at some finite Q^2 since $F(Q^2 = 0) = 1$ by definition. Consequently the absence of zeros in $F_\pi(Q^2)$ is further evidence for a vector gluon. We discuss this in detail in the next section.

5.6. Hadronic Wavefunction Phenomenology

Let us now return to the question of the normalization of exclusive amplitudes in QCD. It should be emphasized that because of the uncertain magnitude of corrections of higher order in $\alpha_s(Q^2)$, comparisons with the normalization of experiment with model predictions could be misleading. Nevertheless, it this section we shall assume that the leading order normalization is at least approximately accurate. If the higher order corrections are indeed small, then the normalization of the proton form factor at large Q^2 is a non-trivial test of the distribution amplitude shape; for example, if the proton wave function has a non-relativistic shape peaked at $x_i \sim 1/3$ then one obtains the wrong sign for the nucleon form factor. Furthermore symmetrical distribution amplitudes predict a very small magnitude for $Q^4 G_M^p(Q^2)$ at large Q^2.

The phenomenology of hadron wavefunctions in QCD is now just beginning. Constraints on the baryon and meson distribution amplitudes have been recently obtained using QCD sum rules and lattice gauge theory. The results are expressed in terms of gauge-invariant moments $< x_j^m >= \int \Pi dx_i \, x_j^m \, \phi(x_i, \mu)$ of the hadron's distribution amplitude. A particularly important challenge is the construction of the baryon distribution amplitude.In the case of the proton form factor, the constants a_{nm} in the QCD prediction for G_M must be computed from moments of the nucleon's distribution amplitude $\phi(x_i, Q)$. There are now extensive theoretical efforts to compute this nonperturbative input directly from QCD. The QCD sum rule analysis of Chernyak *et al.*[16,49] provides constraints on the first 12 moments of $\phi(x, Q)$. Using as a basis the polynomials which are eigenstates of the nucleon evolution equation, one gets a model representation of the nucleon distribution amplitude, as well as its evolution with the momentum transfer scale. The moments of the proton distribution amplitude computed by Chernyak *et al.*, have now been confirmed in an independent analysis by Sachrajda and King.[50]

A three-dimensional "snapshot" of the proton's *uud* wavefunction at equal light-cone time as deduced from QCD sum rules at $\mu \sim 1$ GeV by Chernyak *et al.*[49] and King and Sachrajda[50] is shown in Fig. 25. The QCD sum rule analysis predicts a surprising feature: strong flavor asymmetry in the nucleon's momentum distribution. The computed moments of the distribution amplitude imply that 65% of the proton's momentum in its 3-quark valence state is carried by the u-quark which has the same helicity as the parent hadron.

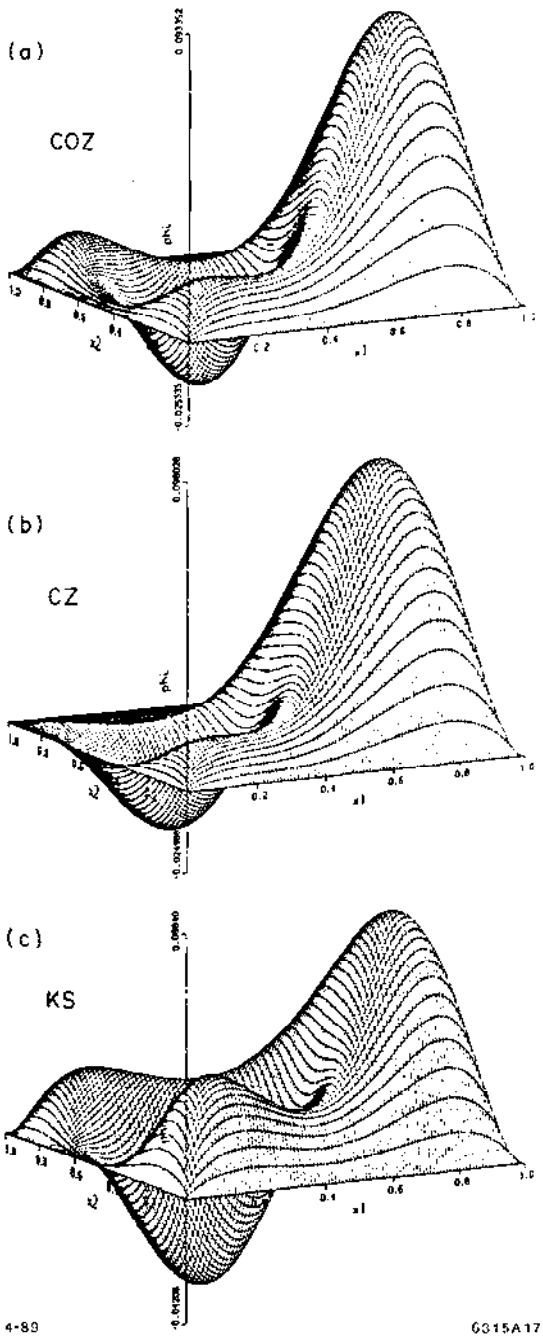

Figure 25. The proton distribution amplitude $\phi_p(x_i, \mu)$ determined at the scale $\mu \sim 1$ GeV from QCD sum rules.

Dziembowski and Mankiewicz[27] have recently shown that the asymmetric form of the CZ distribution amplitude can result from a rotationally-invariant CM wave function transformed to the light cone using free quark dynamics. They find that one can simultaneously fit low energy phenomena (charge radii, magnetic

moments, etc.), the measured high momentum transfer hadron form factors, and the CZ distribution amplitudes with a self-consistent ansatz for the quark wave functions. Thus for the first time one has a somewhat complete model for the relativistic three-quark structure of the hadrons. In the model the transverse size of the valence wave function is not found to be significantly smaller than the mean radius of the proton–averaged over all Fock states as argued in Ref. 51. Dziembowski *et al.* also find that the perturbative QCD contribution to the form factors in their model dominates over the soft contribution (obtained by convoluting the non-perturbative wave functions) at a scale $Q/N \approx 1$ GeV, where N is the number of valence constituents. (This criterion was also derived in Ref. 52.)

Gari and Stefanis[53] have developed a model for the nucleon form factors which incorporates the CZ distribution amplitude predictions at high Q^2 together with VMD constraints at low Q^2. Their analysis predicts sizeable values for the neutron electric form factor at intermediate values of Q^2.

A detailed phenomenological analysis of the nucleon form factors for different shapes of the distribution amplitudes has been given by Ji, Sill, and Lombard-Nelsen.[54] Their results show that the CZ wave function is consistent with the sign and magnitude of the proton form factor at large Q^2 as recently measured by the American University/SLAC collaboration[36] (see Fig. 26).

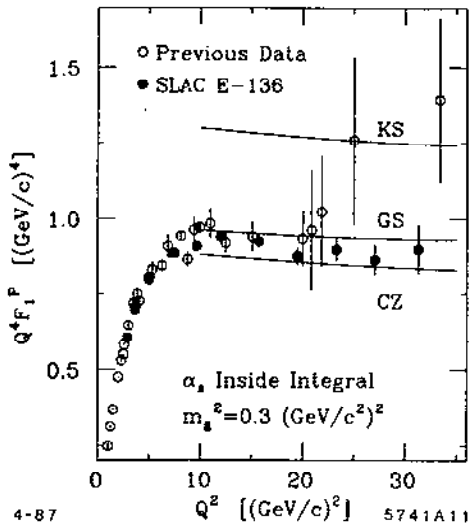

Figure 26. Predictions for the normalization and sign of the proton form factor at high Q^2 using perturbative QCD factorization and QCD sum rule predictions for the proton distribution amplitude (from Ref. 54.) The predictions use forms given by Chernyak and Zhitnitsky, King and Sachrajda,[50] and Gari and Stefanis.[53]

It should be stressed that the magnitude of the proton form factor is sensitive to the $x \sim 1$ dependence of the proton distribution amplitude, where non-perturbative effects could be important.[55] The asymmetry of the distribution amplitude emphasizes contributions from the large x region. Since non-leading corrections are expected when the quark propagator scale $Q^2(1-x)$ is small, in principle relatively large momentum transfer is required to clearly test the perturbative QCD predictions. Chernyak *et al.*[49] have studied this effect in some detail and claim that their QCD sum rule predictions are not significantly changed when higher moments of the distribution amplitude are included.

The moments of distribution amplitudes can also be computed using lattice gauge theory.[14] In the case of the pion distribution amplitudes, there is good agreement of the lattice gauge theory computations of Martinelli and Sachrajda[15] with the QCD sum rule results. This check has strengthened confidence in the reliability of the QCD sum rule method, although the shape of the meson distribution amplitudes are unexpectedly structured: the pion distribution amplitude is broad and has a dip at $x = 1/2$. The QCD sum rule meson distributions, combined with the perturbative QCD factorization predictions, account well for the scaling, normalization of the pion form factor and $\gamma\gamma \to M^+M^-$ cross sections.

In the case of the baryon, the asymmetric three-quark distributions are consistent with the normalization of the baryon form factor at large Q^2 and also the branching ratio for $J/\psi \to p\bar{p}$. The data for large angle Compton scattering $\gamma p \to \gamma p$ are also well described.[56] However, a very recent lattice calculation of the lowest two moments by Martinelli and Sachrajda[15] does not show skewing of the average fraction of momentum of the valence quarks in the proton. This lattice result is in contradiction to the predictions of the QCD sum rules and does cast some doubt on the validity of the model of the proton distribution proposed by Chernyak *et al.*[49] The lattice calculation is performed in the quenched approximation with Wilson fermions and requires an extrapolation to the chiral limit.

The contribution of soft momentum exchange to the hadron form factors is a potentially serious complication when one uses the QCD sum rule model distribution amplitudes. In the analysis of Ref. 24 it was argued that only about 1% of the proton form factor comes from regions of integration in which all the propagators are hard. A new analysis by Dziembowski *et al.*[57] shows that the QCD sum rule[16] distribution amplitudes of Chernyak *et al.*[16] together with the perturbative QCD prediction gives contributions to the form factors which agree with the measured normalization of the pion form factor at $Q^2 >$

4 GeV^2 and proton form factor $Q^2 > 20\ GeV^2$ to within a factor of two. In the calculation the virtuality of the exchanged gluon is restricted to $|k^2| > 0.25\ GeV^2$. The authors assume $\alpha_s = 0.3$ and that the underlying wavefunctions fall off exponentially at the $x \simeq 1$ endpoints. Another model of the proton distribution amplitude with diquark clustering[58] chosen to satisfy the QCD sum rule moments come even closer. Considering the uncertainty in the magnitude of the higher order corrections, one really cannot expect better agreement between the QCD predictions and experiment.

The relative importance of non-perturbative contributions to form factors is also an issue. Unfortunately, there is little that can be said until we have a deeper understanding of the end-point behavior of hadronic wavefunctions, and of the role played by Sudakov form factors in the end-point region. Models have been constructed in which non-perturbative effects persist to high Q.[24] Other models have been constructed in which such effects vanish rapidly as Q increases.[25,26,27]

If the QCD sum rule results are correct then, the light hadrons are highly structured oscillating momentum-space valence wavefunctions. In the case of mesons, the results from both the lattice calculations and QCD sum rules show that the light quarks are highly relativistic. This gives further indication that while nonrelativistic potential models are useful for enumerating the spectrum of hadrons (because they express the relevant degrees of freedom), they may not be reliable in predicting wave function structure.

5.7. Calculating T_H

The calculation of hard-scattering diagrams for exclusive processes in QCD becomes increasingly arduous as the number of incident and final parton lines increases. The tree-graph calculations of T_H have been completed for the meson and baryon form factors, as well as for many exclusive two-photon processes such as $\gamma\gamma \to p\bar{p}$ for both real and virtual photons and various Compton scattering reactions. Further discussion of the two-photon predictions is given in Section 7.

The most efficient computational methods involve two-component spinor techniques where the amplitude itself can be converted to a trace. This method was first used by Bjorken and Chen[59] for their calculation of the QED "trident" amplitudes for $\mu Z \to \mu\mu\mu$. It was further developed by the CALKUL group and applied to exclusive processes by Farrar[60] and Gunion[61] and their co-workers.

The large number of PQCD tree graph (300,000 for pp scattering) may help to explain the relatively large normalization of the pp amplitude at large momentum transfer. For example the nominal one-gluon exchange amplitude $4\pi C_F(s/t)\alpha_s(t)[F_1^p(t)]^2$ gives a contribution only about 10^{-3} of that required by

the large angle pp scattering data. It is clearly necessary to develop highly efficient and automatic methods for evaluating multi-particle hard scattering amplitudes T_H for reactions such as pp scattering. The light-cone quantization method could prove highly effective. In this method one expands the S-matrix in the τ-ordered perturbation theory. For numerical computations one can use a discrete basis, such that in each intermediate state one sums over a complete set of discretized Fock states, defined using periodic or anti-periodic boundary conditions. The matrix elements of the light-cone Hamiltonian $H_{QCD}^{interaction}$ are simple to compute. In the expansion all Feynman diagrams and all time-orderings are automatically summed.

In principle the perturbative QCD predictions can be calculated systematically in powers of $\alpha_s(Q^2)$. In practice the calculations are formidable, and thus far only the next-to-leading correction to the pion form factor and the $\gamma\gamma \to \pi\pi$ amplitude have been systematically studied. The two-photon amplitude analysis is given by Nizic[62] and is discussed further in Section 7. The complete analysis of the meson form factor to this order requires evaluating the one-loop corrections to the hard-scattering amplitude for $\gamma q\bar{q} \to q\bar{q}$, plus a corresponding correction to the kernel for the meson distribution amplitude. The one-loop corrections to T_H for the meson form factor have been evaluated by several groups. Because of different conventions the results differ in detail; however Braaten and Tse[18] have resolved the discrepancies between the three previous calculations. An important feature is the presence of correction terms of order $\frac{\alpha_s}{4\pi}(\frac{11}{3}C_A - \frac{2}{3})\log[(1-x)(1-y)Q^2]$ which sets the scale of the running coupling constant in the leading order contribution at $Q^2_{eff} = (1-x)(1-y)Q^2$. This is consistent with the expectation that the running coupling constant scale is set by the virtuality of the exchanged gluon propagator, just as in Abelian QED. This is also consistent with the automatic scale-fixing scheme of Ref. 63. Thus a significant part of the PQCD higher order corrections can be absorbed by taking the natural choice for the argument of the running coupling constant. The next-to-leading correction to the kernel for the meson distribution amplitude has also been evaluated by several groups. A surprising feature of this analysis is the fact that conformal symmetry cannot be used as a guide to predict the form the results even when the β-function is set to zero.[13] This is discussed in further detail in Section 4.2

5.8. The Pre-QCD Development of Exclusive Reactions

The study of exclusive processes in terms of underlying quark subprocesses in fact began before the discovery of QCD. The advent of the parton model and Bjorken scaling for deep inelastic structure functions in the late 1960's brought a new focus to the structure of form factors and exclusive processes at large momentum transfer. The underlying theme of the parton model was the concept that quarks carried the electromagnetic current within hadrons. The use of time-ordered perturbation theory in an "infinite momentum frame", or equivalently, quantization on the light cone, provided a natural language for hadrons as composites of relativistic partons, *i.e.* point-like constituents.[64] As discussed in Section 3, Drell and Yan[10] introduced Eq. (57) for current matrix elements in terms of a Fock state expansion at infinite momentum. (Later this result was shown to be an exact result using light-cone quantization.)

Drell and Yan suggested that the form factor is dominated by the end-point region $x \approx 1$. Then it is clear from the Drell-Yan formula that the form factor fall-off at large Q^2 is closely related to the $x \to 1$ behavior of the hadron structure function. The relation found by Drell and Yan was

$$F(Q^2) \sim \frac{1}{(Q^2)^n} \quad \text{if} \quad F_2(x, Q^2) \sim (1-x)^{2n-1}.$$

Gribov and Lipatov[65] extended this relationship to fragmentation functions $D(z, Q^2)$ at $z \to 1$, taking into account cancellations due to quark spin. Feynman[66] noted that the Drell-Yan relationship was also true in gauge theory models in which the endpoint behavior of structure functions is suppressed due to the emission of soft or "wee" partons by charged lines. However, as discussed in Section 4, the endpoint region is suppressed in QCD relative to the leading perturbative contributions.

The parton model was extended to exclusive processes such as hadron-hadron scattering and photoproduction by Blankenbecler, Brodsky, and Gunion[67] and by Landshoff and Polkinghorne.[68] It was recognized that independent of specific dynamics, hadrons could interact and scatter simply by exchanging their common constituents. These authors showed that the amplitude due to quark interchange (or rearrangement) could be written in closed form as an overlap of the light-cone wavefunctions of the incident and final hadrons. In order to make definite predictions, model wavefunctions were chosen to reproduce the fall-off of the form factors obtained from the Drell-Yan formula. Two-body exclusive amplitudes in

the "constituent interchange model" then take the form of "fixed-angle" scaling laws

$$\frac{d\sigma}{dt}(AB \to CD) \sim \frac{f(\theta_{cm})}{s^N}$$

where the power N reflects the power-law fall-off of the elastic form factors of the scattered hadrons. The form of the angular dependence $f(\theta_{cm})$ reflects the number of interchanged quarks.

Even though the constituent interchange is model was motivated in part by the Drell-Yan endpoint analysis of form factors, many of the predictions and systematics of quark interchange remain applicable in the QCD analysis.[67] A comprehensive series of measurements of elastic meson nucleon scattering reactions has recently been carried out by Baller *et al.*[69] at BNL. Empirically, the quark interchange amplitudes gives a reasonable account of the scaling, angular dependence, and relative magnitudes of the various channels. For example, the strong differences between K^+p and K^-p scattering is accounted for by u quark interchange in the K^+p amplitude. It is inconsistent with gluon exchange as the dominant amplitude since this produces equal scattering for the two channels. The dominance of quark interchange over gluon exchange is a surprising result which eventually needs to be understood in the context of QCD.

The prediction of fixed angle scaling laws laid the groundwork for the derivation of the "dimensional counting rules." As discussed in Ref. 5, it is natural to assume that at large momentum transfer, an exclusive amplitude factorize as a convolution of hadron wavefunctions which couple the hadrons to their quark constituents with a hard scattering amplitude T_H which scatters the quarks from the initial to final direction. Since the hadron wavefunction is maximal when the quarks are nearly collinear with each parent hadron, the large momentum transfer occurs in T_H. The pre-QCD argument went as follows: the dimension of T_H is $[L^{n-4}]$ where $n = n_A + n_B + n_C + n_D$ is the total number of fields entering T_H. In a renormalizable theory where the coupling constant is dimensionless and masses can be neglected at large momentum transfer, all connected tree-graphs for T_H then scale as $[1/\sqrt{s}]^{n-4}$ at fixed t/s. This immediately gives the dimensional counting law[5]

$$\frac{d\sigma}{dt}(AB \to CD) \sim \frac{f(\theta_{cm})}{s^{n_A+n_B+n_C+n_D-2}}.$$

In the case of incident or final photons or leptons $n = 1$. Specializing to elastic lepton-hadron scattering, this also implies $F(Q^2) \sim 1/(Q^2)^{n_H-1}$ for the spin averaged form factor, where n_H is the number of constituents in hadron H. These

results were obtained independently by Matveev *et al.*[5] on the basis of an "automodality" principle, that the underlying constituent interactions are scale free.

As we have seen, the dimensional counting scaling laws will generally be modified by the accumulation of logarithms from higher loop corrections to the hard scattering amplitude T_H; the phenomenological success of the counting rules in their simplest form thus implies that the loop corrections be somewhat mild. As we have seen, it is the asymptotic freedom property of QCD which in fact makes higher order corrections an exponentiation of a $\log\log Q^2$ series, thus preserving the form of the dimensional counting rules modulo only logarithmic corrections.

6. EXCLUSIVE e^+e^- ANNIHILATION PROCESSES

The study of time-like hadronic form factors using e^+e^- colliding beams can provide very sensitive tests of the QCD helicity selection rule. This follows because the virtual photon in $e^+e^- \to \gamma^* \to h_A\bar{h}_B$ always has spin ± 1 along the beam axis at high energies.[#15] Angular-momentum conservation implies that the virtual photon can "decay" with one of only two possible angular distributions in the center-of-momentum frame: $(1+\cos^2\theta)$ for $|\lambda_A - \lambda_B| = 1$, and $\sin^2\theta$ for $|\lambda_A - \lambda_B| = 0$, where $\lambda_{A,B}$ are the helicities of hadron $h_{A,B}$. Hadronic-helicity conservation, Eq. (7), as required by QCD greatly restricts the possibilities. It implies that $\lambda_A + \lambda_B = 2\lambda_A = -2\lambda_B$. Consequently, angular-momentum conservation requires $|\lambda_A| = |\lambda_B| = \frac{1}{2}$ for baryons and $|\lambda_A| = |\lambda_B| = 0$ for mesons; and the angular distributions are now completely determined:

$$\frac{d\sigma}{d\cos\theta}(e^+e^- \to B\bar{B}) \propto 1 + \cos^2\theta(\text{baryons}),$$
$$\frac{d\sigma}{d\cos\theta}(e^+e^- \to M\bar{M}) \propto \sin^2\theta(\text{mesons}).$$

It should be emphasized that these predictions are far from trivial for vector mesons and for all baryons. For example, one expects distributions like $\sin^2\theta$ for baryon pairs in theories with a scalar or tensor gluon. Simply verifying these angular distributions would give strong evidence in favor of a vector gluon.

#15 This follows from helicity conservation as well, which is a well-known property of QED at high energies. The electron and positron must have opposite helicities; *i.e.* $\gamma_e + \gamma_{\bar{e}} = 0$. since it is the total helicity carried by fermions (alone) which is conserved, and there are no fermions in the intermediate state. In the laboratory frame ($\to p_e = - \to p_{\bar{e}}$), their *spins* must be parallel, resulting in a virtual photon with spin ± 1 along the beam.

The power-law dependence on s of these cross sections is also predicted in QCD, using the dimensional-counting rule. Such "all-orders" predictions for QCD allowed processes are summarized in Table II.[6,70] Processes suppressed in QCD are also listed there; these all violate hadronic-helicity conservation, and are suppressed by powers of m^2/s in QCD. This would not necessarily be the case in scalar or tensor theories.

Table II

Exclusive channels in e^+e^- annihilation. The $h_A\bar{h}_B\gamma^*$ couplings in allowed processes are $-ie(p_A-p_B)^\mu F(s)$ for mesons, $-ie\bar{v}(p_B)\gamma^\mu G(s)u(p_A)$ for baryons, and $-ie^2\epsilon_{\mu\nu\rho}p_M^\nu\epsilon^\rho p_\gamma^\sigma F_{M\gamma}(s)$ for meson-photon final states. Similar predictions apply to decays of heavy-quark vector states, such as $\psi, \psi', \ldots$, produced in e^+e^- collisions.

	$e^+e^- \to h_A(\lambda_A)\bar{h}_B(\lambda_B)$	Angular distribution	$\frac{\sigma(e^+e^-\to h_A\bar{h}_B)}{\sigma(e^+e^-\to\mu^+\mu^-)}$
	$e^+e^- \to \pi^+\pi^-, K^+K^-$	$\sin^2\theta$	$\frac{1}{4}\lvert F(s)\rvert^2 \sim c/s^2$
	$e^+e^- \to \rho^+\rho^-(0), K^{*+}K^{*-}$	$\sin^2\theta$	$\frac{1}{4}\lvert F(s)\rvert^2 \sim c/s^2$
Allowed	$e^+e^- \to \pi^0\gamma(\pm1), \eta\gamma, \eta'\gamma$	$1+\cos^2\theta$	$(\pi\alpha/2)s\lvert F_{M\gamma}(s)\rvert^2 \sim c/s$
in QCD	$e^+e^- \to p(\pm\frac{1}{2})\bar{p}(\mp\frac{1}{2}), n\bar{n}, \ldots$	$1+\cos^2\theta$	$\lvert G(s)\rvert^2 \sim c/s^4$
	$e^+e^- \to p(\pm\frac{1}{2})\bar{\Delta}(\mp\frac{1}{2}), \bar{n}\Delta\ldots$	$1+\cos^2\theta$	$\lvert G(s)\rvert^2 \sim c/s^4$
	$e^+e^- \to \Delta(\pm\frac{1}{2})\bar{\Delta}(\mp\frac{1}{2}), y^*\bar{y}^*, \ldots$	$1+\cos^2\theta$	$\lvert G(s)\rvert^2 \sim c/s4$
	$e^+e^- \to \rho^+(0)\rho^-(\pm1), \pi^+\rho^-, K^+K^{*-}, \ldots$	$1+\cos^2\theta$	$< c/s^3$
Suppressed	$e^+e^- \to \rho^+(\pm1)\rho^-(\pm1), \ldots$	$\sin^2\theta$	$< c/s^3$
in QCD	$e^+e^- \to p(\pm\frac{1}{2})\bar{p}(\pm\frac{1}{2}), p\bar{\Delta}, \Delta\bar{\Delta}, \ldots$	$\sin 2\theta$	$< c/s^5$
	$e^+e^- \to p(\pm\frac{1}{2})\bar{\Delta}(\pm\frac{3}{2}), \Delta\bar{\Delta}, \ldots$	$1+\cos^2\theta$	$< c/s^5$
	$e^+e^- \to \Delta(\pm\frac{3}{2})\bar{\Delta}(\pm\frac{3}{2}), \ldots$	$\sin^2\theta$	$< c/s^5$

Table II

All of these perturbative predictions assume that s is sufficiently far from resonance contributions.

Notice the $e^+e^- \to \pi\rho, \pi\omega, K^*K^*, \ldots$, are all suppressed in QCD. This occurs because the $\gamma - \pi - \rho$ can couple through only a single form factor - $\epsilon^{\mu\nu\tau\sigma}\epsilon_\mu^{(\gamma)}\epsilon_\nu^{(\rho)}p_\tau^{(\pi)}p_\sigma^{(\rho)}F_{\pi\rho}(s)$ — and this requires $\mid \lambda_\rho \mid = 1$ in e^+e^- collisions. Hadronic-helicity conservation requires $\lambda = 0$ for mesons, and thus these amplitudes are suppressed in QCD (although, again, not in scalar or tensor theories). Notice however that the processes $e^+e^- \to \gamma\pi, \gamma\eta, \gamma\eta'$ are allowed by the helicity selection rule; helicity conservation applies only to the hadrons. Unfortunately the form factors governing these last processes are not expected to be large, e.g. $F_{\pi\gamma}(s) \sim 2f_\pi/s$.

These form factors can also tell us about the quark distribution amplitudes $\phi_H(x_i, Q)$. For example sum rules require (to all orders in α_s) that $\pi^+\pi^-, K^+K^-$, and $\rho^+\rho^-$ (helicity-zero) pairs are produced in the ratio of $f_\pi^4 : f_K^4 : 4f_\rho^4 \sim 1 : 2 : 7$, respectively if the π, K, and ρ distribution amplitudes are of similar shape. These ratios must apply at very large energies, where all distribution amplitudes tend to $\phi \propto x(1-x)$. On the other hand, the kaon's distribution amplitude may be quite asymmetric about $x = \frac{1}{2}$ at low energies due to the large difference between s and u, d quark masses. This could enhance K^+K^- production. (Distribution amplitudes for π's and ρ's must be symmetric due to isospin.) The process $e^+e^- \to K_L K_S$ is only possible if the kaon distribution amplitude is asymmetric;[#16] the presence or absence of $K_L K_S$ pairs relative to K^+K^- pairs is thus a sensitive indicator of asymmetry in the wave function.

6.1. J/ψ Decay to Hadron Pairs

The exclusive decays of heavy-quark atoms $(J/\psi, \psi', ...)$ into light hadrons can also be analyzed in QCD.[71] The decay $\psi \to p\bar{p}$, for example, proceeds via diagrams such as those in Fig. 27. Since ψ's produced in e^+e^- collisions must also have spin ± 1 along the beam direction and since they can only couple to light quarks via gluons, all the properties listed in Table II apply to $\psi, \psi', \Upsilon, \Upsilon', ...$ decays as well. Already there is considerable experimental data for the ψ and ψ' decays.[72,73]

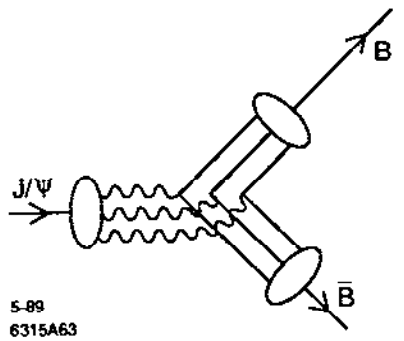

Figure 27. Quark-gluon subprocesses for $\psi \to B\overline{B}$.

#16 For example, this amplitude vanishes under the (stronger) assumption of exact flavor-$SU(3)$ symmetry. This is easily seen by defining G_U parity, in analogy to G parity: $G_U = C\exp(i\pi U_2)$, where the U_i are the isospin-like generators of $SU(3)_f$ which connect the K_0 and $\overline{K}_0$. The final state in $e^+e^- \to K_L K_S$ has positive G_U parity, while the intermediate photon has negative G_U parity. G_U parity is conserved if $SU(3)_f$ is exact, and $e^+e^- \to K_L K_S$ then vanishes.

Perhaps the most significant are the decays $\psi, \psi' \to p\bar{p}, n\bar{n}, ...$ The predicted angular distribution $1+\cos^2\theta$ is consistent with published data.[73] This is important evidence favoring a vector gluon, since scalar- or tensor-gluon theories would predict a distribution of $\sin^2\theta + O(\alpha_s)$. Dimensional-counting rules can be checked by comparing the ψ and ψ' rates into $p\bar{p}$, normalized by the total rates into light-quark hadrons so as to remove dependence upon the heavy-quark wave functions. Theory predicts that the ratio of branching fractions for the $p\bar{p}$ decays of the ψ and ψ' is

$$\frac{B(\psi' \to p\bar{p})}{B(\psi \to p\bar{p})} \sim Q_{e^+e^-}\left(\frac{M_\psi}{M'_\psi}\right)^8,$$

where $Q_{e^+e^-}$ is the ratio of branching fractions into e^+e^-:

$$Q_{e^+e^-} \equiv \frac{B(\psi' \to e^+e^-)}{B(J/\psi \to e^+e^-)} = 0.135 \pm 0.023 \quad .$$

Existing data suggest a ratio $(M_{\psi'}/M_\psi)^n$ with $n = 6 \pm 3$, in good agreement with QCD. One can also use the data for $\psi \to p\bar{p}, \Lambda\overline{\Lambda}, \Xi\Xi, ...,$ to estimate the relative magnitudes of the quark distribution amplitudes for baryons. Correcting for phase space, one obtains $\phi_p \sim 1.04(13)$ $\phi_n \sim 0.82(5)$ $\phi_\Xi \sim 1.08(8)$ $\phi_\Sigma \sim 1.14(5)$ ϕ_Λ by assuming similar functional dependence on the quark momentum fractions x_i for each case.

As is well known, the decay $\psi \to \pi^+\pi^-$ must be electromagnetic if G-parity is conserved by the strong interactions. To leading order in α_s, the decay is through a virtual photon (*i.e.* $\psi \to \gamma^* \to \pi^+\pi^-$) and the rate is determined by the pion's electromagnetic form factor:

$$\frac{\Gamma(\psi \to \pi^+\pi^-)}{\Gamma(\psi \to \mu^+\mu^-)} = \frac{1}{4}[F_\pi(s)]^2[1 + O(\alpha_s(s))],$$

where $s = (3.1GeV)^2$. Taking $F_\pi(s) \simeq (1 - s/m_\rho^2)^{-1}$ gives a rate $\Gamma(\psi \to \pi^+\pi^-) \sim 0.0011\ \Gamma(\psi \to \mu^+\mu^-)$, which compares well with the measured ratio 0.0015(7). This indicates that there is indeed little asymmetry in the pion's wave function.

The same analysis applied to $\psi \to K^+K^-$ suggests that the kaon's wave function is nearly symmetric about $x = \frac{1}{2}$. The ratio $\Gamma(\psi \to K^+K^-)/\Gamma(\psi \to \pi^+\pi^-)$ is 2 ± 1, which agrees with the ratio $(f_K/f_\pi)^4 \sim 2$ expected if π and K have similar quark distribution amplitudes. This conclusion is further supported by measurements of $\psi \to K_L K_S$ which vanishes completely if the K distribution amplitudes are symmetric; experimentally the limit is $\Gamma(\psi \to K_L K_S)/\Gamma(\psi \to K^+K^-) \lesssim \frac{1}{2}$.

6.2. The π-ρ Puzzle

We have emphasized that a central prediction of perturbative QCD for exclusive processes is hadron helicity conservation: to leading order in $1/Q$, the total helicity of hadrons in the initial state must equal the total helicity of hadrons in the final state. This selection rule is independent of any photon or lepton spin appearing in the process. The result follows from (a) neglecting quark mass terms, (b) the vector coupling of gauge particles, and (c) the dominance of valence Fock states with zero angular momentum projection.[6] The result is true in each order of perturbation theory in α_s.

Hadron helicity conservation appears relevant to a puzzling anomaly in the exclusive decays J/ψ and $\psi' \to \rho\pi, K^*\overline{K}$ and possibly other Vector-Pseudoscalar (VP) combinations. One expects the J/ψ and ψ' mesons to decay to hadrons via three gluons or, occasionally, via a single direct photon. In either case the decay proceeds via $|\Psi(0)|^2$, where $\Psi(0)$ is the wave function at the origin in the nonrelativistic quark model for $c\bar{c}$. Thus it is reasonable to expect on the basis of perturbative QCD that for any final hadronic state h that the branching fractions scale like the branching fractions into e^+e^-:

$$Q_h \equiv \frac{B(\psi' \to h)}{B(J/\psi \to h)} \cong Q_{e^+e^-}$$

Usually this is true, as is well documented in Ref. 74 for $p\bar{p}\pi^0$, $2\pi^+2\pi^-\pi^0$, $\pi^+\pi^-\omega$, and $3\pi^+3\pi^-\pi^0$, hadronic channels. The startling exceptions occur for $\rho\pi$ and $K^*\overline{K}$ where the present experimental limits[74] are $Q_{\rho\pi} < 0.0063$ and $Q_{K^*\overline{K}} < 0.0027$.

Perturbative QCD quark helicity conservation implies[6] $Q_{\rho\pi} \equiv [B(\psi' \to \rho\pi)/B(J/\psi \to \rho\pi)] \leq Q_{e^+e^-}[M_{J/\psi}/M_{\psi'}]^6$ This result includes a form factor suppression proportional to $[M_{J/\psi}/M_{\psi'}]^4$ and an additional two powers of the mass ratio due to helicity flip. However, this suppression is not nearly large enough to account for the data.[#17]

From the standpoint of perturbative QCD, the observed suppression of $\psi' \to V\,P$ is to be expected; it is the J/ψ that is anomalous.[75] The ψ' obeys the perturbative QCD theorem that total hadron helicity is conserved in high-momentum

---

#17 There is the possibility is the these form factors are dominated by end-point contributions for which quark masses may be less relevant. Such terms are expected to be strongly suppressed by quickly falling Sudakov form factors. This could also explain the rapid falloff of the $\psi - \pi - \rho$ form factor with increasing M_ψ^2.

transfer exclusive processes. The general validity of the QCD helicity conservation theorem at charmonium energies is of course open to question. An alternative model[76] based on nonperturbative exponential vertex functions, has recently been proposed to account for the anomalous exclusive decays of the J/ψ. However, helicity conservation has received important confirmation in $J/\psi \to p\bar{p}$ where the angular distribution is known experimentally to follow $[1 + \cos^2\theta]$ rather than $\sin^2\theta$ for helicity flip, so the decays $J/\psi \to \pi\rho$, and $K\overline{K}$ seem truly exceptional.

The helicity conservation theorem follows from the assumption of short-range point-like interactions among the constituents in a hard subprocess. One way in which the theorem might fail for $J/\psi \to$ gluons $\to \pi\rho$ is if the intermediate gluons resonate to form a gluonium state $\mathcal{O}$. If such a state exists, has a mass near that of the J/ψ, and is relatively stable, then the subprocess for $J/\psi \to \pi\rho$ occurs over large distances and the helicity conservation theorem need no longer apply. This would also explain why the J/ψ decays into $\pi\rho$ and not the ψ'.

Tuan *et al.*[75] have thus proposed, following Hou and Soni,[77] that the enhancement of $J/\psi \to K^*\overline{K}$ and $J/\psi \to \rho\pi$ decay modes is caused by a quantum mechanical mixing of the J/ψ with a $J^{PC} = 1^{--}$ vector gluonium state $\mathcal{O}$ which causes the breakdown of the QCD helicity theorem. The decay width for $J/\psi \to \rho\pi(K^*\overline{K})$ via the sequence $J/\psi \to \mathcal{O} \to \rho\pi(K^*\overline{K})$ must be substantially larger than the decay width for the (non-pole) continuum process $J/\psi \to 3$ gluons $\to \rho\pi(K^*\overline{K})$. In the other channels (such as $p\bar{p}, p\bar{p}\pi^0, 2\pi^+2\pi^-\pi^0$, etc.), the branching ratios of the $\mathcal{O}$ must be so small that the continuum contribution governed by the QCD theorem dominates over that of the $\mathcal{O}$ pole. For the case of the ψ' the contribution of the $\mathcal{O}$ pole must always be inappreciable in comparison with the continuum process where the QCD theorem holds. The experimental limits on $Q_{\rho\pi}$ and $Q_{K^*\overline{K}}$ are now substantially more stringent than when Hou and Soni made their estimates of $M_{\mathcal{O}}$, $\Gamma_{\mathcal{O}\to\rho\pi}$ and $\Gamma_{\mathcal{O}-K^*\overline{K}}$ in 1982.

A gluonium state of this type was first postulated by Freund and Nambu[78] based on OZI dynamics soon after the discovery of the J/ψ and ψ' mesons. In fact, Freund and Nambu predicted that the $\mathcal{O}$ would decay copiously precisely into $\rho\pi$ and $K^*\overline{K}$ with severe suppression of decays into other modes like $\epsilon^+\epsilon^-$ as required for the solution of the puzzle.

Branching fractions for final states h which can proceed only through the intermediate gluonium state have the ratio:

$$Q_h = Q_{e^+e^-}\frac{(M_{J/\psi} - M_{\mathcal{O}})^2 + \frac{1}{4}\,\Gamma_0^2}{(M_{\psi'} - M_{\mathcal{O}})^2 + \frac{1}{4}\,\Gamma_0^2}\,.$$

It is assumed that the coupling of the J/ψ and ψ' to the gluonium state scales

as the e^+e^- coupling. The value of Q_h is small if the $\mathcal{O}$ is close in mass to the J/ψ. Thus one requires $(M_{J/\psi} - M_{\mathcal{O}})^2 + \frac{1}{4}\,\Gamma_{\mathcal{O}}^2 \lesssim 2.6\,Q_h$ GeV^2. The experimental limit for $Q_{K^*\overline{K}}$ then implies $\left[(M_{J/\psi} - M_{\mathcal{O}})^2 + \frac{1}{4}\,\Gamma_{\mathcal{O}}^2\right]^{1/2} \lesssim 80$ MeV. This implies $\mid M_{J/\psi} - M_{\mathcal{O}} \mid < 80$ MeV and $\Gamma_{\mathcal{O}} < 160$ MeV. Typical allowed values are $M_{\mathcal{O}} =$ 3.0 GeV, $\Gamma_{\mathcal{O}} = 140$ MeV or $M_{\mathcal{O}} = 3.15$ GeV, $\Gamma_{\mathcal{O}} = 140$ MeV. Notice that the gluonium state could be either lighter or heavier than the J/ψ. The branching ratio of the $\mathcal{O}$ into a given channel must exceed that of the J/ψ.

It is not necessarily obvious that a $J^{PC} = 1^{--}$ gluonium state with these parameters would necessarily have been found in experiments to date. One must remember that though $\mathcal{O} \to \rho\pi$ and $\mathcal{O} \to K^*\overline{K}$ are important modes of decay, at a mass of order 3.1 GeV many other modes (albeit less important) are available. Hence, a total width $\Gamma_{\mathcal{O}} \cong 100$ to 150 MeV is quite conceivable. Because of the proximity of $M_{\mathcal{O}}$ to $M_{J/\psi}$, the most important signatures for an $\mathcal{O}$ search via exclusive modes $J/\psi \to K^*\overline{K}h$, $J/\psi \to \rho\pi h$; $h = \pi\pi, \eta, \eta'$, are no longer available by phase-space considerations. However, the search could still be carried out using $\psi' \to K^*\overline{K}h$, $\psi' \to \rho\pi h$; with $h = \pi\pi$, and η. Another way to search for $\mathcal{O}$ in particular, and the three gluon bound states in general, is via the inclusive reaction $\psi' \to (\pi\pi) + X$, where the $\pi\pi$ pair is an isosinglet. The three-gluon bound states such as $\mathcal{O}$ should show up as peaks in the missing mass (*i.e.* mass of X) distribution.

The most direct way to search for the $\mathcal{O}$ is to scan $\overline{p}p$ or e^+e^- annihilation at $\sqrt{s}$ within ~ 100 MeV of the J/ψ, triggering on vector/pseudoscalar decays such as $\pi\rho$ or $\overline{K}K^*$.

The fact that the $\rho\pi$ and $K^*\overline{K}$ channels are strongly suppressed in ψ' decays but not in J/ψ decays clearly implies dynamics beyond the standard charmonium analysis. The hypothesis of a three-gluon state $\mathcal{O}$ with mass within $\cong 100$ MeV of the J/ψ mass provides a natural, perhaps even compelling, explanation of this anomaly. If this description is correct, then the ψ' and J/ψ hadronic decays not only confirm hadron helicity conservation (at the ψ' momentum scale), but they also provide a signal for bound gluonic matter in QCD.

6.3. Form Factor Zeros in QCD

The exclusive pair production of heavy hadrons $|Q_1\overline{Q}_2\rangle$, $|Q_1Q_2Q_3\rangle$ consisting of higher generation quarks ($Q_i = t, b, c$, and possibly s) can be reliably predicted within the framework of perturbative QCD, since the required wavefunction input is essentially determined from nonrelativistic considerations.[79] The results can be applied to e^+e^- annihilation, $\gamma\gamma$ annihilation, and W and Z decay into higher generation pairs. The normalization, angular dependence and helicity structure

can be predicted away from threshold, allowing a detailed study of the basic elements of heavy quark hadronization.

A particularly striking feature of the QCD predictions is the existence of a zero in the form factor and e^+e^- annihilation cross section for zero-helicity hadron pair production close to the specific timelike value $q^2/4M_H^2 = m_h/2m_\ell$ where m_h and m_ℓ are the heavier and lighter quark masses, respectively. This zero reflects the destructive interference between the spin-dependent and spin-independent (Coulomb exchange) couplings of the gluon in QCD. In fact, all pseudoscalar meson form factors are predicted in QCD to reverse sign from spacelike to timelike asymptotic momentum transfer because of their essentially monopole form. For $m_h > 2m_\ell$ the form factor zero occurs in the physical region.

To leading order in $1/q^2$, the production amplitude for hadron pair production is given by the factorized form

$$M_{H\overline{H}} = \int [dx_i] \int [dy_j]\, \phi_H^\dagger(x_i, \widetilde{q}^2)\, \phi_{\overline{H}}^\dagger(y_j, \widetilde{q}^2)\, T_H(x_i, y_j; \widetilde{q}^2, \theta_{C.M})$$

where $[dx_i] = \delta\left(\sum_{k=1}^n x_k - 1\right) \prod_{k=1}^n dx_k$ and $n = 2, 3$ is the number of quarks in the valence Fock state. The scale $\widetilde{q}^2$ is set from higher order calculations, but it reflects the minimum momentum transfer in the process. The main dynamical dependence of the form factor is controlled by the hard scattering amplitude T_H which is computed by replacing each hadron by collinear constituents $P_i^\mu = x_i P_H^\mu$. Since the collinear divergences are summed in ϕ_H, T_H can be systematically computed as a perturbation expansion in $\alpha_s(q^2)$.

The distribution amplitude required for heavy hadron production $\phi_H(x_i, q^2)$ is computed as an integral of the valence light-cone Fock wavefunction up to the scale Q^2. For the case of heavy quark bound states, one can assume that the constituents are sufficiently non-relativistic that gluon emission, higher Fock states, and retardation of the effective potential can be neglected. The analysis of Section 2 is thus relevant. The quark distributions are then controlled by a simple nonrelativistic wavefunction, which can be taken in the model form:

$$\psi_M(x_i, \vec{k}_{\perp i}) = \frac{C}{x_1^2 x_2^2 \left[M_H^2 - \frac{\vec{k}_{\perp 1}^2 + m_1^2}{x_1} - \frac{\vec{k}_{\perp 2}^2 + m_2^2}{x_2}\right]^2}$$

This form is chosen since it coincides with the usual Schrödinger- Coulomb wavefunction in the nonrelativistic limit for hydrogenic atoms and has the correct

large momentum behavior induced from the spin- independent gluon couplings. The wavefunction is peaked at the mass ratio $x_i = m_i/M_H$:

$$\left(x_i - \frac{m_i}{M_H}\right)^2 \sim \frac{\langle k_z^2 \rangle}{M_H^2}$$

where $\langle k_z^2 \rangle$ is evaluated in the rest frame. Normalizing the wavefunction to unit probability gives

$$C^2 = 128\pi \left(\langle v^2 \rangle\right)^{5/2} m_r^5 (m_1 + m_2)$$

where $\langle v^2 \rangle$ is the mean square relative velocity and $m_r = m_1 m_2/(m_1 + m_2)$ is the reduced mass. The corresponding distribution amplitude is

$$\phi(x_i) = \frac{C}{16\pi^2} \frac{1}{[x_1 x_2 M_H^2 - x_2 m_1^2 - x_1 m_2^2]}$$

$$\cong \frac{1}{\sqrt{2\pi}} \frac{\gamma^{3/2}}{M_H^{1/2}} \delta\left(x_1 - \frac{m_1}{m_1 + m_2}\right) .$$

It is easy to see from the structure of T_H for $e^+e^- \to M\overline{M}$ that the spectator quark pair is produced with momentum transfer squared $q^2 x_s y_s = 4m_s^2$. Thus heavy hadron pair production is dominated by diagrams in which the primary coupling of the virtual photon is to the heavier quark pair. The perturbative predictions are thus expected to be accurate even near threshold to leading order in $\alpha_s(4m_\ell^2)$ where m_ℓ is the mass of lighter quark in the meson.

The leading order e^+e^- production helicity amplitudes for higher generation meson ($\lambda = 0, \pm 1$) and baryon ($\lambda = \pm 1/2, \pm 3/2$) pairs are computed in Ref. 79 as a function of q^2 and the quark masses. The analysis is simplified by using the peaked form of the distribution amplitude, Eq. (6). In the case of meson pairs the (unpolarized) e^+e^- annihilation cross section has the general form[#18]

#18 $F_{\lambda\bar{\lambda}}(q^2)$ is the form factor for the production of two mesons which have both spin and helicity (Z-component of spin) as λ and $\bar{\lambda}$ respectively. There are two Lorentz and gauge invariant form factors of vector pair production. However, one of them turns out to be the same as the form factor of pseudoscalar plus vector production multiplied by M_H. Therefore the differential cross section for the production of two mesons with spin 0 or 1 can be represented in terms of three independent form factors.

$$4\pi \frac{d\sigma}{d\Omega}(e^+e^- \to M_\lambda \overline{M}_{\overline{\lambda}}) = \frac{3}{4}\beta\sigma_{e^+e^-\to\mu^+\mu^-}\left[\frac{1}{2}\beta^2\sin^2\theta\right.$$

$$\times\left[|F_{0,0}(q^2)|^2 + \frac{1}{(1-\beta^2)^2}\left\{(3-2\beta^2+3\beta^4)|F_{1,1}(q^2)|^2\right.\right.$$

$$\left.\left. - 4(1+\beta^2)\,\mathrm{Re}\,(F_{1,1}(q^2)F^*_{0,1}(q^2)) + 4|F_{0,1}(q^2)|^2\right\}\right]$$

$$\left. + \frac{3\beta^2}{2(1-\beta^2)}(1+\cos^2\theta)|F_{0,1}(q^2)|^2\right]$$

where $q^2 = s = 4M_H^2\overline{q}^2$ and the meson velocity is $\beta = 1 - \frac{4M_H^2}{q^2}$. The production form factors have the general form

$$F_{\lambda\overline{\lambda}} = \frac{\langle v^2\rangle^2}{(\overline{q}^2)^2}\left(A_{\lambda\overline{\lambda}} + \overline{q}^2 B_{\lambda\overline{\lambda}}\right)$$

where A and B reflect the Coulomb-like and transverse gluon couplings, respectively. The results to leading order in α_s are given in Ref. 79. In general A and B have a slow logarithmic dependence due to the q^2-evolution of the distribution amplitudes. The form factor zero for the case of pseudoscalar pair production reflects the numerator structure of the T_H amplitude.

$$\text{Numerator} \sim e_1\left(\overline{q}^2 - \frac{m_1^2}{4M_H^2}\frac{1}{x_2y_1} - \frac{m_2^2}{4M_H^2}\frac{x_1}{x_2^2y_2}\right)$$

For the peaked wavefunction,

$$F^M_{0,0}(q^2) \propto \frac{1}{(\overline{q}^2)^2}\left\{e_1\left(\overline{q}^2 - \frac{m_1}{2m_2}\right) + e_2\left(\overline{q}^2 - \frac{m_2}{2m_1}\right)\frac{m_2^2}{m_1^2}\right\}$$

If m_1 is much greater than m_2 then the e_1 is dominant and changes sign at $q^2/4M_H^2 = m_1/2m_2$. The contribution of the e_2 term and higher order contributions are small and nearly constant in the region where the e_1 term changes sign; such contributions can displace slightly but not remove the form factor zero.

These results also hold in quantum electrodynamics; e.g. pair production of muonium ($\mu - e$) atoms in e_+e_- annihilation. Gauge theory predicts a zero at $\overline{q}^2 = m_\mu/2m_e$.

These explicit results for form factors also show that the onset of the leading power-law scaling of a form factor is controlled by the ratio of the A and B terms; i.e. when the transverse contributions exceed the Coulomb mass-dominated contributions. The Coulomb contribution to the form factor can also be computed directly from the convolution of the initial and final wavefunctions. Thus, contrary to the claim of Ref. 24 there are no extra factors of $\alpha_s(q^2)$ which suppress the "hard" versus nonperturbative contributions.

The form factors for the heavy hadrons are normalized by the constraint that the Coulomb contribution to the form factor equals the total hadronic charge at $q^2 = 0$. Further, by the correspondence principle, the form factor should agree with the standard non-relativistic calculation at small momentum transfer. All of these constraints are satisfied by the form

$$F^M_{0,0}(q^2) = e_1 \, \frac{16\gamma^4}{(q^2+\gamma^2)^2} \, \left(\frac{M_H^2}{m_2^2}\right)^2 \left(1 - \frac{q^2}{4M_H^2} \, \frac{2m_2}{m_1}\right) + 1 \leftrightarrow 2 \; .$$

At large q^2 the form factor can also be written as

$$F^M_{(0,0)} = e_1 \, \frac{16\pi\alpha_s f_M^2}{9q^2} \, \left(\frac{M_H^2}{m_2^2}\right) + (1 \leftrightarrow 2) \; , \quad \frac{f_M}{2\sqrt{3}} = \int_0^1 dx \, \varphi(x,Q)$$

where $f_M = (6\gamma^3/\pi M_H)^{1/2}$ is the meson decay constant. Detailed results for $F\overline{F}$ and $B_c\overline{B}_c$ production are give in Ref. 79.

At low relative velocity of the hadron pair one also expects resonance contributions to the form factors. For these heavy systems such resonances could be related to $qq\overline{qq}$ bound states. From Watson's theorem, one expects any resonance structure to introduce a final-state phase factor, but not destroy the zero of the underlying QCD prediction.

Analogous calculations of the baryon form factor, retaining the constituent mass structure have also been done. The numerator structure for spin 1/2 baryons has the form

$$A + B\overline{q}^2 + c\overline{q}^4 \; .$$

Thus it is possible to have two form factor zeros; e.g. at spacelike and timelike values of q^2.

Although the measurements are difficult and require large luminosity, the observation of the striking zero structure predicted by QCD would provide a unique test of the theory and its applicability to exclusive processes. The onset of leading power behavior is controlled simply by the mass parameters of the theory.

7. EXCLUSIVE $\gamma\gamma$ REACTIONS

Two-photon reactions have a number of unique features which are especially important for testing QCD, especially in exclusive channels:[80]

1. Any even charge conjugation hadronic state can be created in the annihilation of two photons—an initial state of minimum complexity. Because $\gamma\gamma$ annihilation is complete, there are no spectator hadrons to confuse resonance analyses. Thus, one has a clean environment for identifying the exotic color-singlet even C composites of quarks and gluons $|q\bar{q}>$, $|gg>$, $|ggg>$, $|q\bar{q}g>$, $|qq\bar{q}\bar{q}>$,... which are expected to be present in the few GeV mass range. (Because of mixing, the actual mass eigenstates of QCD may be complicated admixtures of the various Fock components.)
2. The mass and polarization of each of the incident virtual photons can be continuously varied, allowing highly detailed tests of theory. Because a spin-one state cannot couple to two on-shell photons, a $J = 1$ resonance can be uniquely identified by the onset of its production with increasing photon mass.[81]
3. Two-photon physics plays an especially important role in probing dynamical mechanisms. In the low momentum transfer domain, $\gamma\gamma$ reactions such as the total annihilation cross section and exclusive vector meson pair production can give important insights into the nature of diffractive reactions in QCD. Photons in QCD couple directly to the quark currents at any resolution scale (see Fig. 28). Predictions for high momentum transfer $\gamma\gamma$ reactions, including the photon structure functions, $F_2^\gamma(x,Q^2)$ and $F_L^\gamma(x,Q^2)$, high p_T jet production, and exclusive channels are thus much more specific than corresponding hadron-induced reactions. The pointlike coupling of the annihilating photons leads to a host of special features which differ markedly with predictions based on vector meson dominance models.
4. Exclusive $\gamma\gamma$ processes provide a window for viewing the wavefunctions of hadrons in terms of their quark and gluon degrees of freedom. In the case of $\gamma\gamma$ annihilation into hadron pairs, the angular distribution of the production cross section directly reflects the shape of the distribution amplitude (valence wavefunction) of each hadron.

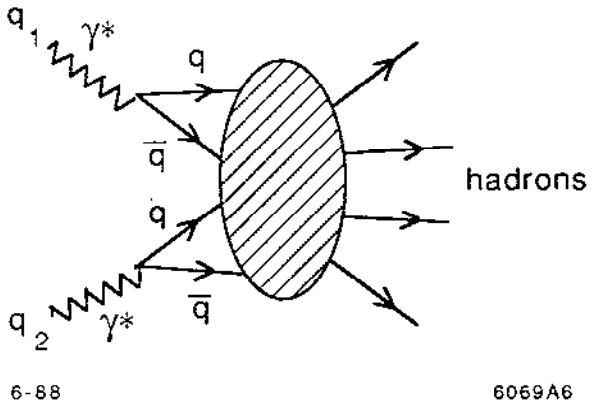

Figure 28. Photon-photon annihilation in QCD. The photons couple directly to one or two quark currents.

Thus far experiment has not been sufficiently precise to measure the logarithmic modification of dimensional counting rules predicted by QCD. Perturbative QCD predictions for $\gamma\gamma$ exclusive processes at high momentum transfer and high invariant pair mass provide some of the most severe tests of the theory.[82] A simple, but still very important example[4] is the Q^2-dependence of the reaction $\gamma^*\gamma \to M$ where M is a pseudoscalar meson such as the η. The invariant amplitude contains only one form factor:

$$M_{\mu\nu} = \epsilon_{\mu\nu\sigma\tau} p_\eta^\sigma q^\tau F_{\gamma\eta}(Q^2) \ .$$

It is easy to see from power counting at large Q^2 that the dominant amplitude (in light-cone gauge) gives $F_{\gamma\eta}(Q^2) \sim 1/Q^2$ and arises from diagrams (see Fig. 29) which have the minimum path carrying Q^2: *i.e.* diagrams in which there is only a single quark propagator between the two photons. The coefficient of $1/Q^2$ involves only the two-particle $q\bar{q}$ distribution amplitude $\phi(x,Q)$, which evolves logarithmically on Q. Higher particle number Fock states give higher power-law falloff contributions to the exclusive amplitude.

The TPC/$\gamma\gamma$ data[83] shown in Fig. 30 are in striking agreement with the predicted QCD power: a fit to the data gives $F_{\gamma\eta}(Q^2) \sim (1/Q^2)^n$ with $n = 1.05 \pm 0.15$. Data for the η' from Pluto and the TPC/$\gamma\gamma$ experiments give similar results, consistent with scale-free behavior of the QCD quark propagator and the point coupling to the quark current for both the real and virtual photons. In the case of deep inelastic lepton scattering, the observation of Bjorken scaling tests these properties when both photons are virtual.

The QCD power law prediction, $F_{\gamma\eta}(Q^2) \sim 1/Q^2$, is consistent with dimensional counting[5] and also emerges from current algebra arguments (when both

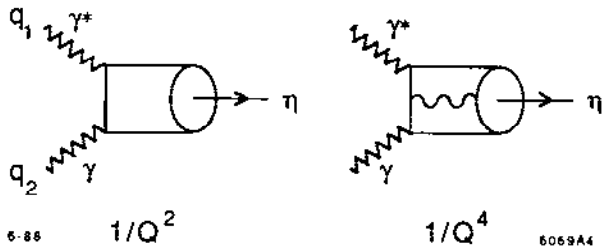

Figure 29. Calculation of the $\gamma - \eta$ transition form factor in QCD from the valence $q\bar{q}$ and $q\bar{q}g$ Fock states.

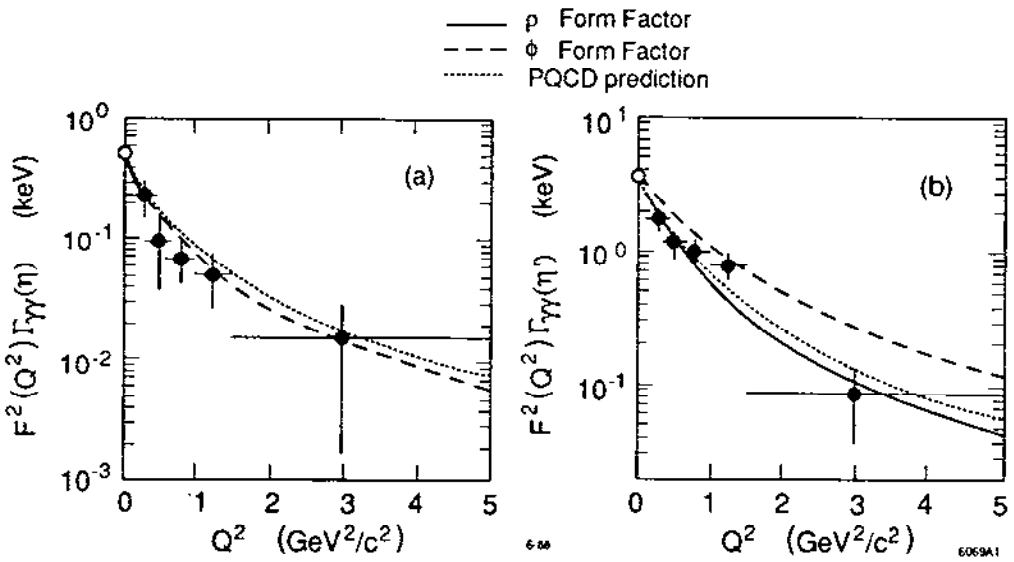

Figure 30. Comparison of TPC/$\gamma\gamma$ data[83] for the $\gamma - \eta$ and $\gamma - \eta'$ transition form factors with the QCD leading twist prediction of Ref. 82. The VMD predictions are also shown. See S. Yellin, this meeting.

photons are very virtual).[84] On the other hand, the $1/Q^2$ falloff is also expected in vector meson dominance models. The QCD and VDM predictions can be readily discriminated by studying $\gamma^*\gamma^* \to \eta$. In VMD one expects a product of form factors; in QCD the falloff of the amplitude is still $1/Q^2$ where Q^2 is a linear combination of Q_1^2 and Q_2^2. It is clearly very important to test this essential feature of QCD.

Exclusive two-body processes $\gamma\gamma \to H\overline{H}$ at large $s = W_{\gamma\gamma}^2 = (q_1 + q_2)^2$ and fixed $\theta_{\rm cm}^{\gamma\gamma}$ provide a particularly important laboratory for testing QCD, since the

large momentum-transfer behavior, helicity structure, and often even the absolute normalization can be rigorously predicted.[82,56] The angular dependence of some of the $\gamma\gamma \to H\overline{H}$ cross sections reflects the shape of the hadron distribution amplitudes $\phi_H(x_i, Q)$. The $\gamma_\lambda \gamma_{\lambda'} \to H\overline{H}$ amplitude can be written as a factorized form

$$\mathcal{M}_{\lambda\lambda'}(W_{\gamma\gamma}, \theta_{\rm cm}) = \int_0^1 [dy_i]\, \phi_H^*(x_i, Q)\, \phi_{\overline{H}}^*(y_i, Q)\, T_{\lambda\lambda'}(x, y; W_{\gamma\gamma}, \theta_{\rm cm})$$

where $T_{\lambda\lambda'}$ is the hard scattering helicity amplitude. To leading order $T \propto \alpha(\alpha_s/W_{\gamma\gamma}^2)^n$ and $d\sigma/dt \sim W_{\gamma\gamma}^{-(2n+2)} f(\theta_{\rm cm})$ where $n = 1$ for meson and $n = 2$ for baryon pairs.

Lowest order predictions for pseudo-scalar and vector-meson pairs for each helicity amplitude are given in Ref. 82. In each case the helicities of the hadron pairs are equal and opposite to leading order in $1/W^2$. The normalization and angular dependence of the leading order predictions for $\gamma\gamma$ annihilation into charged meson pairs are almost model independent; *i.e.* they are insensitive to the precise form of the meson distribution amplitude. If the meson distribution amplitudes is symmetric in x and $(1-x)$, then the same quantity

$$\int_0^1 dx\, \frac{\varphi_\pi(x, Q)}{(1-x)}$$

controls the x-integration for both $F_\pi(Q^2)$ and to high accuracy $M(\gamma\gamma \to \pi^+\pi^-)$. Thus for charged pion pairs one obtains the relation:

$$\frac{\frac{d\sigma}{dt}(\gamma\gamma \to \pi^+\pi^-)}{\frac{d\sigma}{dt}(\gamma\gamma \to \mu^+\mu^-)} \cong \frac{4|F_\pi(s)|^2}{1 - \cos^4\theta_{\rm cm}} .$$

Note that in the case of charged kaon pairs, the asymmetry of the distribution amplitude may give a small correction to this relation.

The scaling behavior, angular behavior, and normalization of the $\gamma\gamma$ exclusive pair production reactions are nontrivial predictions of QCD. Recent Mark II meson pair data and PEP4/PEP9 data[85] for separated $\pi^+\pi^-$ and K^+K^- production in the range $1.6 < W_{\gamma\gamma} < 3.2$ GeV near 90° are in satisfactory agreement with the normalization and energy dependence predicted by QCD (see Fig. 31). In the case of $\pi^0\pi^0$ production, the $\cos\theta_{\rm cm}$ dependence of the cross section can be inverted to determine the x-dependence of the pion distribution amplitude.

The wavefunction of hadrons containing light and heavy quarks such as the K, D-meson are likely to be asymmetric due to the disparity of the quark masses. In a gauge theory one expects that the wavefunction is maximum when the quarks have zero relative velocity; this corresponds to $x_i \propto m_{i\perp}$ where $m_\perp^2 = k_\perp^2 + m^2$. An explicit model for the skewing of the meson distribution amplitudes based on QCD sum rules is given by Benyayoun and Chernyak.[86] These authors also apply their model to two-photon exclusive processes such as $\gamma\gamma \to K^+K^-$ and obtain some modification compared to the strictly symmetric distribution amplitudes. If the same conventions are used to label the quark lines, the calculations of Benyayoun and Chernyak are in complete agreement with those of Ref. 82.

The one-loop corrections to the hard scattering amplitude for meson pairs have been calculated by Nizic.[62] The QCD predictions for mesons containing admixtures of the $|gg\rangle$ Fock state is given by Atkinson, Sucher, and Tsokos.[56]

The perturbative QCD analysis has been extended to baryon-pair production in comprehensive analyses by Farrar *et al.*[60,56] and by Gunion *et al.*[61,56] Predictions are given for the "sideways" Compton process $\gamma\gamma \to p\bar{p}$, $\Delta\overline{\Delta}$ pair production, and the entire decuplet set of baryon pair states. The arduous calculation of 280 $\gamma\gamma \to qqq\overline{qqq}$ diagrams in T_H required for calculating $\gamma\gamma \to B\overline{B}$ is greatly simplified by using two-component spinor techniques. The doubly charged Δ pair is predicted to have a fairly small normalization. Experimentally such resonance pairs may be difficult to identify under the continuum background.

The normalization and angular distribution of the QCD predictions for proton-antiproton production shown in Fig. 32 depend in detail on the form of the nucleon distribution amplitude, and thus provide severe tests of the model form derived by Chernyak, Ogloblin, and Zhitnitsky[49] from QCD sum rules.

An important check of the QCD predictions can be obtained by combining data from $\gamma\gamma \to p\bar{p}$ and the annihilation reaction, $p\bar{p} \to \gamma\gamma$, with large angle Compton scattering $\gamma p \to \gamma p$. The available data[87] for large angle Compton scattering (see Fig. 33), for $5\ GeV^2 < s < 10\ GeV^2$ are consistent with the dimensional counting scaling prediction, $s^6 d\sigma/dt = f(\theta_{cm})$. In general, comparisons between channels related by crossing of the Mandelstam variables place a severe constraint on the angular dependence and analytic form of the underlying QCD exclusive amplitude. Furthermore in $p\bar{p}$ collisions one can study timelike photon production into e^+e^- and examine the virtual photon mass dependence of the Compton amplitude. Predictions for the q^2 dependence of the $p\bar{p} \to \gamma\gamma^*$ amplitude can be obtained by crossing the results of Gunion and Millers.[56]

The region of applicability of the leading power-law predictions for $\gamma\gamma \to$

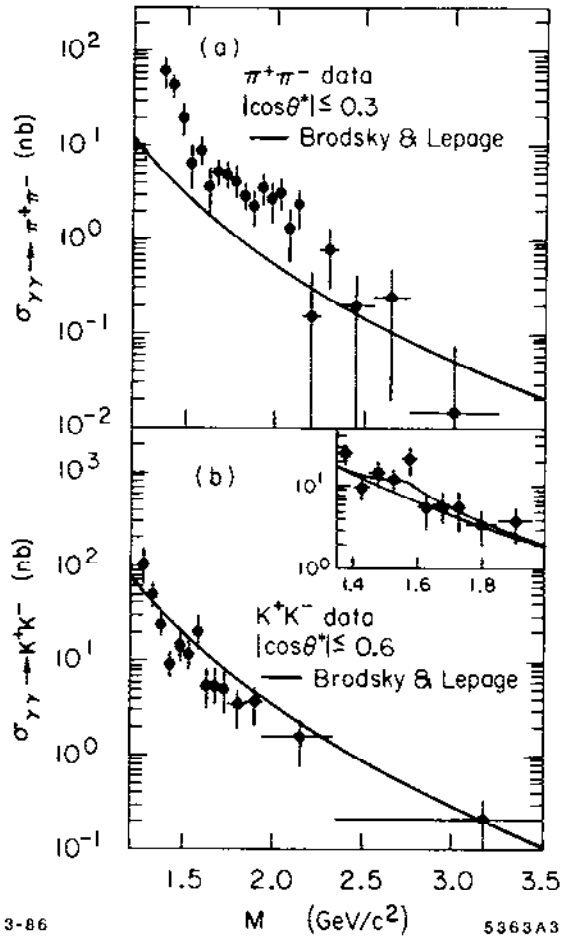

Figure 31. Comparison of $\gamma\gamma \to \pi^+\pi^-$ and $\gamma\gamma \to K^+K^-$ meson pair production data with the parameter-free perturbative QCD prediction of Ref. 82. The theory predicts the normalization and scaling of the cross sections. The data are from the TPC/$\gamma\gamma$ collaboration.[85]

$p\bar{p}$ requires that one be beyond resonance or threshold effects. It presumably is set by the scale where $Q^4 G_M(Q^2)$ is roughly constant, *i.e.* $Q^2 > 3$ GeV^2. Present measurements may thus be too close to threshold for meaningful tests.[88] It should be noted that unlike the case for charged meson pair production, the QCD predictions for baryons are sensitive to the form of the running coupling constant and the endpoint behavior of the wavefunctions.

The QCD predictions for $\gamma\gamma \to H\overline{H}$ can be extended to the case of one or two virtual photons, for measurements in which one or both electrons are tagged. Because of the direct coupling of the photons to the quarks, the Q_1^2 and Q_2^2 dependence of the $\gamma\gamma \to H\overline{H}$ amplitude for transversely polarized photons is minimal at W^2 large and fixed $\theta_{\rm cm}$, since the off-shell quark and gluon propagators

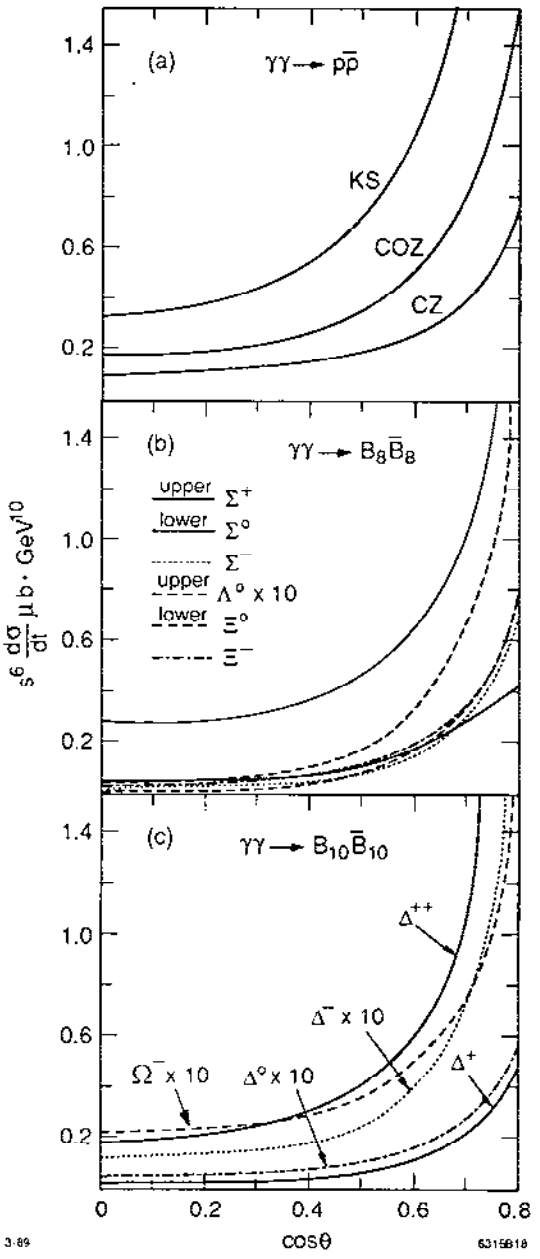

Figure 32. Perturbative QCD predictions by Farrar and Zhang for the $\cos(\theta_{cm})$ dependence of the $\gamma\gamma \rightarrow p\bar{p}$ cross section assuming the King-Sachrajda (KS), Chernyak, Ogloblin, and Zhitnitsky (COZ)[19], and original Chernyak and Zhitnitsky (CZ)[16] forms for the proton distribution amplitude, $\phi_p(x_i, Q)$.

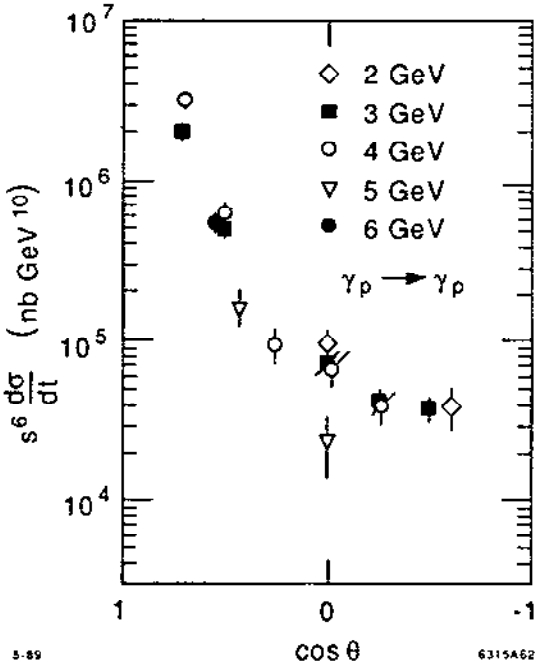

Figure 33. Test of dimensional counting for Compton scattering for $2 < E^{\gamma}_{lab} < 6$ GeV.[87]

in T_H already transfer hard momenta; *i.e.* the 2γ coupling is effectively local for $Q_1^2,\ Q_2^2 \ll p_T^2$. The $\gamma^*\gamma^* \to \overline{B}B$ and $M\overline{M}$ amplitudes for off-shell photons have been calculated by Millers and Gunion.[56] In each case, the predictions show strong sensitivity to the form of the respective baryon and meson distribution amplitudes.

We also note that photon-photon collisions provide a way to measure the running coupling constant in an exclusive channel, independent of the form of hadronic distribution amplitudes.[82] The photon-meson transition form factors $F_{\gamma-M}(Q^2)$, $M = \pi^0, \eta^0, f$, etc., are measurable in tagged $e\gamma \to e'M$ reactions. QCD predicts

$$\alpha_s(Q^2) = \frac{1}{4\pi}\ \frac{F_\pi(Q^2)}{Q^2|F_{\pi\gamma}(Q^2)|^2}$$

where to leading order the pion distribution amplitude enters both numerator and denominator in the same manner.

The complete calculations of the tree-graph structure (see Figs. 34, 35, 36) of both $\gamma\gamma \to M\overline{M}$ and $\gamma\gamma \to B\overline{B}$ amplitudes has now been completed. One can use crossing to compute T_H for $p\overline{p} \to \gamma\gamma$ to leading order in $\alpha_s(p_T^2)$ from the

calculations reported by Farrar, Maina and Neri[56] and Gunion and Millers.[56] Examples of the predicted angular distributions are shown in Figs. 37 and 38.

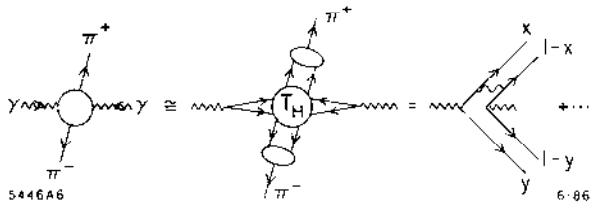

Figure 34. Application of QCD to two-photon production of meson pairs.[85]

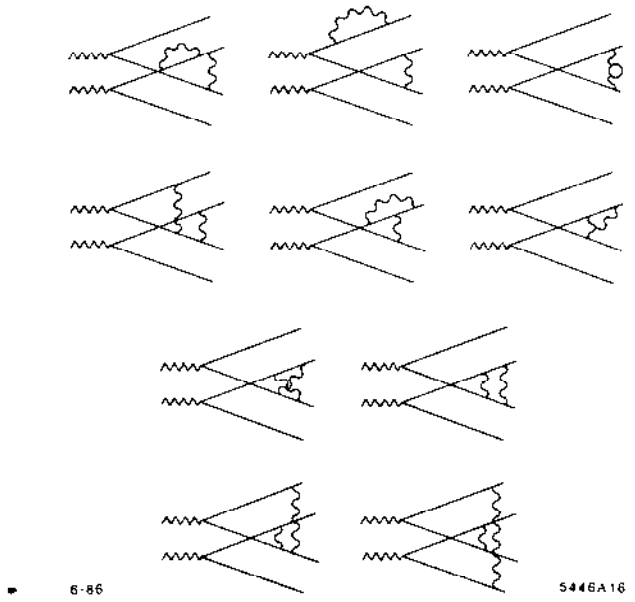

Figure 35. Next-to-leading perturbative contribution to T_H for the process $\gamma\gamma \to M\overline{M}$. The calculation has been done by Nizic.[89]

As discussed in Section 2, a model form for the proton distribution amplitude has been proposedby Chernyak and Zhitnitsky[16] based on QCD sum rules which leads to normalization and sign consistent with the measured proton form factor (see Fig. 21). The CZ sum rule analysis has been confirmed and extended by King and Sachrajda.[50] The CZ proton distribution amplitude yields predictions for $\gamma\gamma \to p\overline{p}$ in rough agreement with the experimental normalization, although the production energy is too low for a clear test. It should be noted that unlike

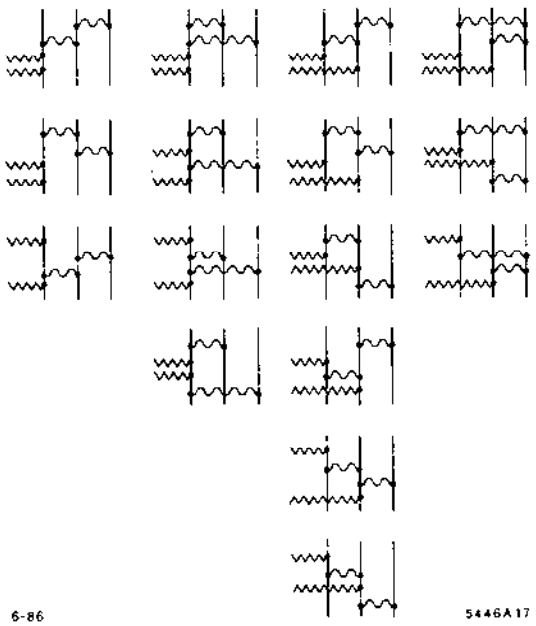

Figure 36. Leading diagrams for $\gamma + \gamma \to \bar{p} + p$ calculated in Ref. 56.

meson pair production[89] the QCD predictions for baryons are highly sensitive to the form of the running coupling constant and the endpoint behavior of the wavefunctions.

It is possible that data from $p\bar{p}$ collisions at energies up to 10 GeV could greatly clarify the question of whether the perturbative QCD predictions are reliable at moderate momentum transfer. As emphasized in Section 4, an important check of the QCD predictions can be obtained by combining data from $p\bar{p} \to \gamma\gamma$, $\gamma\gamma \to p\bar{p}$ with large angle Compton scattering $\gamma p \to \gamma p$. This comparison checks in detail the angular dependence and crossing behavior expected from the theory. Furthermore, in $p\bar{p}$ collisions one can even study time-like photon production into e^+e^- and examine the virtual photon mass dependence of the Compton amplitude. Predictions for the q^2 dependence of the $p\bar{p} \to \gamma\gamma^*$ amplitude can be obtained by crossing the results of Gunion and Millers.[56,61]

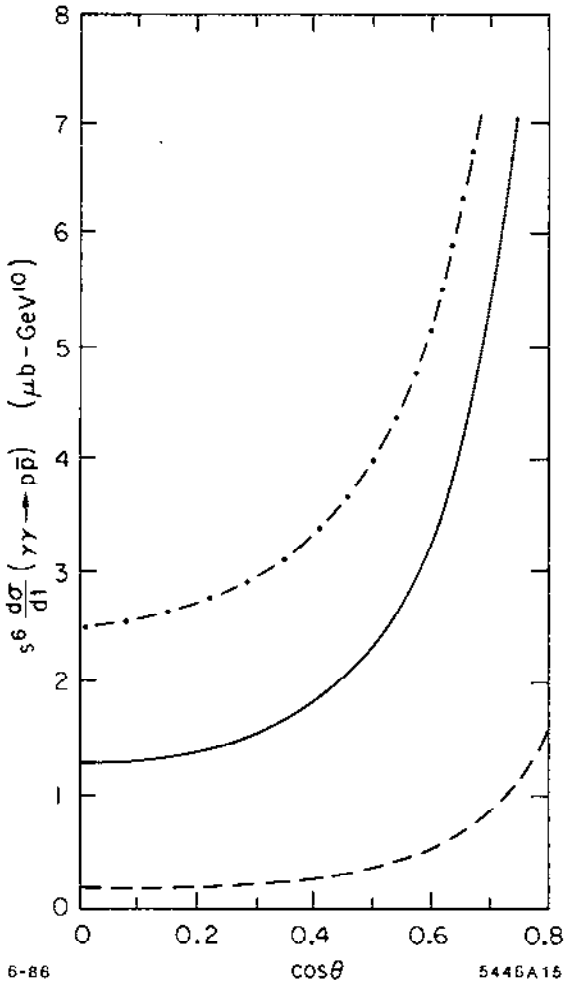

Figure 37. QCD prediction for the scaling and angular distribution for $\gamma + \gamma \to \bar{p} + p$ calculated by Farrar *et al.*[56] The dashed-dot curve corresponds to $4\Lambda^2/s = 0.0016$ and a maximum running coupling constant $\alpha_s^{max} = 0.8$. The solid curve corresponds to $4\Lambda^2/s = 0.016$ and a maximum running coupling constant $\alpha_s^{max} = 0.5$. The dashed curve corresponds to a fixed $\alpha_s = 0.3$. The results are very sensitive to the endpoint behavior of the proton distribution amplitude. The CZ form is assumed.

8. QCD PROCESSES IN NUCLEI

The least-understood process in QCD is *hadronization* -- the mechanism which converts quark and gluon quanta to color-singlet integrally-charged hadrons. One way to study hadronization is to perturb the environment by introducing a nuclear medium surrounding the hard-scattering short distance reaction. This is obviously impractical in the theoretically simplest processes -- e^+e^- or $\gamma\gamma$ annihilation. However, for large momentum transfer reactions occurring in a nuclear target, such as deep inelastic lepton scattering or massive lepton pair production.

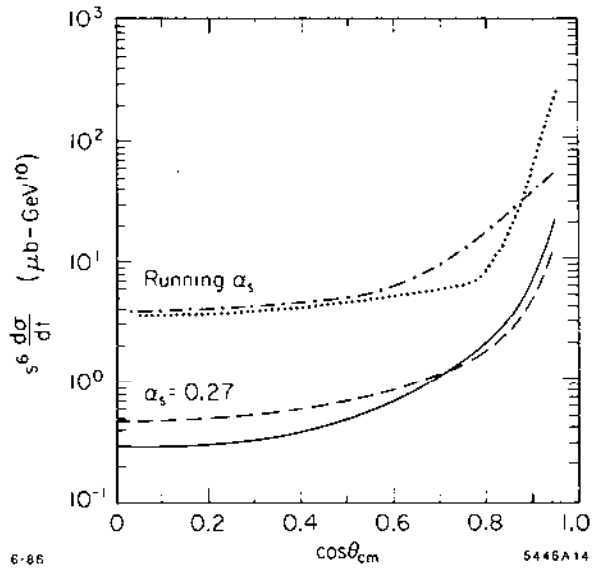

Figure 38. QCD prediction for the scaling and angular distribution for $\gamma + \gamma \to \bar{p} + p$ calculated by Gunion, Sparks and Millers.[56,61] CZ distribution amplitudes are assumed. The solid and running curves are for real photon annihilation. The dashed and dot-dashed curves correspond to one photon space-like, with $Q_1^2/s = 0.1$.

the nuclear medium provides a nontrivial perturbation to jet evolution through the influence of initial- and/or final-state interactions. In the case of large momentum transfer quasiexclusive reactions, one can use a nuclear target to filter and influence the evolution and structure of the hadron wavefunctions themselves. The physics of such nuclear reactions is surprisingly interesting and subtle — involving concepts and novel effects quite orthogonal to usual expectations.

The nucleus thus plays two complimentary roles in quantum chromodynamics:

1. A nuclear target can be used as a control medium or background field to modify or probe quark and gluon subprocesses. Some novel examples are *color transparency*, the predicted transparency of the nucleus to hadrons participating in high-momentum transfer exclusive reactions, and *formation zone phenomena*, the absence of hard, collinear, target-induced radiation by a quark or gluon interacting in a high-momentum transfer inclusive reaction if its energy is large compared to a scale proportional to the length of the target. (Soft radiation and elastic initial-state interactions in the nucleus still occur.) *Coalescence* with co-moving spectators[90] has been discussed as a mechanism which can lead to increased open charm hadroproduction, but which also suppresses forward charmonium production (relative to lepton pairs) in heavy ion collisions.[91] There are also interesting special features of nuclear diffractive amplitudes — high energy hadronic or electromagnetic

reactions which leave the entire nucleus intact and give nonadditive contributions to the nuclear structure function at low x_{Bj}. The Q^2 dependence of diffractive $\gamma^* p \to \rho^0 p$ is found to have a slope in the $t-$dependence $\exp\ bt$ where $b = b(Q^2)$ is of order $1 \sim 2\ GeV^{-2}$, much smaller than expected on the basis of vector meson dominance and $t-$channel factorization.

2. Conversely, the nucleus can be studied as a QCD structure. At short distances nuclear wavefunctions and nuclear interactions necessarily involve *hidden color*, degrees of freedom orthogonal to the channels described by the usual nucleon or isobar degrees of freedom. At asymptotic momentum transfer, the deuteron form factor and distribution amplitude are rigorously calculable. One can also derive new types of testable scaling laws for exclusive nuclear amplitudes in terms of the reduced amplitude formalism.

8.1. Exclusive Nuclear Reactions — Reduced Amplitudes

An ultimate goal of QCD phenomenology is to describe the nuclear force and the structure of nuclei in terms of quark and gluon degrees of freedom. Explicit signals of QCD in nuclei have been elusive, in part because of the fact that an effective Lagrangian containing meson and nucleon degrees of freedom must be in some sense equivalent to QCD if one is limited to low-energy probes. On the other hand, an effective local field theory of nucleon and meson fields cannot correctly describe the observed off-shell falloff of form factors, vertex amplitudes, Z-graph diagrams, etc. because hadron compositeness is not taken into account.

We have already mentioned the prediction $F_d(Q^2) \sim 1/Q^{10}$ which comes from simple quark counting rules, as well as perturbative QCD. One cannot expect this asymptotic prediction to become accurate until very large Q^2 is reached since the momentum transfer has to be shared by at least six constituents. However there is a simple way to isolate the QCD physics due to the compositeness of the nucleus, not the nucleons. The deuteron form factor is the probability amplitude for the deuteron to scatter from p to $p+q$ but remain intact. Note that for vanishing nuclear binding energy $\epsilon_d \to 0$, the deuteron can be regarded as two nucleons sharing the deuteron four-momentum (see Fig. 39). The momentum ℓ is limited by the binding and can thus be neglected. To first approximation the proton and neutron share the deuteron's momentum equally. Since the deuteron form factor contains the probability amplitudes for the proton and neutron to scatter from $p/2$ to $p/2+q/2$; it is natural to define the reduced deuteron form factor[92,93]

$$f_d(Q^2) \equiv \frac{F_d(Q^2)}{F_{1N}\left(\frac{Q^2}{4}\right)\ F_{1N}\left(\frac{Q^2}{4}\right)}.$$

The effect of nucleon compositeness is removed from the reduced form factor. QCD then predicts the scaling

$$f_d(Q^2) \sim \frac{1}{Q^2}$$

i.e. the same scaling law as a meson form factor. Diagrammatically, the extra power of $1/Q^2$ comes from the propagator of the struck quark line, the one propagator not contained in the nucleon form factors. Because of hadron helicity conservation, the prediction is for the leading helicity-conserving deuteron form factor ($\lambda = \lambda' = 0$.) As shown in Fig. 40, this scaling is consistent with experiment for $Q = p_T \gtrsim 1$ GeV.[94]

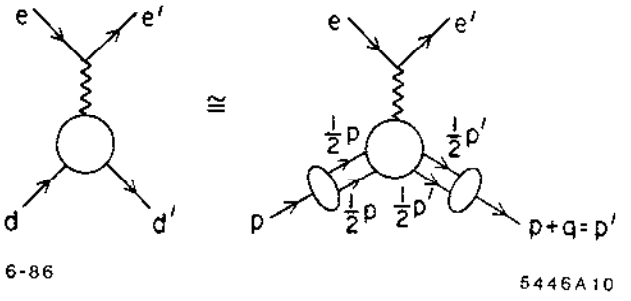

Figure 39. Application of the reduced amplitude formalism to the deuteron form factor at large momentum transfer.

The distinction between the QCD and other treatments of nuclear amplitudes is particularly clear in the reaction $\gamma d \to np$; *i.e.* photodisintegration of the deuteron at fixed center of mass angle. Using dimensional counting, the leading power-law prediction from QCD is simply $\frac{d\sigma}{dt}(\gamma d \to np) \sim \frac{1}{s^{11}} F(\theta_{cm})$. Again we note that the virtual momenta are partitioned among many quarks and gluons, so that finite mass corrections will be significant at low to medium energies. Nevertheless, one can test the basic QCD dynamics in these reactions taking into

account much of the finite-mass, higher-twist corrections by using the "reduced amplitude" formalism.[92,93] Thus the photodisintegration amplitude contains the probability amplitude (*i.e.* nucleon form factors) for the proton and neutron to each remain intact after absorbing momentum transfers $p_p - 1/2 p_d$ and $p_n - 1/2 p_d$, respectively (see Fig. 41). After the form factors are removed, the remaining "reduced" amplitude should scale as $F(\theta_{\rm cm})/p_T$. The single inverse power of transverse momentum p_T is the slowest conceivable in any theory, but it is the unique power predicted by PQCD.

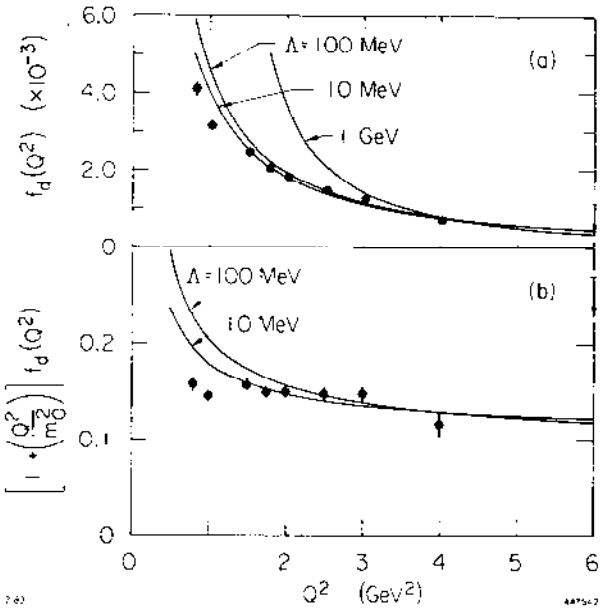

Figure 40. Scaling of the deuteron reduced form factor. The data are summarized in Ref. 92.

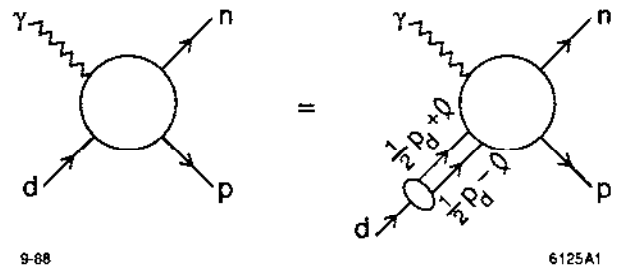

Figure 41. Construction of the reduced nuclear amplitude for two-body inelastic deuteron reactions.[92]

The prediction that $f(\theta_{\rm cm})$ is energy dependent at high-momentum transfer is compared with experiment in Fig. 42. It is particularly striking to see the QCD

prediction verified at incident photon lab energies as low as 1 GeV. A comparison with a standard nuclear physics model with exchange currents is also shown for comparison as the solid curve in Fig. 42(a). The fact that this prediction falls less fast than the data suggests that meson and nucleon compositeness are not taken to into account correctly. An extension of these data to other angles and higher energy would clearly be very valuable.

An important question is whether the normalization of the $\gamma d \rightarrow pn$ amplitude is correctly predicted by perturbative QCD. A recent analysis by Fujita[98] shows that mass corrections to the leading QCD prediction are not significant in the region in which the data show scaling. However Fujita also finds that in a model based on simple one-gluon plus quark-interchange mechanism, normalized to the nucleon-nucleon scattering amplitude, gives a photo-disintegration amplitude with a normalization an order of magnitude below the data. However this model only allows for diagrams in which the photon insertion acts only on the quark lines which couple to the exchanged gluon. It is expected that including other diagrams in which the photon couples to the current of the other four quarks will increase the photo-disintegration amplitude by a large factor.

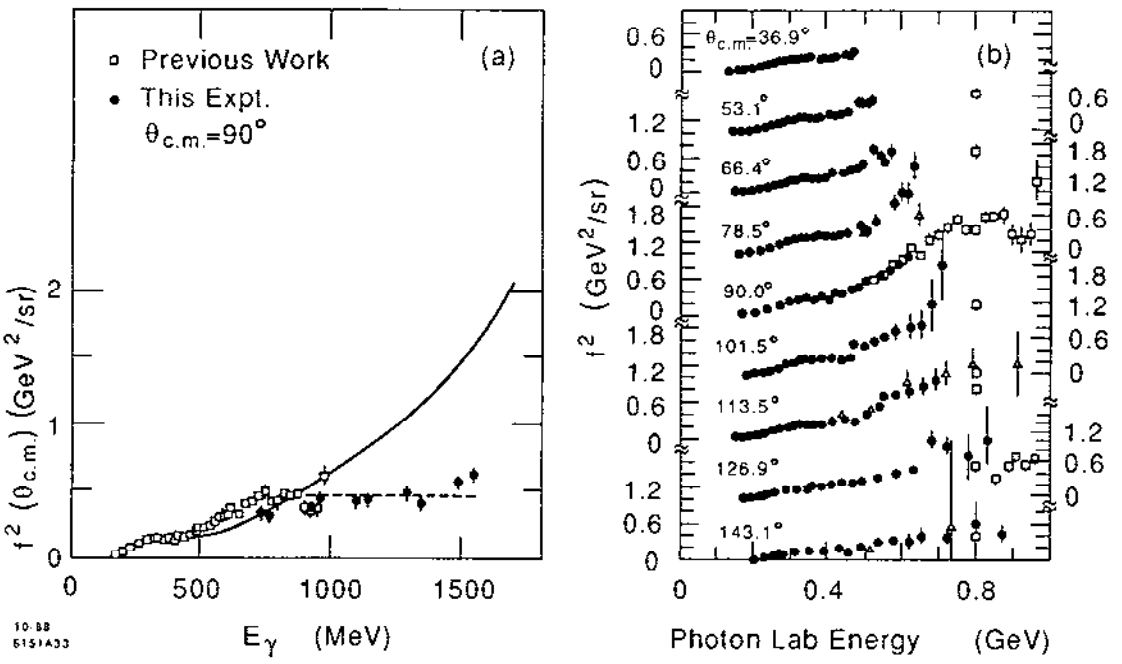

Figure 42. Comparison of deuteron photodisintegration data with the scaling prediction which requires $f^2(\theta_{cm})$ to be at most logarithmically dependent on energy at large momentum transfer. The data in (a) are from the recent experiment of Ref. 95. The nuclear physics prediction shown in (a) is from Ref. 96. The data in (b) are from Ref. 97.

The derivation of the evolution equation for the deuteron and other multi-quark states is given in Refs. 99 and 93. In the case of the deuteron, the evolution equation couples five different color singlet states composed of the six quarks. The leading anomalous dimension for the deuteron distribution amplitude and the helicity-conserving deuteron form factor at asymptotic Q^2 is given in Ref. 99.

There are a number of related tests of QCD and reduced amplitudes which require $\overline{p}$ beams[93] such as $\overline{p}d \to \gamma n$ and $\overline{p}d \to \pi^- p$ in the fixed $\theta_{\rm cm}$ region. These reactions are particularly interesting tests of QCD in nuclei. Dimensional counting rules predict the asymptotic behavior $\frac{d\sigma}{dt}\ (\overline{p}d \to \pi^- p) \sim \frac{1}{(p_T^2)^{12}}\ f(\theta_{\rm cm})$ since there are 14 initial and final quanta involved. Again one notes that the $\overline{p}d \to \pi^- p$ amplitude contains a factor representing the probability amplitude (*i.e.* form factor) for the proton to remain intact after absorbing momentum transfer squared $\hat{t} = (p - 1/2p_d)^2$ and the $\overline{N}N$ time-like form factor at $\hat{s} = (\overline{p} + 1/2p_d)^2$. Thus $\mathcal{M}_{\overline{p}d \to \pi^- p} \sim F_{1N}(\hat{t})\ F_{1N}(\hat{s})\, \mathcal{M}_\tau$, where $\mathcal{M}_\tau$ has the same QCD scaling properties as quark meson scattering. One thus predicts

$$\frac{\frac{d\sigma}{d\Omega}\ (\overline{p}d \to \pi^- p)}{F_{1N}^2(\hat{t})\, F_{1N}^2(\hat{s})} \sim \frac{f(\Omega)}{p_T^2}\ .$$

The reduced amplitude scaling for $\gamma d \to pn$ at large angles and $p_T \gtrsim 1$ GeV (see Fig. 42). One thus expects similar precocious scaling behavior to hold for $\overline{p}d \to \pi^- p$ and other $\overline{p}d$ exclusive reduced amplitudes. Recent analyses by Kondratyuk and Sapozhnikov[100] show that standard nuclear physics wavefunctions and interactions cannot explain the magnitude of the data for two-body anti-proton annihilation reactions such as $\overline{p}d \to \pi^- p$.

8.2. Color Transparency

A striking feature of the QCD description of exclusive processes is "color transparency:"The only part of the hadronic wavefunction that scatters at large momentum transfer is its valence Fock state where the quarks are at small relative impact separation. Such a fluctuation has a small color-dipole moment and thus has negligible interactions with other hadrons. Since such a state stays small over a distance proportional to its energy, this implies that quasi-elastic hadron-nucleon scattering at large momentum transfer as illustrated in Fig. 43 can occur additively on all of the nucleons in a nucleus with minimal attenuation due to elastic or inelastic final state interactions in the nucleus, *i.e.* the nucleus becomes "transparent." By contrast, in conventional Glauber scattering,

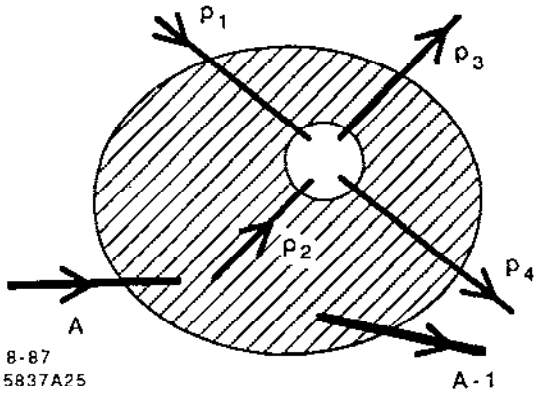

Figure 43. Quasi-elastic pp scattering inside a nuclear target. Normally one expects such processes to be attenuated by elastic and inelastic interactions of the incident proton and the final state interaction of the scattered proton. Perturbative QCD predicts minimal attenuation; *i.e.* "color transparency," at large momentum transfer.[7]

one predicts strong, nearly energy-independent initial and final state attenuation. A detailed discussion of the time and energy scales required for the validity of the PQCD prediction is given in by Farrar *et al.* and Mueller in Ref. 7.

A recent experiment[101] at BNL measuring quasi-elastic $pp \to pp$ scattering at $\theta_{\rm cm} = 90°$ in various nuclei appears to confirm the color transparency prediction—at least for p_{lab} up to 10 GeV/c (see Fig. 44). Descriptions of elastic scattering which involve soft hadronic wavefunctions cannot account for the data. However, at higher energies, $p_{lab} \sim 12$ GeV/c, normal attenuation is observed in the BNL experiment. This is the same kinematical region $E_{\rm cm} \sim 5$ GeV where the large spin correlation in A_{NN} are observed.[102] Both features may be signaling new s-channel physics associated with the onset of charmed hadron production[103] or interference with Landshoff pinch singularity diagrams.[43] We will discuss these possible solutions in Section 9. Clearly, much more testing of the color transparency phenomena is required, particularly in quasi-elastic lepton-proton scattering, Compton scattering, antiproton-proton scattering, etc. The cleanest test of the PQCD prediction is to check for minimal attenuation in large momentum transfer lepton-proton scattering in nuclei since there are no complications from pinch singularities or resonance interference effects.

In Section 5.4 we emphasized the fact that soft initial-state interactions $\overline{p}p \to \overline{\ell}\ell$ are suppressed at high lepton pair mass. This is a remarkable consequence of gauge theory and is quite contrary to normal treatments of initial interactions based on Glauber theory. This novel effect can be studied in quasielastic $\overline{p}A \to \overline{\ell}\ell\ (A-1)$ reaction. in which there are no extra hadrons produced and the

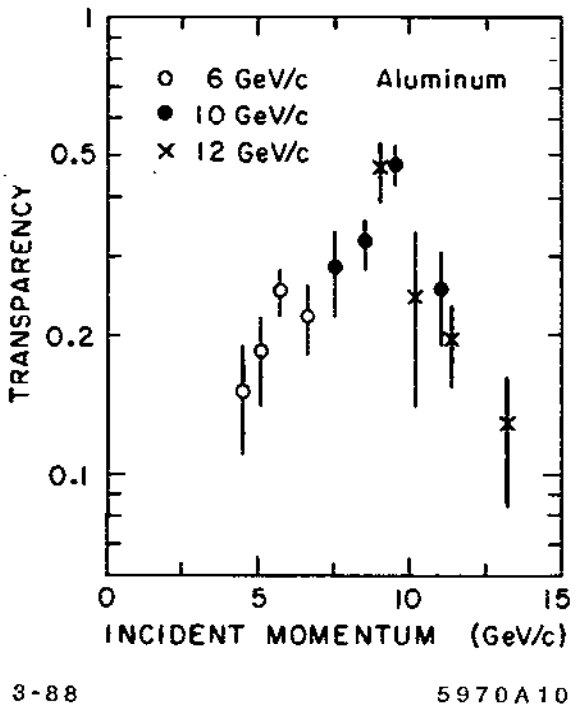

Figure 44. Measurements of the transparency ratio

$$T = \frac{Z_{eff}}{Z} = \frac{d\sigma}{dt}[pA \to p(A-1)] / \frac{d\sigma}{dt}[pA \to pp]$$

near 90° on Aluminum.[101] Conventional theory predicts that T should be small and roughly constant in energy. Perturbative QCD[7] predicts a monotonic rise to $T = 1$.

produced leptons are coplanar with the beam. (The nucleus $(A-1)$ can be left excited). Since PQCD predicts the absence of initial-state elastic and inelastic interactions, the number of such events should be strictly additive in the number Z of protons in the nucleus, every proton in the nucleus is equally available for short-distance annihilation. In traditional Glauber theory only the surface protons can participate because of the strong absorption of the $\overline{p}$ as it traverses the nucleus.

The above description is the ideal result for large s. QCD predicts that additivity is approached monotonically with increasing energy, corresponding to two effects: a) the effective transverse size of the $\overline{p}$ wavefunction is $b_\perp \sim 1/\sqrt{s}$, and b) the formation time for the $\overline{p}$ is sufficiently long, such that the Fock state stays small during transit of the nucleus.

The color transparency phenomena is also important to test in purely hadronic quasiexclusive antiproton-nuclear reactions. For large p_T one predicts

$$\frac{d\sigma}{dt\,dy}\,(\bar{p}A \to \pi^+\pi^- + (A-1)) \simeq \sum_{p\epsilon A} G_{p/A}(y)\,\frac{d\sigma}{dt}\,(\bar{p}p \to \pi^+\pi^-) \quad ,$$

where $G_{p/A}(y)$ is the probability distribution to find the proton in the nucleus with light-cone momentum fraction $y = (p^0 + p^z)/(p^0_A + p^z_A)$, and

$$\frac{d\sigma}{dt}(\bar{p}p \to \pi^+\pi^-) \simeq \left(\frac{1}{p_T^2}\right)^8 f(\cos\theta_{\rm cm}) \; .$$

The distribution $G_{p/A}(y)$ can also be measured in $eA \to ep(A-1)$ quasiexclusive reactions. A remarkable feature of the above prediction is that there are no corrections required from initial-state absorption of the $\bar{p}$ as it traverses the nucleus, nor final-state interactions of the outgoing pions. Again the basic point is that the only part of hadron wavefunctions which is involved in the large p_T reaction is $\psi_H(b_\perp \sim \mathcal{O}(1/p_T))$. *i.e.* the amplitude where all the valence quarks are at small relative impact parameter. These configurations correspond to small color singlet states which, because of color cancellations, have negligible hadronic interactions in the target. Measurements of these reactions thus test a fundamental feature of the Fock state description of large p_T exclusive reactions.

Another interesting feature which can be probed in such reactions is the behavior of $G_{p/A}(y)$ for y well away from the Fermi distribution peak at $y \sim m_N/M_A$. For $y \to 1$ spectator counting rules[104] predict $G_{p/A}(y) \sim (1-y)^{2N_s-1} = (1-y)^{6A-7}$ where $N_s = 3(A-1)$ is the number of quark spectators required to "stop" ($y_i \to 0$) as $y \to 1$. This simple formula has been quite successful in accounting for distributions measured in the forward fragmentation of nuclei at the BEVALAC.[105] Color transparency can also be studied by measuring quasiexclusive J/ψ production by anti-protons in a nuclear target $\bar{p}A \to J/\psi(A-1)$ where the nucleus is left in a ground or excited state, but extra hadrons are not created (see Fig. 45). The cross section involves a convolution of the $\bar{p}p \to J/\psi$ subprocess cross section with the distribution $G_{p/A}(y)$ where $y = (p^0 + p^3)/(p^0_A + p^3_A)$ is the boost-invariant light-cone fraction for protons in the nucleus. This distribution can be determined from quasiexclusive lepton-nucleon scattering $\ell A \to \ell p(A-1)$.

In first approximation $\bar{p}p \to J/\psi$ involves $qqq + \overline{qqq}$ annihilation into three charmed quarks. The transverse momentum integrations are controlled by the charm mass scale and thus only the Fock state of the incident antiproton which contains three antiquarks at small impact separation can annihilate. Again it follows that this state has a relatively small color dipole moment, and thus it

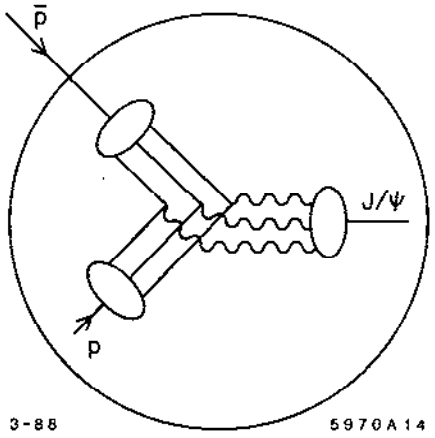

Figure 45. Schematic representation of quasielastic charmonium production in $\bar{p}A$ reactions.

should have a longer than usual mean-free path in nuclear matter; *i.e.* color transparency. Unlike traditional expectations, QCD predicts that the $\bar{p}p$ annihilation into charmonium is not restricted to the front surface of the nucleus. The exact nuclear dependence depends on the formation time for the physical $\bar{p}$ to couple to the small $\overline{qqq}$ configuration, $\tau_F \propto E_p$. It may be possible to study the effect of finite formation time by varying the beam energy, E_p, and using the Fermi-motion of the nucleon to stay at the J/ψ resonance. Since the J/ψ is produced at nonrelativistic velocities in this low energy experiment, it is formed inside the nucleus. The A-dependence of the quasiexclusive reaction can thus be used to determine the J/ψ-nucleon cross section at low energies. For a normal hadronic reaction $\bar{p}A \rightarrow HX$, we expect $A_{\rm eff} \sim A^{1/3}$, corresponding to absorption in the initial and final state. In the case of $\bar{p}A \rightarrow J/\psi\ X$ one expects $A_{\rm eff}$ much closer to A^1 if color transparency is fully effective and $\sigma(J/\psi\ N)$ is small.

9. SPIN CORRELATIONS IN PROTON-PROTON SCATTERING

One of the most serious challenges to quantum chromodynamics is the behavior of the spin-spin correlation asymmetry $A_{NN} = \frac{[d\sigma(\uparrow\uparrow) - d\sigma(\uparrow\downarrow)]}{[d\sigma(\uparrow\uparrow) + d\sigma(\uparrow\downarrow)]}$ measured in large momentum transfer pp elastic scattering (see Fig. 46). At $p_{lab} = 11.75$ GeV/c and $\theta_{\rm cm} = \pi/2$, A_{NN} rises to $\simeq 60\%$, corresponding to four times more probability for protons to scatter with their incident spins both normal to the scattering plane and parallel, rather than normal and opposite.

The polarized cross section shows a striking energy and angular dependence not expected from the slowly-changing perturbative QCD predictions. However,

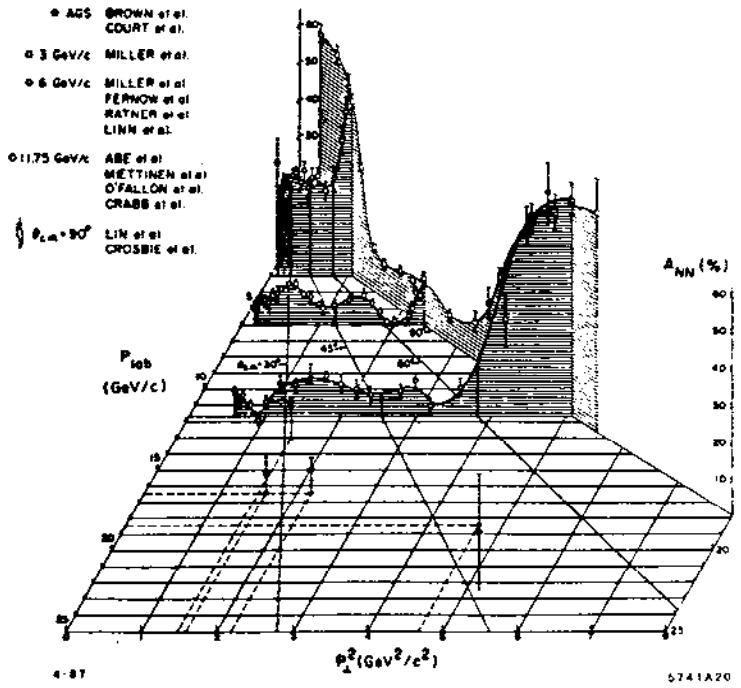

Figure 46. The spin-spin correlation A_{NN} for elastic pp scattering with beam and target protons polarized normal to the scattering plane.[106] $A_{NN} = 60\%$ implies that it is four times more probable for the protons to scatter with spins parallel rather than antiparallel.

the unpolarized data is in first approximation consistent with the fixed angle scaling law $s^{10}d\sigma/dt(pp \to pp) = f(\theta_{CM})$ expected from the perturbative analysis (see Fig. 23). The onset of new structure[107] at $s \simeq 23$ GeV^2 is a sign of new degrees of freedom in the two-baryon system. In this section, we will discuss a possible explanation[103] for (1) the observed spin correlations, (2) the deviations from fixed-angle scaling laws, and (3) the anomalous energy dependence of absorptive corrections to quasielastic pp scattering in nuclear targets, in terms of a simple model based on two $J = L = S = 1$ broad resonances (or threshold enhancements) interfering with a perturbative QCD quark-interchange background amplitude. The structures in the $pp \to pp$ amplitude may be associated with the onset of strange and charmed thresholds. If this view is correct, large angle pp elastic scattering would have been virtually featureless for $p_{lab} \geq 5$ GeV/c, had it not been for the onset of heavy flavor production. As a further illustration of the threshold effect, one can see the effect in A_{NN} due to a narrow $^3F_3$ pp resonance at $\sqrt{s} = 2.17$ GeV ($p_{lab} = 1.26$ GeV/c) associated with the $p\Delta$ threshold.

The perturbative QCD analysis[2] of exclusive amplitudes assumes that large momentum transfer exclusive scattering reactions are controlled by short distance

quark-gluon subprocesses, and that corrections from quark masses and intrinsic transverse momenta can be ignored. The main predictions are fixed-angle scaling laws[5] (with small corrections due to evolution of the distribution amplitudes, the running coupling constant, and pinch singularities), hadron helicity conservation,[6] and the novel phenomenon, "color transparency."

As discussed in Section 8.2, a test of color transparency in large momentum transfer quasielastic pp scattering at $\theta_{\rm cm} \simeq \pi/2$ has recently been carried out at BNL using several nuclear targets (C, Al, Pb).[101] The attenuation at $p_{lab} = 10$ GeV/c in the various nuclear targets was observed to be in fact much less than that predicted by traditional Glauber theory (see Fig. 44). This appears to support the color transparency prediction.

The expectation from perturbative QCD is that the transparency effect should become even more apparent as the momentum transfer rises. Nevertheless, at $p_{lab} = 12$ GeV/c, normal attenuation was observed. One can explain this surprising result if the scattering at $p_{lab} = 12$ GeV/c ($\sqrt{s} = 4.93$ GeV), is dominated by an s-channel B=2 resonance (or resonance-like structure) with mass near 5 GeV, since unlike a hard-scattering reaction, a resonance couples to the fully-interacting large-scale structure of the proton. If the resonance has spin $S = 1$, this can also explain the large spin correlation A_{NN} measured nearly at the same momentum, $p_{lab} = 11.75$ GeV/c. Conversely, in the momentum range $p_{lab} = 5$ to 10 GeV/c one predicts that the perturbative hard-scattering amplitude is dominant at large angles. The experimental observation of diminished attenuation at $p_{lab} = 10$ GeV/c thus provides support for the QCD description of exclusive reactions and color transparency.

What could cause a resonance at $\sqrt{s} = 5$ GeV, more than 3 GeV beyond the pp threshold? There are a number of possibilities: (a) a multigluonic excitation such as $|qqqqqqggg\rangle$, (b) a "hidden color" color singlet $|qqqqqq\rangle$ excitation,[108] or (c) a "hidden flavor" $|qqqqqqQ\overline{Q}\rangle$ excitation, which is the most interesting possibility, since it is so predictive. As in QED, where final state interactions give large enhancement factors for attractive channels in which $Z\alpha/v_{rel}$ is large, one expects resonances or threshold enhancements in QCD in color-singlet channels at heavy quark production thresholds since all the produced quarks have similar velocities.[109] One thus can expect resonant behavior at $M^* = 2.55$ GeV and $M^* = 5.08$ GeV, corresponding to the threshold values for open strangeness: $pp \to \Lambda K^+ p$, and open charm: $pp \to \Lambda_c D^0 p$, respectively. In any case, the structure at 5 GeV is highly inelastic: its branching ratio to the proton-proton channel is $B^{pp} \simeq 1.5\%$.

A model for this phenomenon is given in Ref. 103 In order not to over com-

plicate the phenomenology; the simplest Breit–Wigner parameterization of the resonances was used. There has not been an attempt to optimize the parameters of the model to obtain a best fit. It is possible that what is identified a single resonance is actually a cluster of resonances.

The background component of the model is the perturbative QCD amplitude. Although complete calculations are not yet available, many features of the QCD predictions are understood, including the approximate s^{-4} scaling of the $pp \to pp$ amplitude at fixed $\theta_{\rm cm}$ and the dominance of those amplitudes that conserve hadron helicity.[6] Furthermore, recent data comparing different exclusive two-body scattering channels from BNL[33] show that quark interchange amplitudes[110] dominate quark annihilation or gluon exchange contributions. Assuming the usual symmetries, there are five independent pp helicity amplitudes: $\phi_1 = M(++,++)$, $\phi_2 = M(--,++)$, $\phi_3 = M(+-,+-)$, $\phi_4 = M(-+,+-)$, $\phi_5 = M(++,+-)$. The helicity amplitudes for quark interchange have a definite relationship:[40]

$$\phi_1(\mathrm{PQCD}) = 2\phi_3(\mathrm{PQCD}) = -2\phi_4(\mathrm{PQCD})$$
$$= 4\pi C F(t)F(u)[\frac{t-m_d^2}{u-m_d^2} + (u \leftrightarrow t)]e^{i\delta} \quad .$$

The hadron helicity nonconserving amplitudes, $\phi_2(\mathrm{PQCD})$ and $\phi_5(\mathrm{PQCD})$ are zero. This form is consistent with the nominal power-law dependence predicted by perturbative QCD and also gives a good representation of the angular distribution over a broad range of energies.[111] Here $F(t)$ is the helicity conserving proton form factor, taken as the standard dipole form: $F(t) = (1 - t/m_d^2)^{-2}$, with $m_d^2 = 0.71$ GeV^2. As shown in Ref. 40, the PQCD-quark-interchange structure alone predicts $A_{NN} \simeq 1/3$, nearly independent of energy and angle.

Because of the rapid fixed-angle s^{-4} falloff of the perturbative QCD amplitude, even a very weakly-coupled resonance can have a sizeable effect at large momentum transfer. The large empirical values for A_{NN} suggest a resonant $pp \to pp$ amplitude with $J = L = S = 1$ since this gives $A_{NN} = 1$ (in absence of background) and a smooth angular distribution. Because of the Pauli principle, an $S = 1$ di-proton resonances must have odd parity and thus odd orbital angular momentum. The the two non-zero helicity amplitudes for a $J = L = S = 1$ resonance can be parameterized in Breit–Wigner form:

$$\phi_3(\mathrm{resonance}) = 12\pi \frac{\sqrt{s}}{p_{\rm cm}} d^1_{1,1}(\theta_{\rm cm}) \frac{\frac{1}{2}\Gamma^{pp}(s)}{M^* - E_{\rm cm} - \frac{i}{2}\Gamma} \quad ,$$

$$\phi_4(\text{resonance}) = -12\pi \frac{\sqrt{s}}{p_{\rm cm}} d^1_{-1,1}(\theta_{\rm cm}) \frac{\frac{1}{2}\Gamma^{pp}(s)}{M^* - E_{\rm cm} - \frac{i}{2}\Gamma} \quad .$$

(The ${}^3F_3$ resonance amplitudes have the same form with $d^3_{\pm 1,1}$ replacing $d^1_{\pm 1,1}$.) As in the case of a narrow resonance like the Z^0, the partial width into nucleon pairs is proportional to the square of the time-like proton form factor: $\Gamma^{pp}(s)/\Gamma = B^{pp}|F(s)|^2/|F(M^{*2})|^2$, corresponding to the formation of two protons at this invariant energy. The resonant amplitudes then die away by one inverse power of $(E_{\rm cm} - M^*)$ relative to the dominant PQCD amplitudes. (In this sense, they are higher twist contributions relative to the leading twist perturbative QCD amplitudes.) The model is thus very simple: each pp helicity amplitude ϕ_i is the coherent sum of PQCD plus resonance components: $\phi = \phi(\text{PQCD}) + \Sigma\phi(\text{resonance})$. Because of pinch singularities and higher-order corrections, the hard QCD amplitudes are expected to have a nontrivial phase;[43] the model allows for a constant phase δ in $\phi(\text{PQCD})$. Because of the absence of the ϕ_5 helicity-flip amplitude, the model predicts zero single spin asymmetry A_N. This is consistent with the large angle data at $p_{lab} = 11.75$ GeV/c.[112]

At low transverse momentum, $p_T \leq 1.5$ GeV, the power-law fall-off of $\phi(\text{PQCD})$ in s disagrees with the more slowly falling large-angle data, and one has little guidance from basic theory. The main interest in this low-energy region is to illustrate the effects of resonances and threshold effects on A_{NN}. In order to keep the model tractable, one can extend the background quark interchange and the resonance amplitudes at low energies using the same forms as above but replacing the dipole form factor by a phenomenological form $F(t) \propto e^{-1/2\beta\sqrt{|t|}}$. A kinematic factor of $\sqrt{s}/2p_{\rm cm}$ is included in the background amplitude. The value $\beta = 0.85$ GeV^{-1} then gives a good fit to $d\sigma/dt$ at $\theta_{\rm cm} = \pi/2$ for $p_{lab} \leq 5.5$ GeV/c.[113] The normalizations are chosen to maintain continuity of the amplitudes.

The predictions of the model and comparison with experiment are shown in Figs. 47–52. The following parameters are chosen: $C = 2.9 \times 10^3$, $\delta = -1$ for the normalization and phase of $\phi(\text{PQCD})$. The mass, width and pp branching ratio for the three resonances are $M^*_d = 2.17$ GeV, $\Gamma_d = 0.04$ GeV, $B^{pp}_d = 1$; $M^*_s = 2.55$ GeV, $\Gamma_s = 1.6$ GeV, $B^{pp}_s = 0.65$; and $M^*_c = 5.08$ GeV, $\Gamma_c = 1.0$ GeV, $B^{pp}_c = 0.0155$, respectively. As shown in Figs. 47 and 48, the deviations from the simple scaling predicted by the PQCD amplitudes are readily accounted for by the resonance structures. The cusp which appears in Fig. 48 marks the change in regime below $p_{lab} = 5.5$ GeV/c where PQCD becomes inapplicable. It is interesting to note that in this energy region normal attenuation of quasielastic pp scattering is observed.[101] The angular distribution (normalized to the data

at $\theta_{cm} = \pi/2$) is predicted to broaden relative to the steeper perturbative QCD form, when the resonance dominates. As shown in Fig. 49 this is consistent with experiment, comparing data at $p_{lab} = 7.1$ and 12.1 GeV/c.

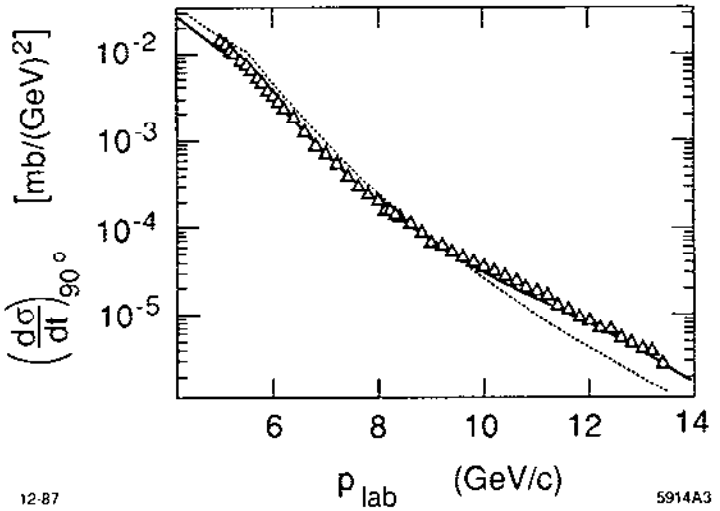

Figure 47. Prediction (solid curve) for $d\sigma/dt(pp \to pp)$ at $\theta_{cm} = \pi/2$ compared with the data of Akerlof *et al.*[113] The dotted line is the background PQCD prediction.

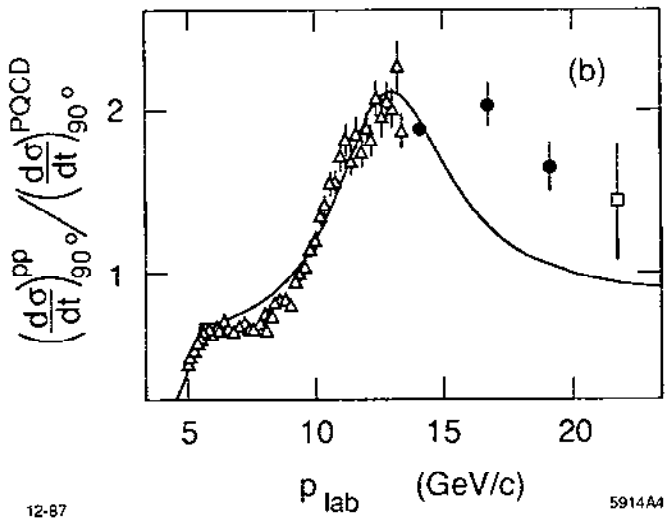

Figure 48. Ratio of $d\sigma/dt(pp \to pp)$ at $\theta_{cm} = \pi/2$ to the PQCD prediction. The data[113] are from Akerlof *et al.* (open triangles), Allaby *et al.* (solid dots) and Cocconi *et al.* (open square). The cusp at $p_{lab} = 5.5$ GeV/c indicates the change of regime from PQCD.

The most striking test of the model is its prediction for the spin correlation A_{NN} shown in Fig. 50. The rise of A_{NN} to $\simeq 60\%$ at $p_{lab} = 11.75$ GeV/c is correctly reproduced by the high energy J=1 resonance interfering with ϕ(PQCD). The narrow peak which appears in the data of Fig. 50 corresponds to the onset

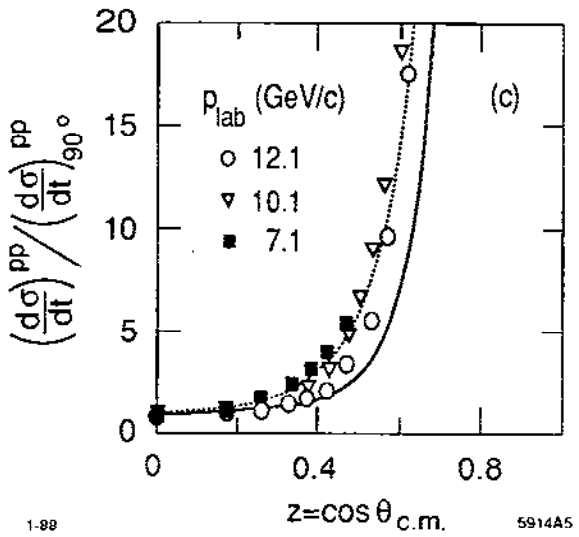

Figure 49. The $pp \to pp$ angular distribution normalized at $\theta_{cm} = \pi/2$. The data are from the compilation given in Sivers *et al.*, Ref. 32. The solid and dotted lines are predictions for p_{lab} = 12.1 and 7.1 GeV/c, respectively, showing the broadening near resonance.

of the $pp \to p\Delta(1232)$ channel which can be interpreted as a $uuuuddq\bar{q}$ resonant state. Because of spin-color statistics one expects in this case a higher orbital momentum state, such as a pp $^3F_3$ resonance. The model is also consistent with the recent high-energy data point for A_{NN} at p_{lab} = 18.5 GeV/c and p_T^2 = 4.7 GeV^2 (see Fig. 51). The data show a dramatic decrease of A_{NN} to zero or negative values. This is explained in the model by the destructive interference effects above the resonance region. The same effect accounts for the depression of A_{NN} for $p_{lab} \approx 6$ GeV/c shown in Fig. 50. The comparison of the angular dependence of A_{NN} with data at p_{lab} = 11.75 GeV/c is shown in Fig. 52. The agreement with the data[114] for the longitudinal spin correlation A_{LL} at the same p_{lab} is somewhat worse.

The simple model discussed here shows that many features can be naturally explained with only a few ingredients: a perturbative QCD background plus resonant amplitudes associated with rapid changes of the inelastic pp cross section. The model provides a good description of the s and t dependence of the differential cross section, including its "oscillatory" dependence[115] in s at fixed θ_{cm}, and the broadening of the angular distribution near the resonances. Most important, it gives a consistent explanation for the striking behavior of both the spin-spin correlations and the anomalous energy dependence of the attenuation of quasielastic pp scattering in nuclei. It is predicted that color transparency should reappear at higher energies ($p_{lab} \geq 16$ GeV/c), and also at smaller angles ($\theta_{cm} \approx 60°$) at p_{lab} = 12 GeV/c where the perturbative QCD amplitude dominates. If the J=1 resonance structures in A_{NN} are indeed associated with heavy

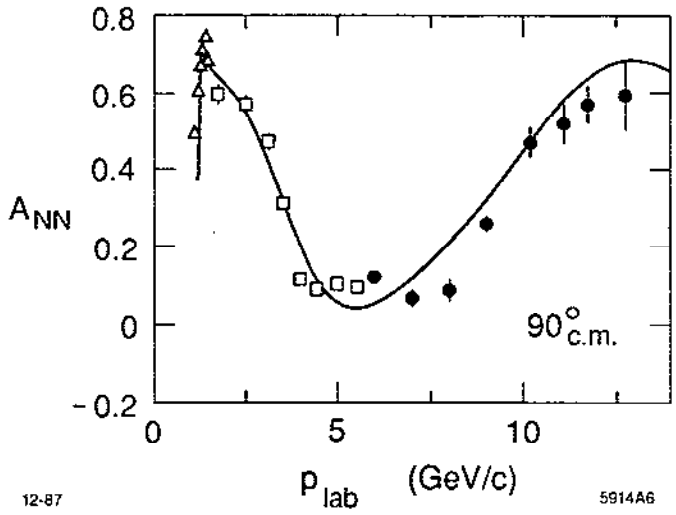

Figure 50. A_{NN} as a function of p_{lab} at $\theta_{cm} = \pi/2$. The data[113] are from Crosbie *et al.* (solid dots), Lin *et al.* (open squares) and Bhatia *et al.* (open triangles). The peak at $p_{lab} = 1.26$ GeV/c corresponds to the $p\Delta$ threshold. The data are well reproduced by the interference of the broad resonant structures at the strange ($p_{lab} = 2.35$ GeV/c) and charm ($p_{lab} = 12.8$ GeV/c) thresholds, interfering with a PQCD background. The value of A_{NN} from PQCD alone is 1/3.

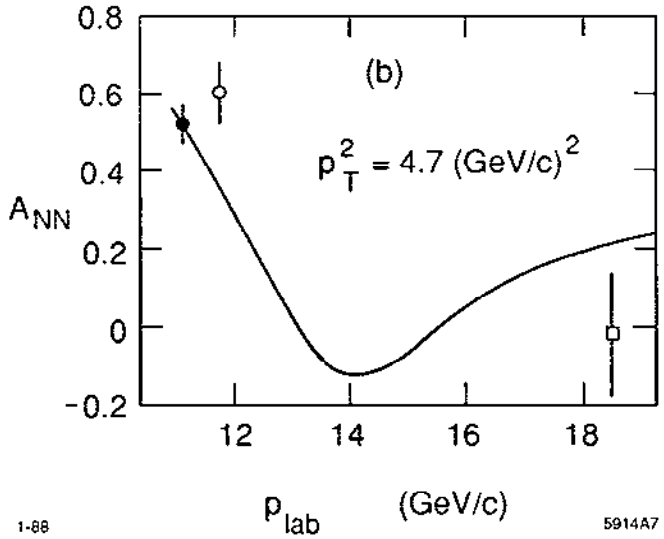

Figure 51. A_{NN} at fixed $p_T^2 = (4.7$ GeV/c$)^2$. The data point[113] at $p_{lab} = 18.5$ GeV/c is from Court *et al.*

quark degrees of freedom, then the model predicts inelastic pp cross sections of the order of 1 mb and 1μb for the production of strange and charmed hadrons near their respective thresholds.[116] Thus a crucial test of the heavy quark hypothesis for explaining A_{NN}, rather than hidden color or gluonic excitations, is the observation of significant charm hadron production at $p_{lab} \geq 12$ GeV/c.

Recently Ralston and Pire[43] have proposed that the oscillations of the pp elastic cross section and the apparent breakdown of color transparency are associated

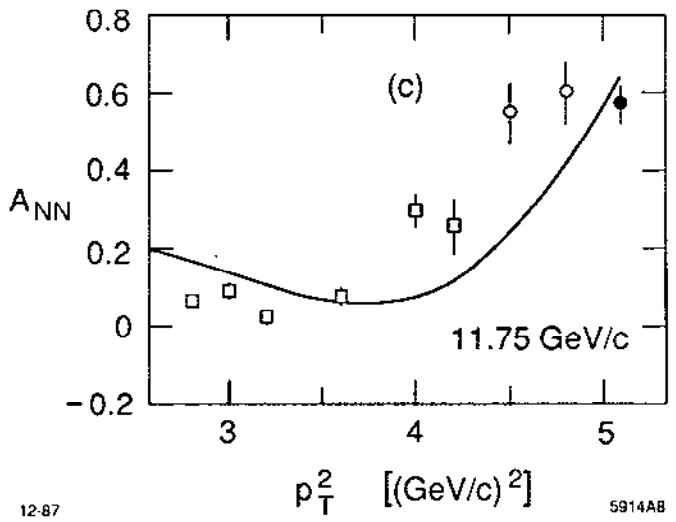

Figure 52. A_{NN} as a function of transverse momentum. The data[106] are from Crabb *et al.* (open circles) and O'Fallon *et al.* (open squares). Diffractive contributions should be included for $p_T^2 \leq 3$ GeV^2.

with the dominance of the Landshoff pinch contributions at $\sqrt{s} \sim 5$ GeV. The oscillating behavior of $d\sigma/dt$ is due to the energy dependence of the relative phase between the pinch and hard-scattering contributions. Color transparency will disappear whenever the pinch contributions are dominant since such contributions could couple to wavefunctions of large transverse size. The large spin correlation in A_{NN} is not readily explained in the Ralston-Pire model. Clearly more data and analysis are needed to discriminate between the pinch and resonance models.

10. CONCLUSIONS

The understanding of exclusive processes is a crucial challenge to QCD. The analysis of these reactions is more complex than that of inclusive reactions since the detailed predictions necessarily depend on the form of the hadronic wavefunctions, the behavior of the running coupling constant, and analytically complex contributions from pinch and endpoint singularities. Unlike inclusive reactions, where the leading power contributions can be computed from an incoherent probabilistic form, exclusive reactions require the understanding of the phase and spin structure of hadronic amplitudes. These complications are also a virtue of exclusive reactions, since they allow a window on basic features of the theory which are extremely difficult to obtain in any other way. The perturbative QCD analysis is based on a factorization theorem so that only one distribution amplitude is required to describe the interaction of a given hadron in any large momentum transfer exclusive reaction. In some cases the predictions for exclusive processes in PQCD are completely rigorous in the sense that the results can be derived to

all orders in perturbation theory. In particular the PQCD results for the pion form factor, the transition form factor $F_{\gamma\pi}(Q^2)$, and the $\gamma\gamma \to \pi\pi$ amplitudes are theorems of QCD and are as rigorous as the predictions for $R_{e^+e^-}(s)$, the evolution equations for the structure functions, etc. Although the perturbative QCD analysis is complex, it is hard to imagine that any other viable description would be simpler. At this point there is no other theoretical approach which provides as comprehensive a description of exclusive phenomena.

The application of perturbative QCD to exclusive processes has in fact been quite successful. The power laws predicted for form factors and fixed angle scattering amplitudes have been confirmed by experiment, ranging from the theoretically simplest reactions $\gamma^*\gamma \to \eta$ to the most complicated reactions such as $pp \to pp$. The application to nuclear exclusive amplitudes such as the deuteron form factor and $\gamma d \to np$ have also been surprisingly successful. Taken together with input from distribution amplitudes predicted by QCD sum rules, the sign and magnitude of the meson form factors, the $\gamma\gamma \to \pi^+\pi^-$, K^+K^-, the Compton amplitude $\gamma p \to \gamma p$ and the proton form factor are all apparent, though model dependent, successes of the theory.

The fact that PQCD scaling laws appear to hold even at momentum transfer as low as 1 GeV/c suggests that the QCD running coupling constant is rather slowly changing even at momentum transfers of order 200 MeV. Barring a conspiracy between non-perturbative and perturbative contributions, the evidence from exclusive reactions is that $\Lambda^{QCD}_{\overline{MS}}$ is of order 100 MeV or even smaller. Alternatively the running coupling constant may "freeze" at the low effective momenta characteristic of exclusive processes. Thus the analysis of exclusive reactions provides important information on the basic parameters of QCD.

As we discussed in Section 8.2, recent BNL data for pp quasi-elastic scattering in nuclei at $\theta_{cm} = \frac{\pi}{2}$ shows that the number of effective protons in the nucleus rises with the momentum transfer as predicted by color transparency at least up to $p_{lab} = 10\ GeV/c$. This remarkable empirical result clearly rules out any description of exclusive reactions based on soft wavefunctions. The observation of the onset of color transparency in quasi-elastic $pp \to pp$ scattering appears to be an outstanding validation of a fundamental feature of perturbative QCD phenomenology. The tests of color transparency address directly the central dynamical assumption of the perturbative analysis, that exclusive reactions at high momentum transfer are controlled by Fock components of the hadron wavefunction with small transverse size.

However, in direct contradiction to PQCD expectations, the BNL data at higher momentum, $p_{lab} = 12\ GeV/c$, indicates normal Glauber attenuation. Be-

cause of the importance of this and other anomalies and the challenges they pose to the theory, we have devoted several sections of this article to these topics and their possible resolution.

The successes of fixed-angle scaling laws could of course be illusory, perhaps due to soft hadronic mechanisms which temporarily simulate the dimensional counting rules at a range of intermediate momentum transfer. If such a description is correct, then the perturbative contributions become dominant only at very large momentum transfer. Quantities such as $Q^2F_\pi(Q^2)$ would drop from the present plateau to the PQCD prediction, but at a high value of Q^2, much higher than the natural scales of the theory. An important question is whether a soft hadronic model can also account for the normalization of the cross sections for other exclusive processes besides form factor measurements. For example, consider hadronic Compton amplitudes such as $\gamma p \to \gamma p$ or $\gamma\gamma \to \pi^+\pi^-$. As we have shown in Section 7, the data appear to scale in momentum transfer according to the perturbative QCD predictions. One can consider a simple model where the hadronic Compton amplitude is given by the product of a point-like Compton amplitude multiplied by the corresponding hadronic form factor. This model predicts $d\sigma/dt(\gamma p \to \gamma p) \simeq 5\ pb/GeV^2$ at $s = 8\ GeV^2$, $\theta_{cm} = \pi/2$ compared to the experimental value of 300 pb/GeV^2 (see Fig. 33). The same simple model predicts $\sigma(\gamma\gamma \to \pi^+\pi^-) \simeq 0.1\ nb$ at $s = 5\ GeV^2$ compared to the experimental value of 2 nb (see Fig. 31).

The above estimates are also characteristic of the soft-scattering models in which the end-point large x regime dominates so that the Compton amplitude is given by the sum of coherent point-like quark Compton amplitudes with $x_q \simeq 1$ multiplied by the electromagnetic form factor. Again one has the problem that the normalization of data for large angle Compton scattering is one to two orders of magnitude larger than predicted. In contrast, in the perturbative QCD description there are many more contributing coherent hard scattering amplitudes for Compton scattering than lepton-proton scattering, so the large relative magnitude of the proton Compton cross section can be accounted for. In the case of large angle pp scattering, the large normalization of the data relative to that obtained by simply multiplying form factors can be understood as a consequence of the many coherent contributions to T_H for this process. We also emphasize that the observation of color transparency in the BNL experiment implies minimal attenuation of the incident and outgoing protons and thus appears to exclude any model in which the full size of the hadron participates in the hard scattering reaction.

Questions have been raised recently[24] on a number of questions concerning the application of perturbative QCD to exclusive reactions in the momentum

transfer range presently accessible to experiment. The issues involved are very important for understanding the basis of virtually all perturbative QCD predictions. The debate is not on the validity of the predictions but on the appropriate range of their applicability because of possible complications such as nonperturbative effects. The questions raised highlight the importance of further experimental tests of exclusive processes.

As we have discussed in this article, there are, in addition to the numerous successes of the theory, a number of major conflicts between perturbative QCD predictions for exclusive processes and experiment which can not be readily blamed on higher contributions in $\alpha_s(Q^2)$. For example, the helicity selection rule appears to be broken in $\pi p \to \rho^0 p$ scattering at large angles, the $J/\psi \to \pi\rho$ and $J/\psi \to KK^*$ decays. The strong spin correlations seen in large angle pp scattering at $\sqrt{s} = 5\ GeV$ are not explained by PQCD mechanisms. Color transparency appears to fail at the same energy. Small but systematic deviations or oscillations are observed relative to the PQCD power-law behavior. In each case, the data seems to indicate the intrusion of soft non-perturbative QCD mechanisms such as resonances perhaps due to gluonic or color excitations or heavy quark threshold effects. The presence of contributions from Landshoff pinch singularities may also be indicated.

Thus exclusive reactions still remain a challenge to theory. A crucial requirement for future progress is the computation of hadron light-cone wavefunctions directly from QCD. Unfortunately it appears very difficult to obtain much more than the leading moments of the distribution amplitude from either lattice gauge theory or QCD sum rules. The discretized light-cone quantization method reviewed in Appendix III shows promise, but so far solutions have been limited to QCD in one space and one time dimension. The computation of hadronic structure functions, magnetic moments, and electroweak decay amplitudes also require this non-perturbative input. The detailed understanding of the relative role of perturbative and non-perturbative contributions to exclusive amplitudes will unquestionably require a fuller understanding of the hadronic wavefunctions.

Much more theoretical work is also required to compute the hard scattering amplitudes for experimentally accessible exclusive processes, and to understand in detail how to integrate over the pinch and endpoint singularities, taking into account Sudakov suppression in the non-Abelian theory. The computerized algebraic methods now available can be used to compute the hard-scattering quark-gluon amplitude T_H for processes as complicated as $pp \to pp$ and the deuteron form factor. Each Feynman diagram which contributes to T_H represents a particular overlap of the participating hadron wavefunctions. Considering the uncertainties in the wavefunctions and the myriad number of diagrams contributing

to pp scattering, even getting the correct order of magnitude of the large angle cross section would be a triumph of the theory. Computations of the higher order corrections to high momentum transfer exclusive reactions will eventually also be needed.

More precise predictions for color transparency is needed, particularly ep quasi-elastic scattering in nuclei. The analysis requires computing the detailed parameters which control the color transparency effect due to smallness of the participating Fock state amplitude, and by uncertainties involving the role of formation zone physics, which controls the length of time the hadron can stay small as it traverses the nucleus.

The experimental study of exclusive reactions is also in its infancy. Much more experimental input is required particularly from ep, γp, $\bar{p}p$, and $\gamma\gamma$ initial states. Ratios of processes such as $\gamma\gamma \to p\bar{p}$ and $\Delta^{++}\overline{\Delta}^{++}$ can isolate important features of the baryon wavefunctions. The ratio of the square transition form factor for $\gamma^*\gamma \to \pi^0$ to the pion form factor provides a wave-function independent determination of $\alpha_s(Q^2)$. It is important to confirm the color transparency phenomena, particularly in the simplest channels such as ep quasi-elastic scattering. It is important to verify that both elastic and inelastic initial and final state interactions are suppressed in the nucleus. Once this phenomena is validated it can be used as a "color filter" to separate soft and hard contributions to a large range of exclusive reactions.

We have emphasized in this article that the correctness of the PQCD description of exclusive processes is by no means settled. There is now a strong challenge to design decisive experimental and theoretical tests of the theory. If the theory survives, the reward is high: through exclusive reactions we can explore both the behavior of QCD and the structure of hadrons.

APPENDIX I
BARYON FORM FACTORS AND EVOLUTION EQUATIONS

The meson form factor analysis given in Section 3 is the prototype for the calculation of the QCD hard scattering contribution for the whole range of exclusive processes at large momentum transfer. Away from possible special points in the x_i integrations a general hadronic amplitude can be written to leading order in $1/Q^2$ as a convolution of a connected hard-scattering amplitude T_H convoluted with the meson and baryon distribution amplitudes:

$$\phi_M(x,Q) = \int^{|\mathcal{E}|<Q^2} \frac{d^2k_\perp}{16\pi^2}\psi^Q_{q\bar{q}}(x,\vec{k}_\perp) \quad ,$$

and

$$\phi_B(x_i,Q) = \int^{|\mathcal{E}|<Q^2} [d^2k_\perp]\psi_{qqq}(x_i,\vec{k}_{\perp i}) \ .$$

The hard scattering amplitude T_H is computed by replacing each external hadron line by massless valence quarks each collinear with the hadron's momentum $p_i^\mu \cong x_i p_H^\mu$. For example the baryon form factor at large Q^2 has the form[4,6]

$$G_M(Q^2) = \int [dx][dy]\phi^*(y_i,\overline{Q})T_H(x,y;Q^2)\phi(x,\overline{Q})$$

where T_H is the $3q+\gamma \to 3q'$ amplitude. For the proton and neutron we have to leading order $[C_B = 2/3]$

$$T_p = \frac{128\pi^2 C_B^2}{(Q^2+M_0^2)^2}\ T_1$$
$$T_n = \frac{128\pi^2 C_B^2}{3(Q^2+M_0^2)^2}\ [T_1 - T_2]$$

where

$$T_1 = -\frac{\alpha_s(x_3y_3Q^2)\ \alpha_s(1-x_1)(1-y_1)Q^2)}{x_3(1-x_1)^2\ y_3(1-y_1)^2} + \frac{\alpha_s(x_2y_2Q^2)\ \alpha_s\left((1-x_1)(1-y_1)Q^2\right)}{x_2(1-x_1)^2\ y_2(1-y_1)^2} - \frac{\alpha_s(x_2y_2Q^2)\ \alpha_s(x_3y_3Q^2)}{x_2x_3(1-x_3)\ y_2y_3(1-y_1)}$$

and

$$T_2 = -\frac{\alpha_s(x_1y_1Q^2)\ \alpha_s(x_3y_3Q^2)}{x_1x_3(1-x_1)\ y_1y_3(1-y_3)} \ .$$

T_1 corresponds to the amplitude where the photon interacts with the quarks (1) and (2) which have helicity parallel to the nucleon helicity, and T_2 corresponds to the amplitude where the quark with opposite helicity is struck. The running coupling constants have arguments $\hat{Q}^2$ corresponding to the gluon momentum transfer of each diagram. Only the large Q^2 behavior is predicted by the theory; we utilize the parameter M_0 to represent the effect of power-law suppressed terms from mass insertions, higher Fock states, etc.

The Q^2-evolution of the baryon distribution amplitude can be derived from the operator product expansion of three quark fields or from the gluon exchange kernel, in parallel with derivation of Eq. (90). The baryon evolution equation to leading order in α_s is[6]

$$x_1x_2x_3\left\{\frac{\partial}{\partial\zeta}\tilde{\phi}(x_i,Q)+\frac{3}{2}\frac{C_F}{\beta_0}\tilde{\phi}(x_i,Q)\right\}=\frac{C_B}{\beta_0}\int_0^1[dy]V(x_i,y_i)\tilde{\phi}(y_i,Q).$$

Here $\phi=x_1x_2x_3\tilde{\phi},\zeta=\log(\log Q^2/\Lambda^2)$, $C_F=(n_c^2-1)/2n_c=4/3$, $C_B=(n_c+1)/2n_c=2/3$, $\beta=11-(2/3)n_f$, and $V(x_i,y_i)$ is computed to leading order in α_s from the single-gluon-exchange kernel [see Fig. 19(b)]:

$$\begin{aligned}V(x_i,y_i)&=2x_ix_2x_3\sum_{i\neq j}\theta(y_i-x_i)\delta(x_k-y_k)\frac{y_j}{x_j}\left(\frac{\delta_{h,\bar{h}_j}}{x_i+x_j}+\frac{\Delta}{y_i-x_i}\right)\\&=V(y_i,x_i)\quad .\end{aligned}$$

The infrared singularity at $x_i=y_i$ is cancelled because the baryon is a color singlet.

The evolution equation automatically sums to leading order in $\alpha_s(Q^2)$ all of the contributions from multiple gluon exchange which determine the tail of the valence wavefunction and thus the Q^2-dependence of the distribution amplitude. The general solution of this equation is

$$\phi(x_i,Q)=x_1x_2x_3\sum_{n=0}^{\infty}a_n\left(\ell n\frac{Q^2}{\Lambda^2}\right)^{-\gamma_n}\quad\phi_n(x_i)\quad ,$$

where the anomalous dimensions γ_n and the eigenfunctions $\tilde{\phi}_n(x_i)$ satisfy the characteristic equation:

$$x_1x_2x_3\left(-\gamma_n+\frac{3C_F}{2\beta}\right)\tilde{\phi}_n(x_i)=\frac{C_B}{\beta}\int_0^1[dy]\;V(x_i,y_i)\,\tilde{\phi}_n(y_i)\quad .$$

A useful technique for obtaining the solution to the evolution equations is to construct completely antisymmetric representations as a polynomial orthonormal

basis for the distribution amplitude of multiquark bound states. In this way one obtain a distinctive classification of nucleon (N) and delta (Δ) wave functions and the corresponding Q^2 dependence which discriminates N and Δ form factors. This technique is developed in detail in Ref. 117.

Taking into account the evolution of the baryon distribution amplitude, the nucleon magnetic form factors at large Q^2, has the form[4,6]

$$G_M(Q^2) \to \frac{\alpha_s^2(Q^2)}{Q^4} \sum_{n,m} b_{nm} \left(\log \frac{Q^2}{\Lambda^2} \right)^{\gamma_n^B - \gamma_n^B} \left[1 + \mathcal{O}\left(\alpha_s(Q^2), \frac{m^2}{Q^2} \right) \right]$$

where the γ_n are computable anomalous dimensions of the baryon three-quark wave function at short distance and the b_{mn} are determined from the value of the distribution amplitude $\phi_B(x, Q_0^2)$ at a given point Q_0^2 and the normalization of T_H. Asymptotically, the dominant term has the minimum anomalous dimension. The dominant part of the form factor comes from the region of the x_i integration where each quark has a finite fraction of the light cone momentum. The integrations over x_i and y_i have potential endpoint singularities. However, it is easily seen that any anomalous contribution [*e.g.* from the region $x_2, x_3 \sim \mathcal{O}(m/Q), x_1 \sim 1 - \mathcal{O}(m/Q)$] is asymptotically suppressed at large Q^2 by a Sudakov form factor arising from the virtual correction to the $\bar{q}\gamma q$ vertex when the quark legs are near-on-shell [$p^2 \sim \mathcal{O}(mQ)$].[6,19] This Sudakov suppression of the endpoint region requires an all orders resummation of perturbative contributions, and thus the derivation of the baryon form factors is not as rigorous as for the meson form factor, which has no such endpoint singularity.[19]

One can also use PQCD to predict ratios of various baryon and isobar form factors assuming isospin or $SU(3)$-flavor symmetry for the basic wave function structure. Results for the neutral weak and charged weak form factors assuming standard $SU(2) \times U(1)$ symmetry are given in Ref. 47.

APPENDIX II
LIGHT CONE QUANTIZATION AND PERTURBATION THEORY

In this Appendix, we outline the canonical quantization of QCD in $A^+ = 0$ gauge. The discussion follows that given in Refs. 4 and 51. This proceeds in several steps. First we identify the independent dynamical degrees of freedom in the Lagrangian. The theory is quantized by defining commutation relations for these dynamical fields at a given light-cone time $\tau = t + z$ (we choose $\tau = 0$). These commutation relations lead immediately to the definition of the Fock state basis. Expressing dependent fields in terms of the independent fields, we then

derive a light-cone Hamiltonian, which determines the evolution of the state space with changing τ. Finally we derive the rules for τ-ordered perturbation theory.

The major purpose of this exercise is to illustrate the origins and nature of the Fock state expansion, and of light-cone perturbation theory. We will ignore subtleties due to the large scale structure of non-Abelian gauge fields (e.g. 'instantons'), chiral symmetry breaking, and the like. Although these have a profound effect on the structure of the vacuum, the theory can still be described with a Fock state basis and some sort of effective Hamiltonian. Furthermore, the short distance interactions of the theory are unaffected by this structure, or at least this is the central ansatz of perturbative QCD.

Quantization

The Lagrangian (density) for QCD can be written

$$\mathcal{L} = -\frac{1}{2}\,\mathrm{Tr}\,(F^{\mu\nu}\,F_{\mu\nu}) + \overline{\psi}\,(i\,\not{D} - m)\,\psi$$

where $F^{\mu\nu} = \partial^\mu A^\nu - \partial^\nu A^\mu + ig[A^\mu, A^\nu]$ and $iD^\mu = i\partial^\mu - gA^\mu$. Here the gauge field A^μ is a traceless 3×3 color matrix ($A^\mu \equiv \sum_a A^{a\mu}T^a$, $\mathrm{Tr}(T^aT^b) = 1/2\delta^{ab}$, $[T^a, T^b] = ic^{abc}T^c, \ldots$), and the quark field ψ is a color triplet spinor (for simplicity, we include only one flavor). At a given light-cone time, say $\tau = 0$, the independent dynamical fields are $\psi_\pm \equiv \Lambda_\pm\psi$ and $A^i_\perp$ with conjugate fields $i\psi^\dagger_+$ and $\partial^+A^i_\perp$, where $\Lambda_\pm = \gamma^o\gamma^\pm/2$ are projection operators ($\Lambda_+\Lambda_- = 0$, $\Lambda_\pm^2 = \Lambda_\pm$, $\Lambda_+ + \Lambda_- = 1$) and $\partial^\pm = \partial^0 \pm \partial^3$. Using the equations of motion, the remaining fields in $\mathcal{L}$ can be expressed in terms of ψ_+, $A^i_\perp$:

$$\begin{aligned}
\psi_- \equiv \Lambda_-\psi &= \frac{1}{i\partial^+}\left[i\vec{D}_\perp\cdot\vec{\alpha}_\perp + \beta m\right]\psi_+ \\
&= \widetilde{\psi}_- - \frac{1}{i\partial^+}\,g\vec{A}_\perp\cdot\vec{\alpha}_\perp\,\psi_+\ , \\
A^+ &= 0\ , \\
A^- &= \frac{2}{i\partial^+}\,i\vec{\partial}_\perp\cdot\vec{A}_\perp + \frac{2g}{(i\partial^+)^2}\left\{\left[i\partial^+A^i_\perp, A^i_\perp\right] + 2\psi^\dagger_+\,T^a\,\psi_+\,T^a\right\} \\
&\equiv \widetilde{A}^- + \frac{2g}{(i\partial^+)^2}\left\{\left[i\partial^+A^i_\perp, A^i_\perp\right] + 2\psi^\dagger_+\,T^a\,\psi_+\,T^a\right\}\ ,
\end{aligned}$$

with $\beta = \gamma^o$ and $\vec{\alpha}_\perp = \gamma^o\vec{\gamma}$.

To quantize, we expand the fields at $\tau = 0$ in terms of creation and annihilation operators,

$$\psi_+(x) = \int\limits_{k^+>0} \frac{dk^+\, d^2k_\perp}{k^+\, 16\pi^3} \sum_\lambda \Big\{ b(\underline{k},\lambda)\; u_+(\underline{k},\lambda)\; e^{-ik\cdot x} + d^\dagger(\underline{k},\lambda)\; v_+(\underline{k},\lambda)\; e^{ik\cdot x} \Big\} \;, \quad \tau = x^+ = 0$$

$$A^i_\perp(x) = \int\limits_{k^+>0} \frac{dk^+\, d^2k_\perp}{k^+\, 16\pi^3} \sum_\lambda \Big\{ a(\underline{k},\lambda)\; \epsilon^i_\perp(\lambda)\; e^{-ik\cdot x} + c\,c^\cdot \Big\} \;, \quad \tau = x^+ = 0 \;,$$

with commutation relations ($\underline{k} = (k^+, \vec{k}_\perp)$):

$$\begin{aligned} \Big\{ b(\underline{k},\lambda),\; b^\dagger(\underline{p},\lambda) \Big\} &= \Big\{ d(\underline{k},\lambda),\; d^\dagger(\underline{p},\lambda') \Big\} \\ &= \Big[a(\underline{k},\lambda),\; a^\dagger(\underline{p},\lambda') \Big] \\ &= 16\pi^3\, k^+\, \delta^3(\underline{k}-\underline{p})\, \delta_{\lambda\lambda'} \;, \\ \{b,b\} = \{d,d\} &= \ldots = 0 \;, \end{aligned}$$

where λ is the quark or gluon helicity. These definitions imply canonical commutation relations for the fields with their conjugates ($\tau = x^+ = y^+ = 0$, $\underline{x} = (x^-, x_\perp), \ldots$):

$$\Big\{ \psi_+(\underline{x}),\; \psi^\dagger_+(\underline{y}) \Big\} = \Lambda_+\, \delta^3(\underline{x}-\underline{y}) \;,$$

$$\Big[A^i(\underline{x}),\; \partial^+ A^j_\perp(\underline{y}) \Big] = i\delta^{ij}\, \delta^3(\underline{x}-\underline{y}) \;.$$

The creation and annihilation operators define the Fock state basis for the theory at $\tau = 0$, with a vacuum $|0\rangle$ defined such that $b\,|0\rangle = d\,|0\rangle = a\,|0\rangle = 0$. The evolution of these states with τ is governed by the light-cone Hamiltonian, $H_{LC} = P^-$, conjugate to τ. The Hamiltonian can be readily expressed in terms of ψ_+ and $A^i_\perp$:

$$H_{LC} = H_0 + V \;,$$

where

$$H_0 = \int d^3x \left\{ \mathrm{Tr}\left(\partial_\perp^i A_\perp^j \partial_\perp^i A_\perp^j\right) + \psi_+^\dagger \left(i\partial_\perp \cdot \alpha_\perp + \beta m\right) \frac{1}{i\partial^+} \left(i\partial_\perp \cdot \alpha_\perp + \beta m\right) \psi_+ \right\}$$

$$= \sum_{\substack{\lambda \\ \text{colors}}} \int \frac{dk^+ \, d^2k_\perp}{16\pi^3 \, k^+} \left\{ a^\dagger(\underline{k},\lambda)\, a(\underline{k},\lambda) \frac{k_\perp^2}{k^+} + b^\dagger(\underline{k},\lambda)\, b(\underline{k},\lambda) \right.$$

$$\left. \times \frac{k_\perp^2 + m^2}{k^+} + d^\dagger(\underline{k},\lambda)\, b(\underline{k},\lambda) \frac{k_\perp^2 + m^2}{k^+} \right\} + \text{constant}$$

is the free Hamiltonian and V the interaction:

$$V = \int d^3x \left\{ 2g \, \mathrm{Tr}\left(i\partial^\mu \tilde{A}^\nu \left[\tilde{A}_\mu, \tilde{A}_\nu\right]\right) - \frac{g^2}{2} \mathrm{Tr}\left(\left[\tilde{A}^\mu, \tilde{A}^\nu\right]\left[\tilde{A}_\mu, \tilde{A}_\nu\right]\right) \right.$$

$$+ g\bar{\tilde{\psi}} \not{A} \tilde{\psi} + g^2 \, \mathrm{Tr}\left(\left[i\partial^+ \tilde{A}^\mu, \tilde{A}_\mu\right] \frac{1}{(i\partial^+)^2} \left[i\partial^+ \tilde{A}^\nu, \tilde{A}_\nu\right]\right)$$

$$+ g^2 \bar{\tilde{\psi}} \not{A} \frac{\gamma^+}{2i\partial^+} \not{A} \tilde{\psi} - g^2 \bar{\tilde{\psi}} \gamma^+ \left(\frac{1}{(i\partial^+)^2} \left[i\partial^+ \tilde{A}^\nu, \tilde{A}_\nu\right]\right) \tilde{\psi}$$

$$\left. + \frac{g^2}{2} \, \bar{\psi}\gamma^+ \, T^a \psi \, \frac{1}{(i\partial^+)^2} \, \bar{\psi}\gamma^+ \, T^a \psi \right\} \, ,$$

with $\tilde{\psi} = \tilde{\psi}_- + \psi_+$ ($\to \psi$ as $g \to 0$) and $\tilde{A}^\mu = (0, \tilde{A}^-, A_\perp^i)$ ($\to A^\mu$ as $g \to 0$). The Fock states are obviously eigenstates of H_0 with

$$H_0 \left|n : k_i^+, k_{\perp i}\right\rangle = \sum_i \left(\frac{k_\perp^2 + m^2}{k^+}\right)_i \left|n : k_i^+, k_{\perp i}\right\rangle \, .$$

It is equally obvious that they are not eigenstates of V, though any matrix element of V between Fock states is trivially evaluated. The first three terms in V correspond to the familiar three and four gluon vertices, and the gluon-quark vertex [Fig. 53(a)]. The remaining terms represent new four-quanta interactions containing instantaneous fermion and gluon propagators [Fig. 53(b)]. All terms conserve total three-momentum $\underline{k} = (k^+, \vec{k}_\perp)$, because of the integral over $\underline{x}$ in V. Furthermore, all Fock states other than the vacuum have total $k^+ > 0$, since each individual bare quantum has $k^+ > 0$. Consequently the Fock state vacuum

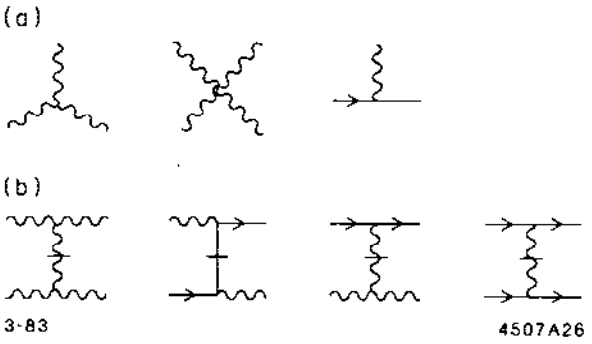

Figure 53. Diagrams which appear in the interaction Hamiltonian for QCD on the light cone. The propagators with horizontal bars represent "instantaneous" gluon and quark exchange which arise from reduction of the dependent fields in $A^+ = 0$ gauge. (a) Basic interaction vertices in QCD. (b) "Instantaneous" contributions.

must be an eigenstate of V and therefore an eigenstate of the full light-cone Hamiltonian.

Light-Cone Perturbation Theory

We define light-cone Green's functions to be the probability amplitudes that a state starting in Fock state $|i\rangle$ ends up in Fock state $|f\rangle$ a (light-cone) time τ later

$$\langle f|i\rangle\ G(f,i;\tau) \equiv \langle f|e^{-iH_{LC}\tau/2}|i\rangle$$

$$= i\int \frac{d\epsilon}{2\pi}\ e^{-i\epsilon\tau/2}\ G(f,i;\epsilon)\,\langle f|i\rangle\ ,$$

where Fourier transform $G(f,i;\epsilon)$ can be written

$$\langle f|i\rangle\ G(f,i;\epsilon) = \left\langle f\left|\frac{1}{\epsilon - H_{LC} + i0_+}\right|i\right\rangle$$

$$= \left\langle f\left|\frac{1}{\epsilon - H_{LC} + i0_+} + \frac{1}{\epsilon - H_0 + i0_+}\,V\,\frac{1}{\epsilon - H_0 + i0_+}\right.\right.$$

$$\left.\left. + \frac{1}{\epsilon - H_0 + i0_+}\,V\,\frac{1}{\epsilon - H_0 + i0_+}\,V\,\frac{1}{\epsilon - H_0 + i0_+} + \ldots\right|i\right\rangle\ .$$

The rules for τ-ordered perturbation theory follow immediately when $(\epsilon - H_0)^{-1}$ is replaced by its spectral decomposition.

$$\frac{1}{\epsilon - H_0 + i0_+} = \sum_{n,\lambda_i}\int \tilde{\prod}\ \frac{dk_i^+\,d^2k_{\perp i}}{16\pi^3\,k_i^+}\ \frac{|n:\underline{k}_i,\lambda_i\rangle\ \langle n:\underline{k}_i,\lambda_i|}{\epsilon - \sum_i (k^2+m^2)_i/k_i^+ + i0_+}$$

The sum becomes a sum over all states n intermediate between two interactions.

To calculate $G(f,i;\epsilon)$ perturbatively then, all τ-ordered diagrams must be considered, the contribution from each graph computed according to the following rules:

1. Assign a momentum k^μ to each line such that the total $k^+, k_\perp$ are conserved at each vertex, and such that $k^2 = m^2$, *i.e.* $k^- = (k^2 + m^2)/k^+$. With fermions associate an on-shell spinor.

$$u(\underline{k},\lambda) = \frac{1}{\sqrt{k^+}}\left(k^+ + \beta m + \vec{\alpha}_\perp \cdot \vec{k}_\perp\right) \begin{cases} \chi(\uparrow) & \lambda = \uparrow \\ \chi(\downarrow) & \lambda = \downarrow \end{cases}$$

   or

$$v(\underline{k},\lambda) = \frac{1}{\sqrt{k^+}}\left(k^+ - \beta m + \vec{\alpha}_\perp \cdot \vec{k}_\perp\right) \begin{cases} \chi(\downarrow) & \lambda = \uparrow \\ \chi(\uparrow) & \lambda = \downarrow \end{cases}$$

   where $\chi(\uparrow) = 1/\sqrt{2}\,(1,0,1,0)$ and $\chi(\downarrow) = 1/\sqrt{2}\,(0,1,0,-1)^T$. For gluon lines, assign a polarization vector $\epsilon^\mu = (0,\ 2\vec{\epsilon}_\perp \cdot \vec{k}_\perp/k^+,\ \vec{\epsilon}_\perp)$ where $\vec{\epsilon}_\perp(\uparrow) = -1/\sqrt{2}\,(1,i)$ and $\vec{\epsilon}_\perp(\downarrow) = 1/\sqrt{2}\,(1,-i)$.
2. Include a factor $\theta(k^+)/k^+$ for each internal line.
3. For each vertex include factors as illustrated in Fig. 54. To convert incoming into outgoing lines or vice versa replace

$$u \leftrightarrow v\ , \qquad \overline{u} \leftrightarrow -\overline{v}\ , \qquad \epsilon \leftrightarrow \epsilon^*$$

   in any of these vertices.
4. For each intermediate state there is a factor

$$\frac{1}{\epsilon - \sum\limits_{\text{interm}} k^- + i0_+}$$

   where ϵ is the incident P^-, and the sum is over all particles in the intermediate state.
5. Integrate $\int dk^+ d^2k_\perp/16\pi^3$ over each independent k, and sum over internal helicities and colors.
6. Include a factor -1 for each closed fermion loop, for each fermion line that both begins and ends in the initial state (*i.e.* $\overline{v}\ldots u$), and for each diagram in which fermion lines are interchanged in either of the initial or final states.

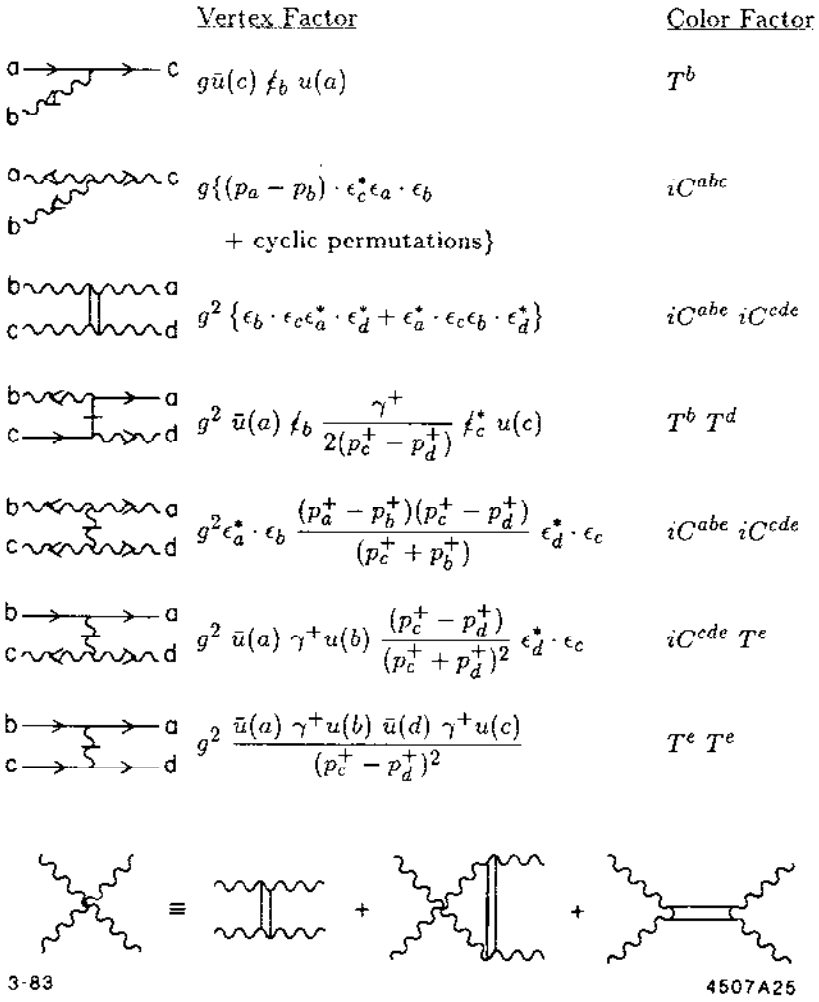

Figure 54. Graphical rules for QCD in light-cone perturbation theory.

As an illustration, the second diagram in Fig. 54 contributes

$$\frac{1}{\epsilon-\sum_{i=b,d}\left(\frac{k_\perp^2+m^2}{k^+}\right)_i}\cdot\frac{\theta(k_a^+-k_b^+)}{k_a^+-k_b^+}$$

$$\times\frac{g^2\sum_\lambda\bar{u}(b)\,\epsilon^*(\underline{k}_a-\underline{k}_b,\lambda)\,u(a)\,\bar{u}(d)\,\not{\epsilon}(\underline{k}_a-\underline{k}_b,\lambda)\,u(c)}{\epsilon-\sum_{i=b,c}\left(\frac{k_\perp^2+m^2}{k^+}\right)_i-\frac{(k_{\perp a}-k_{\perp b})^2}{k_a^+-k_b^+}}\cdot\frac{1}{\epsilon-\sum_{i=a,c}\left(\frac{k_\perp^2+m^2}{k^+}\right)_i}$$

(times a color factor) to the $q\bar{q}\to q\bar{q}$ Green's function. (The vertices for quarks and gluons of definite helicity have very simple expressions in terms of the momenta of the particles.) The same rules apply for scattering amplitudes, but with

propagators omitted for external lines, and with $\epsilon = P^-$ of the initial (and final) states.

Finally, notice that this quantization procedure and perturbation theory (graph by graph) are manifestly invariant under a large class of Lorentz transformations:

1. boosts along the 3-direction — *i.e.* $p^+ \to Kp^+$, $p^- \to K^{-1}p^-$, $p_\perp \to p_\perp$ for each momentum;
2. transverse boosts — *i.e.* $p^+ \to p^+$, $p^- \to p^- + 2p_\perp \cdot Q_\perp + p^+ Q_\perp^2$, $p_\perp \to p_\perp + p^+ Q_\perp$ for each momentum ($Q_\perp$ like K is dimensionless);
3. rotations about the 3-direction.

It is these invariances which lead to the frame independence of the Fock state wave functions.

APPENDIX III
A NONPERTURBATIVE ANALYSIS OF EXCLUSIVE REACTIONS– DISCRETIZED LIGHT-CONE QUANTIZATION

Only a small fraction of exclusive processes can be addressed by perturbative QCD analyses. Despite the simplicity of the e^+e^- and $\gamma\gamma$ initial state, the full complexity of hadron dynamics is involved in understanding resonance production, exclusive channels near threshold, jet hadronization, the hadronic contribution to the photon structure function, and the total e^+e^- or $\gamma\gamma$ annihilation cross section. A primary question is whether we can ever hope to confront QCD directly in its nonperturbative domain. Lattice gauge theory and effective Lagrangian methods such as the Skyrme model offer some hope in understanding the low-lying hadron spectrum but dynamical computations relevant to $\gamma\gamma$ annihilation appear intractable. Considerable information[16] on the spectrum and the moments of hadron valence wavefunctions has been obtained using the ITEP QCD sum rule method, but the region of applicability of this method to dynamical problems appears limited.

Recently a new method for analysing QCD in the nonperturbative domain has been developed: discretized light-cone quantization (DLCQ).[118] The method has the potential for providing detailed information on all the hadron's Fock light-cone components. DLCQ has been used to obtain the complete spectrum of neutral states in QED[8] and QCD[119] in one space and one time for any mass and coupling constant. The QED results agree with the Schwinger solution at infinite coupling. We will review the QCD[1+1] results below. Studies of QED in 3+1 dimensions are now underway.[120] Thus one can envision a nonperturbative

TABLE III

Table III. Comparison Between Time-Ordered and τ-Ordered Perturbation Theory

Equal t	Equal $\tau = t + z$
$k^o = \sqrt{\vec{k}^2 + m^2}$ (particle mass shell)	$k^- = \frac{k_\perp^2 + m^2}{k^+}$ (particle mass shell)
$\sum \vec{k}$ conserved	$\sum \vec{k}_\perp,\ k^+$ conserved
$\mathcal{M}_{ab} = V_{ab} + \sum_c V_{ac} \frac{1}{\sum_a k^o - \sum_c k^o + i\epsilon} V_{ac}$	$\mathcal{M}_{ab} = V_{ab} + \sum_c V_{ac} \frac{1}{\sum_a k^- - \sum_c k^- + i\epsilon} V_{cb}$
$n!$ time-ordered contributions	$k^+ > 0$ only
Fock states $\psi_n(\vec{k}_i)$	Fock states $\psi_n(\vec{k}_{\perp i}, x_i)$
$\sum_{i=1}^{n} \vec{k}_i = \vec{P} = 0$	$x = \frac{k^+}{P^+}\ ,\ \sum_{i=1}^{n} x_i = 1\ ,\ \sum_{i=1}^{n} \vec{k}_{\perp i} = 0$ $(0 < x_i < 1)$
$\mathcal{E} = P^o - \sum_{i=1}^{n} k_i^o$	$\mathcal{E} = P^+ \left(P^- - \sum_{i=1}^{n} k_i^- \right)$
$= M - \sum_{i=1}^{n} \sqrt{k_i^2 + m_i^2}$	$= M^2 - \sum_{i=1}^{n} \left(\frac{k_\perp^2 + m^2}{x} \right)_i$

method which in principle could allow a quantitative confrontation of QCD with the data even at low energies and momentum transfer.

The basic idea of DLCQ is as follows: QCD dynamics takes a rather simple form when quantized at equal light-cone "time" $\tau = t + z/c$. In light-cone gauge $A^+ = A^0 + A^z = 0$, the QCD light-cone Hamiltonian

$$H_{\rm QCD} = H_0 + gH_1 + g^2 H_2$$

contains the usual 3-point and 4-point interactions plus induced terms from instantaneous gluon exchange and instantaneous quark exchange diagrams. The perturbative vacuum is an eigenstate of $H_{\rm QCD}$ and serves as the lowest state in constructing a complete basis set of color singlet Fock states of H_0 in momentum space. Solving QCD is then equivalent to solving the eigenvalue problem:

$$H_{\rm QCD}|\Psi>= M^2|\Psi>$$

as a matrix equation on the free Fock basis. The set of eigenvalues $\{M^2\}$ represents the spectrum of the color-singlet states in QCD. The Fock projections of the eigenfunction corresponding to each hadron eigenvalue gives the quark and gluon Fock state wavefunctions $\psi_n(x_i, k_{\perp i}, \lambda_i)$ required to compute structure functions, distribution amplitudes, decay amplitudes, etc. For example, as shown by Drell and Yan,[10] the form-factor of a hadron can be computed at any momentum transfer Q from an overlap integral of the ψ_n summed over particle number n. The e^+e^- annihilation cross section into a given $J = 1$ hadronic channel can be computed directly from its $\psi_{q\bar{q}}$ Fock state wavefunction.

The light-cone momentum space Fock basis becomes discrete and amenable to computer representation if one chooses (anti-)periodic boundary conditions for the quark and gluon fields along the $z^- = z - ct$ and $z_\perp$ directions. In the case of renormalizable theories, a covariant ultraviolet cutoff Λ is introduced which limits the maximum invariant mass of the particles in any Fock state. One thus obtains a finite matrix representation of $H^{(\Lambda)}_{\rm QCD}$ which has a straightforward continuum limit. The entire analysis is frame independent, and fermions present no special difficulties.

Since H_{LC}, P^+, $\vec{P}_\perp$, and the conserved charges all commute, H_{LC} is block diagonal. By choosing periodic (or antiperiodic) boundary conditions for the basis states along the negative light-cone $\psi(z^- = +L) = \pm\psi(z^- = -L)$, the Fock basis becomes restricted to finite dimensional representations. The eigenvalue problem thus reduces to the diagonalization of a finite Hermitian matrix. To see this,

note that periodicity in z^- requires $P^+ = \frac{2\pi}{L}K$, $k_i^+ = \frac{2\pi}{L}\, n_i$, $\sum_{i=1}^{n} n_i = K$. The dimension of the representation corresponds to the number of partitions of the integer K as a sum of positive integers n. For a finite resolution K, the wavefunction is sampled at the discrete points

$$x_i = \frac{k_i^+}{P^+} = \frac{n_i}{K} = \left\{ \frac{1}{K}, \quad \frac{2}{K}, \quad \cdots \frac{K-1}{K} \right\} \quad .$$

The continuum limit is clearly $K \to \infty$.

One can easily show that P^- scales as L. One thus defines $P^- \equiv \frac{L}{2\pi}H$. The eigenstates with $P^2 = M^2$ at fixed P^+ and $\vec{P}_\perp = 0$ thus satisfy $H_{LC}\,|\Psi\rangle = KH\,|\Psi\rangle = M^2\,|\Psi\rangle$, independent of L (which corresponds to a Lorentz boost factor).

The basis of the DLCQ method is thus conceptually simple: one quantizes the independent fields at equal light-cone time τ and requires them to be periodic or antiperiodic in light-cone space with period $2L$. The commuting operators, the light-cone momentum $P^+ = \frac{2\pi}{L}K$ and the light cone energy $P^- = \frac{L}{2\pi}H$ are constructed explicitly in a Fock space representation and diagonalized simultaneously. The eigenvalues give the physical spectrum: the invariant mass squared $M^2 = P^\nu P_\nu$. The eigenfunctions give the wavefunctions at equal τ and allow one to compute the current matrix elements, structure functions, and distribution amplitudes required for physical processes. All of these quantities are manifestly independent of L, since $M^2 = P^+P^- = HK$. Lorentz-invariance is violated by periodicity, but re-established at the end of the calculation by going to the continuum limit: $L \to \infty$, $K \to \infty$ with P^+ finite. In the case of gauge theory, the use of the light-cone gauge $A^+ = 0$ eliminates negative metric states in both Abelian and non-Abelian theories.

Since continuum as well as single hadron color singlet hadronic wavefunctions are obtained by the diagonalization of H_{LC}, one can also calculate scattering amplitudes as well as decay rates from overlap matrix elements of the interaction Hamiltonian for the weak or electromagnetic interactions. An important point is that all higher Fock amplitudes including spectator gluons are kept in the light-cone quantization approach; such contributions cannot generally be neglected in decay amplitudes involving light quarks.

The simplest application of DLCQ to local gauge theory is QED in one-space and one-time dimensions. Since $A^+ = 0$ is a physical gauge there are no photon degrees of freedom. Explicit forms for the matrix representation of H_{QED} are given in Ref. 8.

The basic interactions which occur in H_{LC}(QCD) are illustrated in Fig. 53. Recently Hornbostel[119] has used DLCQ to obtain the complete color-singlet spectrum of QCD in one space and one time dimension for $N_C = 2, 3, 4$. The hadronic spectra are obtained as a function of quark mass and QCD coupling constant (see Fig. 55). Where they are available, the spectra agree with results obtained earlier;

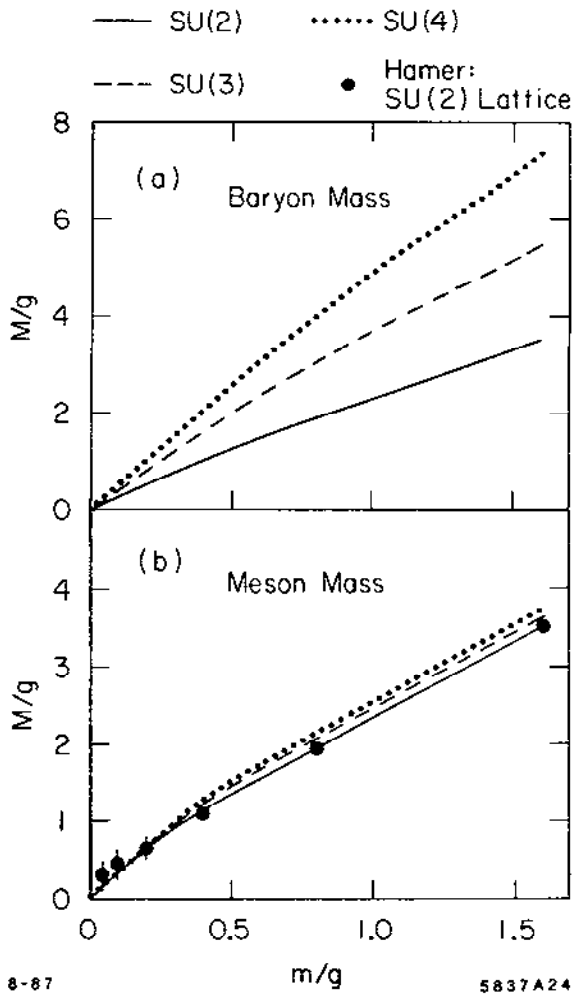

Figure 55. The baryon and meson spectrum in QCD [1+1] computed in DLCQ for $N_C = 2, 3, 4$ as a function of quark mass and coupling constant.[119]

in particular, the lowest meson mass in SU(2) agrees within errors with lattice Hamiltonian results.[121] The meson mass at $N_C = 4$ is close to the value obtained in the large N_C limit. The method also provides the first results for the baryon spectrum in a non-Abelian gauge theory. The lowest baryon mass is shown in

Fig. 55 as a function of coupling constant. The ratio of meson to baryon mass as a function of N_C also agrees at strong coupling with results obtained by Frishman and Sonnenschein.[122] Precise values for the mass eigenvalue can be obtained by extrapolation to large K since the functional dependence in $1/K$ is understood.

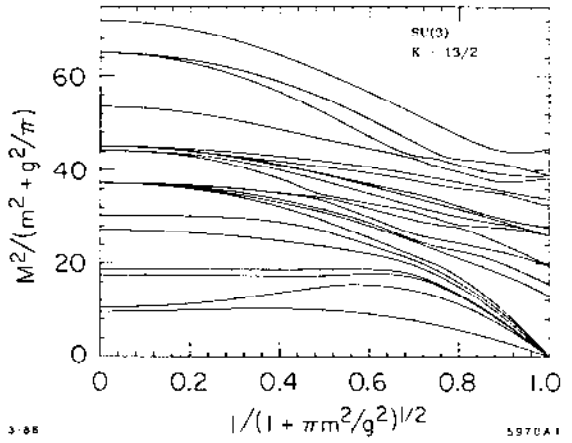

Figure 56. Representative baryon spectrum for QCD in one-space and one-time dimension.[119]

As emphasized above, when the light-cone Hamiltonian is diagonalized for a finite resolution K, one gets a complete set of eigenvalues corresponding to the total dimension of the Fock state basis. A representative example of the spectrum is shown in Fig. 56 for baryon states ($B = 1$) as a function of the dimensionless variable $\lambda = 1/(1 + \pi m^2/g^2)$. Antiperiodic boundary conditions are used. Note that spectrum automatically includes continuum states with $B = 1$.

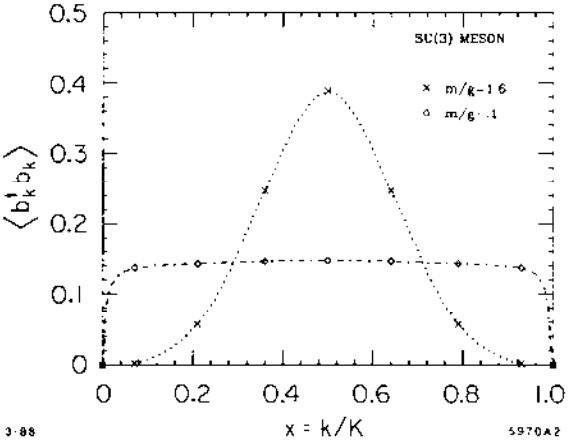

Figure 57. The meson quark momentum distribution in QCD[1+1] computed using DLCQ.[119]

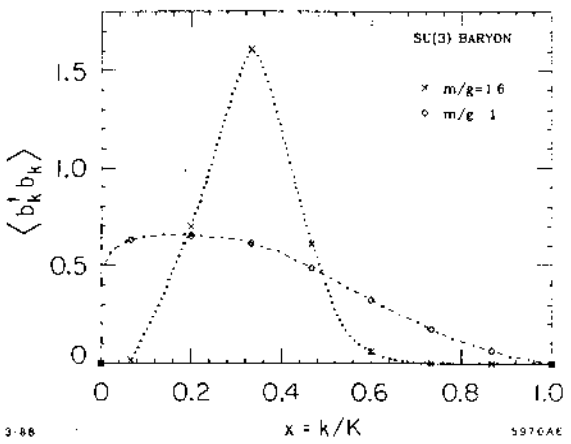

Figure 58. The baryon quark momentum distribution in QCD[1+1] computed using DLCQ.[119]

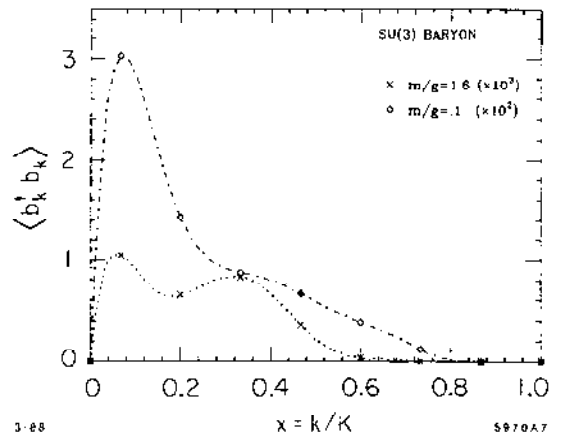

Figure 59. Contribution to the baryon quark momentum distribution from $qqq\overline{qq}$ states for QCD[1+1].[119]

The structure functions for the lowest meson and baryon states in SU(3) at two different coupling strengths $m/g = 1.6$ and $m/g = 0.1$ are shown in Figs. 57 and 58. Higher Fock states have a very small probability; representative contributions to the baryon structure functions are shown in Figs. 59 and 60. For comparison, the valence wavefunction of a higher mass state which can be identified as a composite of meson pairs (analogous to a nucleus) is shown in Fig. 61. The interactions of the quarks in the pair state produce Fermi motion beyond $x = 0.5$. Although these results are for one time one space theory they do suggest that the sea quark distributions in physical hadrons may be highly structured.

In the case of gauge theory in 3+1 dimensions, one also takes the $k_\perp^i =$

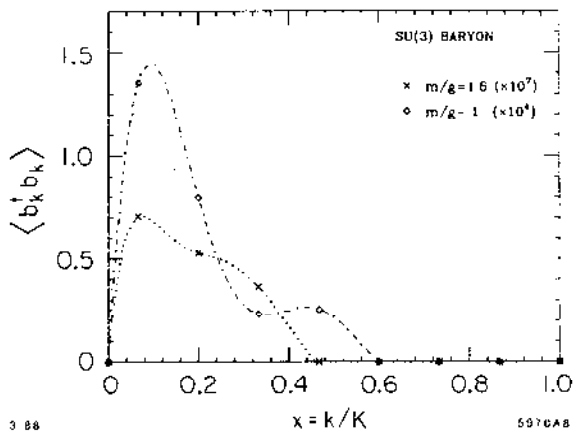

Figure 60. Contribution to the baryon quark momentum distribution from $qqq\overline{qqq}$ states for QCD[1+1].[119]

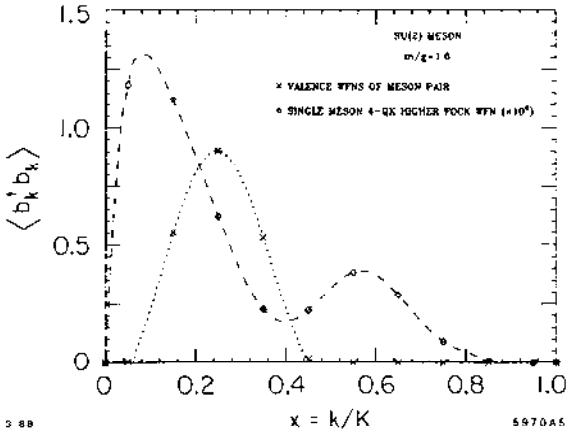

Figure 61. Comparison of the meson quark distributions in the $qq\overline{qq}$ Fock sate with that of a continuum meson pair state. The structure in the former may be due to the fact that these four-particle wavefunctions are orthogonal.[119]

$(2\pi/L_\perp)n^i_\perp$ as discrete variables on a finite cartesian basis. The theory is covariantly regulated if one restricts states by the condition

$$\sum_i \frac{k^2_{\perp i} + m_i^2}{x_i} \leq \Lambda^2 \quad ,$$

where Λ is the ultraviolet cutoff. In effect, states with total light-cone kinetic energy beyond Λ^2 are cut off. In a renormalizable theory physical quantities are independent of physics beyond the ultraviolet regulator; the only dependence on Λ appears in the coupling constant and mass parameters of the Hamiltonian.

consistent with the renormalization group.[123] The resolution parameters need to be taken sufficiently large such that the theory is controlled by the continuum regulator Λ, rather than the discrete scales of the momentum space basis.

There are a number of important advantages of the DLCQ method which have emerged from this study of two-dimensional field theories. They are as follows:

1. The Fock space is denumerable and finite in particle number for any fixed resolution K. In the case of gauge theory in 3+1 dimensions, one expects that photon or gluon quanta with zero four-momentum decouple from neutral or color-singlet bound states, and thus need not be included in the Fock basis.
2. Because one is using a discrete momentum space representation, rather than a space-time lattice, there are no special difficulties with fermions: *e.g.* no fermion doubling, fermion determinants, or necessity for a quenched approximation. Furthermore, the discretized theory has basically the same ultraviolet structure as the continuum theory. It should be emphasized that unlike lattice calculations, there is no constraint or relationship between the physical size of the bound state and the length scale L.
3. The DLCQ method has the remarkable feature of generating the complete spectrum of the theory; bound states and continuum states alike. These can be separated by tracing their minimum Fock state content down to small coupling constant since the continuum states have higher particle number content. In lattice gauge theory it appears intractable to obtain information on excited or scattering states or their correlations. The wavefunctions generated at equal light cone time have the immediate form required for relativistic scattering problems. In particular one can calculate the relativistic form factor from the matrix element of currents.
4. DLCQ is basically a relativistic many-body theory, including particle number creation and destruction, and is thus a basis for relativistic nuclear and atomic problems. In the nonrelativistic limit the theory is equivalent to the many-body Schrödinger theory.

Whether QCD can be solved using DLCQ — considering its large number of degrees of freedom is unclear. The studies for Abelian and non-Abelian gauge theory carried out so far in 1+1 dimensions give grounds for optimism.

ACKNOWLEDGEMENTS

We wish to thank the following: G. de Teramond, J. F. Gunion, J. R. Hiller, K. Hornbostel, C. R. Ji, A. H. Mueller, H. C. Pauli, D. E. Soper, A. Tang and S. F. Tuan.

REFERENCES

1. For general reviews of QCD see J. C. Collins and D. E. Soper, Ann. Rev. Nucl. Part. Sci., 37, 383 (1987); E. Reya, Phys. Rept. 69, 195 (1981); and A. H. Mueller, Lectures on Perturbative QCD given at the Theoretical Advanced Study Institute, New Haven, 1985.
2. General QCD analyses of exclusive processes are given in Ref. 4, S. J. Brodsky and G. P. Lepage, SLAC-PUB-2294, presented at the Workshop on Current Topics in High Energy Physics, Cal Tech (Feb. 1979), S. J. Brodsky, in the Proc. of the La Jolla Inst. Summer Workshop on QCD, La Jolla (1978), A. V. Efremov and A. V. Radyushkin, Phys. Lett. B94, 245 (1980), V. L. Chernyak, V. G. Serbo, and A. R. Zhitnitskii, Yad. Fiz. 31, 1069 (1980), S. J. Brodsky, Y. Frishman, G. P. Lepage, and C. Sachrajda, Phys. Lett. 91B, 239 (1980), and A. Duncan and A. H. Mueller, Phys. Rev. D21, 1636 (1980).
3. QCD predictions for the pion form factor at asymptotic Q^2 were first obtained by V. L. Chernyak, A. R. Zhitnitskii, and V. G. Serbo, JETP Lett. 26, 594 (1977), D. R. Jackson, Ph.D. Thesis, Cal Tech (1977), and G. Farrar and D. Jackson, Phys. Rev. Lett. 43, 246 (1979). See also A. M. Polyakov, Proc. of the Int. Symp. on Lepton and Photon Interactions at High Energies, Stanford (1975), and G. Parisi, Phys. Lett. 84B, 225 (1979). See also S. J. Brodsky and G. P. Lepage, in *High Energy Physics–1980*, proceedings of the XXth International Conference, Madison, Wisconsin, edited by L. Durand and L. G. Pondrom (AIP, New York, 1981); p. 568. A. V. Efremov and A. V. Radyushkin, Rev. Nuovo Cimento 3, 1 (1980); Phys. Lett. 94B, 245 (1980). V. L. Chernyak and A. R. Zhitnitsky, JETP Lett. 25, 11 (1977); G. Parisi, Phys. Lett. 43, 246 (1979); M. K. Chase, Nucl. Phys. B167, 125 (1980).
4. G. P. Lepage and S. J. Brodsky, Phys. Rev. D22, 2157 (1980); Phys. Lett. 87B, 359 (1979); Phys. Rev. Lett. 43, 545, 1625(E) (1979).
5. S. J. Brodsky and G. R. Farrar, Phys. Rev. Lett. 31, 1153 (1973), and Phys. Rev. D11, 1309 (1975); See also V. A. Matveev, R. M. Muradyan and A. V. Tavkheldize, Lett. Nuovo Cimento 7, 719 (1973).
6. S. J. Brodsky and G. P. Lepage, Phys. Rev. D24, 2848 (1981).
7. A. H. Mueller, Proc. XVII Recontre de Moriond (1982); S. J. Brodsky, Proc. XIII Int. Symp. on Multiparticle Dynamics, Volendam (1982). See also G. Bertsch, A. S. Goldhaber, and J. F. Gunion, Phys. Rev. Lett. 47, 297 (1981); G. R. Farrar, H. Liu, L. L. Frankfurt, M. J. Strikmann, Phys. Rev. Lett. 61, 686 (1988); A. H. Mueller, CU-TP-415, talk given at

the DPF meeting, Stoors, Conn (1988), and CU-TP-412 talk given at the Workshop on Nuclear and Particle Physics on the Light-Cone, Los Alamos, (1988).

8. T. Eller, H. C. Pauli and S. J. Brodsky, Phys. Rev. D35, 1493 (1987).
9. P. A. M. Dirac, Rev. Mod. Phys. 21, 392 (1949). Further references to light-cone quantization are given in Ref. 8.
10. S. D. Drell and T. M. Yan, Phys. Rev. Lett. 24, 181 (1970).
11. S. J. Brodsky, Y. Frishman, G. P. Lepage and C. Sachrajda, Phys. Lett. 91B, 239 (1980).
12. M. Peskin, Phys. Lett. 88B, 128 (1979); A. Duncan and A. H. Mueller. Phys. Lett. 90B, 159 (1980); Phys. Rev. D 21, 1636 (1980).
13. S. J. Brodsky, Y. Frishman, G. Peter Lepage Phys. Lett. 167B, 347, (1986); S. J. Brodsky, P. Damgaard, Y. Frishman, G. Peter Lepage Phys. Rev. D33, 1881, (1986).
14. S. Gottlieb and A. S. Kronfeld, Phys. Rev. D33, 227–233 (1986); CLNS-85/646, June 1985.
15. G. Martinelli and C. T. Sachrajda, Phys. Lett. 190B, 151, 196B, 184, (1987); Phys. Lett. B217, 319, (1989).
16. V. L. Chernyak and I. R. Zhitnitskii, Phys. Rept. 112, 1783 (1984). Xiao-Duang Xiang, Wang Xin-Nian and Huang Tao, BIHEP-TH-84, 23 and 29, 1984.
17. F. del Aguila and M. K. Chase, Nucl. Phys. B193, 517 (1982). E. Braaten, Phys. Rev. D28, 524 (1982). R. D. Field, R. Gupta, S. Ottos, and L. Chang, Nucl. Phys. B186, 429 (1981). F.-M. Dittes and A. V. Radyushkin, Sov. J. Phys. 34, 293 (1981), Phys. Lett. 134B, 359 (1984). M. H. Sarmadi, University of Pittsburgh Ph. D. thesis (1982), Phys. Lett. 143B, 471 (1984). G. R. Katz, Phys. Rev D31, 652 (1985).
18. E. Braaten and S.-M. Tse, Phys. Rev. D35, 2255 (1987).
19. A. Duncan and A. Mueller, Phys. Rev. D21, 636 (1980); Phys. Lett. 98B, 159 (1980); A. Mueller, Ref. 1.
20. P. V. Landshoff, Phys. Rev. D10, 1024 (1974). See also P. Cvitanovic, *ibid.* 10, 338 (1974); S. J. Brodsky and G. Farrar, *ibid.* 11, 1309 (1975).
21. A.H. Mueller, Phys. Rept. 73, 237 (1981). See also S. S. Kanwal, Phys. Lett. 294, 1984).
22. P. V. Landshoff and D. J. Pritchard, Z. Phys. C6, 9 (1980)
23. J. Botts and G. Sterman, Stony Brook preprint ITP-SB-89-7.

24. N. Isgur and C.H. Llewellyn Smith, Phys. Rev. Lett. 52, 1080 (1984). G. P. Korchemskii, A. V. Radyushkin, Sov. J. Nucl. Phys. 45, 910 (1987) and refs. therein.
25. C. Carlson and F. Gross, Phys. Rev. Lett. 53, 127 (1984); Phys. Rev. D36 2060 (1987).
26. O. C. Jacob and L. S. Kisslinger, Phys. Rev. Lett. 56, 225 (1986).
27. Z. Dziembowski and L. Mankiewicz, Phys. Rev. Lett. 58, 2175 (1987); Z. Dziembowski, Phys. Rev. D37, 768, 778, 2030 (1988)
28. J. Ashman *et al.*, Phys. Lett. 206B, 384 (1988).
29. See *e.g.* S. J. Brodsky, J. Ellis and M. Karliner, Phys. Lett. 206B, 309 (1988).
30. S. J. Brodsky, SLAC–PUB–4342 and in the *Proceedings of the VIIIth Nuclear and Particle Physics Summer School*, Launceston, Australia, 1987.
31. Arguments for the conservation of baryon chirality in large-momentum transfer processes have been given by B. L. Ioffe, Phys. Lett. 63B, 425 (1976). For some processes this rule leads to predictions which differ from the QCD results given here. The QCD helicity conservation rule also differs from the electroproduction helicity rules given in O. Nachtmann, Nucl. Phys. B115, 61 (1976).
32. D. Sivers, S. J. Brodsky, and R. Blankenbecler, Phys. Rep. 23C, 1, (1976).
33. G. C. Blazey *et al.*, Phys. Rev. Lett. 55, 1820 (1985); G. C. Blazey, Ph.D. Thesis, University of Minnesota (1987); B. R. Baller, Ph.D. Thesis, University of Minnesota (1987); D. S. Barton, *et al.*, J. de Phys. 46, C2, Supp. 2 (1985). For a review, see D. Sivers, Ref. 32.
34. V. D. Burkert, CEBAF-PR-87-006.
35. M. D. Mestayer, SLAC-Report 214 (1978) F. Martin, *et al.*, Phys. Rev. Lett. 38, 1320 (1977); W. P. Schultz, *et al.*, Phys. Rev. Lett. 38, 259 (1977); R. G. Arnold, *et al.*, Phys. Rev. Lett. 40, 1429 (1978); SLAC-PUB-2373 (1979); B. T. Chertok, Phys. Lett. 41, 1155 (1978); D. Day, *et al.*, Phys. Rev. Lett. 43, 1143 (1979). Summaries of the data for nucleon and nuclear form factors at large Q^2 are given in B. T. Chertok, in Progress in Particle and Nuclear Physics, Proceeding of the International School of Nuclear Physics, 5th Course, Erice (1978), and Proceedings of the XVI Rencontre de Moriond, Les Arcs, Savoie, France, 1981.
36. R. G. Arnold *et al.*, Phys. Rev. Lett. 57, 174 (1986).
37. R. L. Anderson *et al.*, Phys. Rev. Lett. 30, 627 (1973).
38. A. W. Hendry, Phys. Rev. D10, 2300 (1974).

39. G. R. Court *et al.*, UM-HE-86-03, April 1986, 14 pp.

40. S. J. Brodsky, C. E. Carlson and H. J. Lipkin, Phys. Rev. D20, 2278 (1979); G. R. Farrar, S. Gottlieb, D. Sivers and G. Thomas, Phys. Rev. D20, 202 (1979).

41. G. R. Farrar, RU-85-46, 1986.

42. S. J. Brodsky, C. E. Carlson and H. J. Lipkin, Ref. 40; H. J. Lipkin, (private communication).

43. J. P. Ralston and B. Pire, Phys. Rev. Lett. 57, 2330 (1986); Phys. Lett. 117B, 233 (1982).

44. S. Gupta, Phys. Rev. D24, 1169 (1981).

45. P. H. Damgaard, Nucl. Phys. B211, 435,(1983).

46. G. R. Farrar, G. Sterman, and H. Zhang, Rutgers Preprint 89-07 (1989).

47. S. J. Brodsky, G. P. Lepage, and S. A. A. Zaidi, Phys. Rev. D23, 1152 (1981).

48. A. Yokosawa, contributed to the 1980 International Symposium on High Energy Physics with Polarized Targets, Lausanne, Switzerland, 1980 (unpublished). For the review of the model calculations for the *pp* spin asymmetries, see S. J. Brodsky and G. P. Lepage in *High Energy Physics with Polarized Beams and Polarized Targets*; J. Szwed, Jagellonian University Report No. TPJU-13/80, 1980 (unpublished) and references therein. A review of the nucleon-nucleon scattering experiments is given by A. Yokosawa, Phys. Rep. 64, 47 (1980).

49. V. L. Chernyak, A. A. Ogloblin and I. R. Zhitnitsky, Novosibirsk preprints INP 87-135,136, and references therein. See also Xiao-Duang Xiang, Wang Xin-Nian, and Huang Tao, BIHEP-TH-84, 23 and 29, 1984, and M. J. Lavelle, ICTP-84-85-12; Nucl. Phys. B260, 323 (1985).

50. I. D. King and C. T. Sachrajda, Nucl. Phys. B279, 785 (1987).

51. G. P. Lepage, S. J. Brodsky, Tao Huang and P. B. Mackenzie, published in the *Proceedings of the Banff Summer Institute*, 1981.

52. S.J. Brodsky and B.T. Chertok, Phys. Rev. Lett. 37, 269 (1976); Phys. Rev. D114, 3003 (1976).

53. M. Gari and N. Stefanis, Phys. Lett. B175, 462 (1986), M. Gari and N. Stefanis, Phys. Lett. 187B, 401 (1987).

54. C-R Ji, A. F. Sill and R. M. Lombard-Nelsen, Phys. Rev. D36, 165 (1987).

55. See also G. R. Farrar, presented to the Workshop on Quantum Chromodynamics at Santa Barbara, 1988.

56. G. W. Atkinson, J. Sucher, and K. Tsokos, Phys. Lett. 137B, 407 (1984); G. R. Farrar, E. Maina, and F. Neri, Nucl. Phys. B259, 702 (1985) Err.-ibid. B263, 746 (1986).; E. Maina, Rutgers Ph.D. Thesis (1985); J. F. Gunion, D. Millers, and K. Sparks, Phys. Rev. D33, 689 (1986); P. H. Damgaard, Nucl. Phys. B211, 435 (1983); B. Nezic, Ph.D. Thesis, Cornell University (1985); D. Millers and J. F. Gunion, Phys. Rev. D34, 2657 (1986).

57. Z. Dziembowski, G. R. Farrar, H. Zhang, and L. Mankiewicz, contribution to the 12th Int. Conf. on Few Body Problems in Physics, Vancouver, 1989.

58. Z. Dziembowski and J. Franklin contribution to the 12th Int. Conf. on Few Body Problems in Physics, Vancouver, 1989.

59. J. D. Bjorken and M. C. Chen Phys. Rev. 154, 1335 (1966).

60. G. R. Farrar RU-88-47, Invited talk given at Workshop on Particle and Nuclear Physics on the Light Cone, Los Alamos, New Mexico, 1988; G. R. Farrar, H. Zhang, A. A. Globlin and I. R. Zhitnitsky, Nucl. Phys. B311, 585 (1989); G. R. Farrar, E. Maina, and F. Neri, Phys. Rev. Lett. 53, 28 and, 742 (1984).

61. J. F. Gunion, D. Millers, and K. Sparks, Phys. Rev. D33, 689 (1986); D. Millers and J. F. Gunion, Phys. Rev. D34, 2657 (1986).

62. B. Nizic Phys. Rev. D35, 80 (1987)

63. S. J. Brodsky, G. P. Lepage, P. B. Mackenzie, Phys. Rev. D28, 228 (1983.)

64. The connection of the parton model to QCD is discussed in G. Altarelli, Phys. Rep. 81, No. 1, 1982.

65. V. N. Gribov and L. V. Lipatov, Sov. Jour. Nucl Phys. 15, 438, 675 (1972).

66. R. P. Feynman, Photon-Hadron Interactions, (W. A. Benjamin, Reading, Mass. 1972).

67. J. F. Gunion, S. J. Brodsky and R. Blankenbecler, Phys. Rev. D8, 287 (1973); Phys. Lett. 39B, 649 (1972); see also Ref. 32. References to fixed angle scattering are given in this review.

68. P. V. Landshoff, J. C. Polkinghorne Phys. Rev. D10, 891 (1974).

69. B. R. Baller, et al., Phys. Rev. Lett. 60, 1118 (1988).

70. See also A. I. Vainshtein and V. I. Zakharov, Phys. Lett. 72B, 368 (1978); G. R. Farrar and D. R. Jackson, Phys. Rev. Lett. 35, 1416 (1975); B. Ioffe, Ref. 31).

71. For other applications, see A. Duncan and A. H. Mueller, Phys. Lett. 93B, 119 (1980); see also S. Gupta, Ref. 44.

72. Unless otherwise noted, the data used here is from the compilation of the Particle Data Group, Rev. Mod. Phys. 52, S1 (1980).

73. I. Peruzzi *et al.*, Phys. Rev. D17, 2901 (1978).

74. M. E. B. Franklin, Ph.D Thesis (1982), SLAC–254, UC–34d; M. E. B. Franklin *et al.*, Phys. Rev. Lett. 51, 963 (1983); G. Trilling, in *Proceedings of the Twenty-First International Conference on High Energy Physics*, Paris, July 26–31, 1982; E. Bloom, ibid.

75. S. J. Brodsky, G. P. Lepage and San Fu Tuan, Phys. Rev. Lett. 59, 621 (1987).

76. M. Chaichian, N. A. Tornqvist HU-TFT-88-11 (1988).

77. Wei-Shou Hou and A. Soni, Phys. Rev. Lett. 50, 569 (1983).

78. P. G. O. Freund and Y. Nambu, Phys. Rev. Lett. 34, 1645 (1975).

79. S. J. Brodsky and C. R. Ji, Phys. Rev. Lett. 55, 2257 (1985).

80. For general discussions of $\gamma\gamma$ annihilation in $e^+e^- \to e^+e^-X$ reactions, see S. J. Brodsky, T. Kinoshita, and H. Terazawa, Phys. Rev. Lett. 25, 972 (1970), Phys. Rev. D4, 1532 (1971), V. E. Balakin, V. M. Budnev, and I. F. Ginzburg, JETP Lett. 11, 388 (1970), N. Arteaga-Romero, A. Jaccarini, and P. Kessler, Phys. Rev. D3, 1569 (1971), R. W. Brown and I. J. Muzinich, Phys. Rev. D4, 1496 (1971), and C. E. Carlson and W.-K. Tung, Phys. Rev. D4, 2873 (1971). Reviews and further references are given in H. Kolanoski and P. M. Zerwas, DESY 87-175 (1987), H. Kolanoski, *Two-Photon Physics in e^+e^- Storage Rings*, Springer–Verlag (1984), and Ch. Berger and W. Wagner, Phys. Rep. 136 (1987); J. H. Field, University of Paris Preprint LPNHE 84-04 (1984).

81. G. Köpp, T. F. Walsh, and P. Zerwas, Nucl. Phys. B70, 461 (1974). F. M. Renard, Proc. of the Vth International Workshop on $\gamma\gamma$ Interactions, and Nuovo Cim. 80, 1 (1984). Backgrounds to the $C = +$, $J = 1$ signal can occur from tagged $e^+e^- \to e^+e^-X$ events which produce $C = -$ resonances.

82. S. J. Brodsky and G. P. Lepage, Phys. Rev. D24, 1808 (1981).

83. H. Aihara *et al.*, Phys. Rev. Lett. 57, 51, 404 (1986). Mark II data for combined charged meson pair production are also in good agreement with the PQCD predictions. See J. Boyer *et al.*, Phys. Rev. Lett. 56, 207 (1986).

84. H. Suura, T. F. Walsh, and B. L. Young, Lett. Nuovo Cimento 4, 505 (1972). See also M. K. Chase, Nucl. Phys. B167, 125 (1980).

85. J. Boyer *et al.*, Ref. 83; TPC/Two Gamma Collaboration (H. Aihara *et al.*), Phys. Rev. Lett. 57, 404 (1986).

86. M. Benyayoun and V. L. Chernyak, College de France preprint LPC 89 10 (1989).

87. M. A. Shupe, et al., Phys. Rev. D19, 1921 (1979).

88. A simple method for estimating hadron pair production cross sections near threshold in $\gamma\gamma$ collisions is given in S. J. Brodsky, G. Köpp, and P. M. Zerwas, Phys. Rev. Lett. 58, 443 (1987).

89. See Ref. 82. The next-to-leading order evaluation of T_H for these processes is given by B. Nezic, Ph.D. Thesis, Cornell University (1985).

90. S. J. Brodsky, J. F. Gunion and D. E. Soper, Phys. Rev. D36, 2710 (1987).

91. S.J. Brodsky and A. H. Mueller

92. See Ref. 52 and S. J. Brodsky and J. R. Hiller, Phys. Rev. C28, 475 (1983).

93. C. R. Ji and S. J. Brodsky, Phys. Rev. D34, 1460 (1986); D33, 1951, 1406, 2653, (1986). For a review of multi-quark evolution, see S. J. Brodsky, C.-R. Ji, SLAC-PUB-3747, (1985).

94. The data are compiled in Brodsky and Hiller, Ref. 92.

95. J. Napolitano *et al.*, ANL preprint PHY–5265–ME–88 (1988).

96. T. S.-H. Lee, ANL preprint (1988).

97. H. Myers *et al.*, Phys. Rev. 121, 630 (1961); R. Ching and C. Schaerf, Phys. Rev. 141, 1320 (1966); P. Dougan *et al.*, Z. Phys. A 276, 55 (1976).

98. T. Fujita, MPI-Heidelberg preprint, 1989.

99. S. J. Brodsky, C.-R. Ji, G. P. Lepage, Phys. Rev. Lett. 51, 83 (1983).

100. L.A. Kondratyuk and M. G. Sapozhnikov, Dubna preprint E4-88-808.

101. A. S. Carroll, *et al.*, Phys. Rev. Lett. 61, 1698 (1988).

102. G. R. Court *et al.*, Phys. Rev. Lett. 57, 507 (1986).

103. S. J. Brodsky and G. de Teramond, Phys. Rev. Lett. 60, 1924 (1988).

104. R. Blankenbecler and S. J. Brodsky, Phys. Rev. D10, 2973 (1974).

105. I. A. Schmidt and R. Blankenbecler, Phys. Rev. D15, 3321 (1977).

106. See Ref. 102; T. S. Bhatia *et al.*, Phys. Rev. Lett. 49, 1135 (1982); E. A. Crosbie *et al.*, Phys. Rev. D23, 600 (1981); A. Lin *et al.*, Phys. Lett. 74B, 273 (1978); D. G. Crabb *et al.*, Phys. Rev. Lett. 41, 1257 (1978); J. R. O'Fallon *et al.*, Phys. Rev. Lett. 39, 733 (1977); For a review, see A. D. Krisch, UM–HE–86–39 (1987).

107. For other attempts to explain the spin correlation data, see C. Avilez, G. Cocho and M. Moreno, Phys. Rev. D24, 634 (1981); G. R. Farrar, Phys. Rev. Lett. 56, 1643 (1986), Err-ibid. 56, 2771 (1986); H. J. Lipkin, Nature 324, 14 (1986); S. M. Troshin and N. E. Tyurin, JETP Lett. 44, 149 (1986) [Pisma Zh. Eksp. Teor. Fiz. 44, 117 (1986)]; G. Preparata and J. Soffer, Phys. Lett. 180B, 281 (1986); S. V. Goloskokov, S. P. Kuleshov

and O. V. Seljugin, *Proceedings of the VII International Symposium on High Energy Spin Physics*, Protvino (1986); C. Bourrely and J. Soffer, Phys. Rev. D35, 145 (1987).

108. There are five different combinations of six quarks which yield a color singlet B=2 state. It is expected that these QCD degrees of freedom should be expressed as B=2 resonances. See, *e.g.* S. J. Brodsky and C. R. Ji, Ref. 93.

109. For other examples of threshold enhancements in QCD, see S. J. Brodsky, J. F. Gunion and D. E. Soper, Ref. 90 and also Ref. 88. Resonances are often associated with the onset of a new threshold. For a discussion, see D. Bugg, Presented at the IV LEAR Workshop, Villars-Sur-Ollon, Switzerland, September 6–13, 1987.

110. J. F. Gunion, R. Blankenbecler and S. J. Brodsky, Phys. Rev. D6, 2652 (1972).

111. With the above normalization, the unpolarized pp elastic cross section is $d\sigma/dt = \Sigma_{i=1,2,...5} \mid \phi_i^2 \mid /(128\pi s p_{\rm cm}^2)$.

112. At low momentum transfers one expects the presence of both helicity-conserving and helicity nonconserving pomeron amplitudes. It is possible that the data for A_N at $p_{lab} = 11.75$ GeV/c can be understood over the full angular range in these terms. The large value of $A_N = 24 \pm 8\%$ at $p_{lab} = 28$ GeV/c and $p_T^2 = 6.5$ GeV^2 remains an open problem. See P. R. Cameron *et al.*, Phys. Rev. D32, 3070 (1985).

113. K. Abe *et al.*, Phys. Rev. D12, 1 (1975), and references therein. The high energy data for $d\sigma/dt$ at $\theta_{\rm cm} = \pi/2$ are from C. W. Akerlof *et al.*, Phys. Rev. 159, 1138 (1967); G. Cocconi *et al.*, Phys. Rev. Lett. 11, 499 (1963); J. V. Allaby *et al.*, Phys. Lett. 23, 389 (1966).

114. I. P. Auer *et al.*, Phys. Rev. Lett. 52, 808 (1984). Comparison with the low energy data for A_{LL} at $\theta_{\rm cm} = \pi/2$ suggests that the resonant amplitude below $p_{lab} = 5.5$ GeV/c has more structure than the single resonance form adopted here. See I. P. Auer *et al.*, Phys. Rev. Lett. 48, 1150 (1982).

115. See Ref. 38 and N. Jahren and J. Hiller, University of Minnesota preprint. 1987.

116. The neutral strange inclusive pp cross section measured at $p_{lab} = 5.5$ GeV/c is 0.45 ± 0.04 mb; see G. Alexander *et al.*, Phys. Rev. 154, 1284 (1967).

117. Phys. Rev. D33, 1951 (1986).

118. H. C. Pauli and S. J. Brodsky, Phys. Rev. D32, 1993, 2001 (1985) and Ref. 8.

119. K. Hornbostel, SLAC-0333, Dec 1988; K. Hornbostel, S. J. Brodsky, and H. C. Pauli, SLAC-PUB-4678, Talk presented to Workshop on Relativistic Many Body Physics, Columbus, Ohio, June, 1988.

120. S. J. Brodsky, H. C. Pauli, and A. Tang, in preparation.

121. C. J. Burden and C. J. Hamer, Phys. Rev. D37, 479 (1988), and references therein.

122. Y. Frishman and J. Sonnenschein, Nucl. Phys. B294, 801 (1987), and Nucl. Phys. B301, 346 (1988).

123. For a discussion of renormalization in light-cone perturbation theory, see S. J. Brodsky, R. Roskies and R. Suaya, Phys. Rev. D8, 4574 (1974), and also Ref. 4.